“Proteomic investigation of serine/threonine phosphorylation in *Streptococcus pneumoniae*”

I n a u g u r a l d i s s e r t a t i o n

zur

Erlangung des akademischen Grades eines

Doktors der Naturwissenschaften (Dr. rer. nat.)

der

Mathematisch-Naturwissenschaftlichen Fakultät

der

Universität Greifswald

vorgelegt von

Claudia Hirschfeld

Greifswald, den 24.07.2020

Dekan:	Herr Prof. Dr. Gerald Kerth
1. Gutachter:	Frau Prof. Dr. Dörte Becher
2. Gutachter:	Herr Prof. Dr. Jan Maarten van Dijl
Tag der Promotion:	27.11.2020

TABLE OF CONTENT

LIST OF FIGURES

LIST OF TABLES

ABBREVIATIONS

ABC	ATP-binding cassette
BR	Biological replicate
CDM	Chemically defined medium
CID	Collision-induced dissociation
EM	Electron microscopy
ESI	Electron spray ionization
ESTK	Eukaryotic-type Serine/Threonine protein kinases
ESTP	Eukaryotic-type Serine/Threonine protein phosphatase
FC	Fold change
FDR	False discovery rate
FESEM	Field scanning electron microscopy
LC	Liquid chromatography
LFQ	Label-free quantification
m/z	Mass-over-charge ratio
MALDI	Matrix-assisted laser desorption/ionization
MS	Mass spectrometry
MS/MS	Tandem mass spectrometry
NCBI	National Center for Biotechnology Information
PAGE	Polyacrylamide gel electrophoresis
PCA	Principal component analysis
PSM	Peptide spectral match
PTM	Post-translational modification
RPMI	Roswell Park Memorial Institute (specific CDM)
RPMI *modi*	Modified RPMI medium
RT	Room temperature
SAM	Significance analysis of microarrays
SCX	Strong cation exchange chromatography
SILAC	Stable isotope labeling by amino acids in cell culture
TEM	Transmission electron microscopy
THY	Todd-Hewitt broth with yeast extract
TOF	Time-of-flight

1. SUMMARY

Streptococcus pneumoniae is a commensal of the human upper respiratory tract and moreover, the causative agent of several life-threatening diseases including pneumonia, sepsis, otitis media, and meningitis. Due to the worldwide rise of resistance to antibiotics in pneumococci the understanding of its physiology is of increasing importance. In this context, the analysis of the pneumococcal proteome is helpful as comprehensive data on protein abundances in *S. pneumoniae* may provide an extensive source of information to facilitate the development of new vaccines and drug treatments.

It is known that protein phosphorylation on serine, threonine and tyrosine residues is a major regulatory post-translational modification in pathogenic bacteria. This reversible post-translational modification enables the translation of extracellular signals into cellular responses and therewith adaptation to a steadily changing environment. Consequently, it is of particular interest to gather precise information about the phosphoproteome of pneumococci. *S. pneumoniae* encodes a single Serine/Threonine kinase-phosphatase couple known as StkP-PhpP.

To address the global impact and physiological importance of StkP and PhpP which are closely linked to the regulation of cell morphology, growth and cell division in *S. pneumoniae,* proteomics with an emphasis on phosphorylation and dephosphorylation events on Ser and Thr residues was applied. Thus, the non-encapsulated pneumococcal D39Δ*cps* strain (WT), a kinase (Δ*stkP*) and phosphatase mutant (Δ*phpP*) were analyzed in in a mass spectrometry based label-free quantification experiment. The global proteome analysis of the mutants deficient for *stkP* or *phpP* already proved the essential role of StkP-PhpP in the protein regulation of the pneumococcus. Proteins with significantly altered abundances were detected in diverse functional groups in both mutants. Noticeable changes in the proteome of the *stkP* deletion mutant were observed in metabolic processes such as “Amino acid metabolism” and also in pathways regulating genetic and environmental information processing like “Transcription” and “Signal transduction”. Prominent changes in the metabolism of DNA, nucleotides, carbohydrates, cofactors and vitamins as well as in the categories “Transport and binding proteins” and “Glycan biosynthesis and metabolism” have been additionally detected in the proteome of the phosphatase mutant. Still, the quantitative comparison of WT and mutants revealed more significantly altered proteins in Δ*phpP* than in Δ*stkP*. Moreover, the results indicated that the loss of function of PhpP causes an increased abundance of proteins in the pneumococcal phosphate uptake system Pst. Furthermore, the obtained quantitative proteomic data revealed an influence of StkP and PhpP on the two-component systems ComDE, LiaRS, CiaRH, and VicRK.

Recent studies of the pneumococcal StkP/PhpP couple demonstrated that both proteins play an essential role in cell growth, cell division and separation. Growth analyses and the phenotypic

characterization of the mutants by electron-microscopy performed within this work pointed out that Δ*phpP* and Δ*stkP* had different growth characteristics and abnormal cell division and cell separation. Nevertheless, the morphological effects could not be explained by changes in protein abundances on a global scale. So, the in-depth analysis of the phosphoproteome was mandatory to deliver further information of PhpP and StkP and their influence in cell division and peptidoglycan synthesis by modulating proteins involved in this mechanisms.

For more detailed insights into the activity, targets and target sites of PhpP and StkP the advantages of phosphopeptide enrichment using titanium dioxide and spectral library based data evaluation were combined. Indeed, the application of an adapted workflow for phosphoproteome analyses and the use of a recently constructed broad spectral library, including a large number of phosphopeptides (504) highly enhanced the reliable and reproducible identification of phosphorylated proteins in this work.

Finally, already known targets and target sites of StkP and PhpP, detected and described in other studies using different experimental procedures, have been identified as a proof of principle applying the mass spectrometry based phosphoproteome approach presented in this work. Referring to the role of StkP in cell division and cell separation a number of proteins participating in cell wall synthesis and cell division that are apparently phosphorylated by StkP was identified. In comparison to StkP, the physiological function and role of the co-expressed phosphatase PhpP is poorly understood. But, especially the list of previously unknown putative target substrates of PhpP has been extended remarkably in this work. Among others, five proteins with direct involvement in cell division (DivIVA, GpsB) and peptidoglycan biosynthesis (MltG, MreC, MacP) can be found under the new putative targets of PhpP.

All in all, this work provides a complex and comprehensive protein repository of high proteome coverage of *S. pneumoniae* D39 including identification of yet unknown serine/threonine/tyrosine phosphorylation, which might contribute to support various research interests within the scientific community and will facilitate further investigations of this important human pathogen.

2. ZUSAMMENFASSUNG

Streptococcus pneumoniae ist ein Kommensale der oberen Atemwege des Menschen und darüber hinaus der Erreger mehrerer lebensbedrohlicher Krankheiten, einschließlich Lungenentzündung, Sepsis, Mittelohrentzündung und Meningitis. Aufgrund des weltweiten Anstiegs der Antibiotika-resistenz bei Pneumokokken gewinnt das Verständnis seiner Physiologie zunehmend an Bedeutung. In diesem Zusammenhang ist auch die Analyse des Pneumokokken-Proteoms von großer Wichtigkeit. Ausführliche Daten zur Abundanz bestimmter Proteine in *S. pneumoniae* können eine umfassende Informationsbasis für die Entwicklung neuer Impfstoffe und Arzneimittelbehandlungen bilden.

Dabei ist bekannt, dass die Proteinphosphorylierung an Serin-, Threonin- und Tyrosinresten eine zentrale regulatorische Rolle bei pathogenen Bakterien spielt. Jene reversible posttranslationale Modifikation ermöglicht auch die Übersetzung extrazellulärer Signale in zelluläre Antworten und damit die Anpassung der Bakterien an eine sich ständig ändernde Umgebung. Somit ist es von besonderem Interesse, weiterführende Informationen, vor allem auch über das Phosphoproteom, von Pneumokokken zu sammeln. Im Genom von *S. pneumoniae* ist ein einzelnes Serin/Threonin-Kinase-Phosphatase-Paar kodiert, das als StkP-PhpP bezeichnet wird. StkP und PhpP werden mit der Regulation der Zellmorphologie, des Wachstums und der Zellteilung bei *S. pneumoniae* in Verbindung gebracht. Um ihren globalen Einfluss und die physiologische Relevanz näher zu charakterisieren, wurden aktuelle Methoden der mikrobiellen Proteomik mit Schwerpunkt auf Phosphorylierungs- und Dephosphorylierungsereignissen an Ser- und Thr-Seitenketten angewendet. Mittels Massenspektrometrie wurden der unbekapselte Pneumokokken-Stamm D39Δ*cps* (WT), eine Kinase- (Δ*stkP*) und eine Phosphatase-Mutante (Δ*phpP*) analysiert. Zur Untersuchung von Unterschieden in Proteinabundanzen zwischen dem Wildtyp und den Mutanten wurde eine markierungsfreie Quantifizierungsstrategie gewählt. Bereits die globale Proteomanalyse der Deletions-Mutanten hat eine tragende Rolle von StkP-PhpP bei der Proteinregulation in Pneumokokken herausgestellt. Proteine mit signifikant veränderter Abundanz wurden in beiden Mutanten in verschiedenen funktionellen Kategorien aufgezeigt. Auffällige Veränderungen im Proteom der *stkP*-Deletionsmutante wurden bei Stoffwechselprozessen wie dem „Aminosäuremetabolismus“ und auch bei Wegen zur Regulierung der Verarbeitung genetischer und umweltbezogener Informationen wie „Transkription“ und „Signaltransduktion“ beobachtet. Im Proteom der Phosphatase-Mutante wurden zusätzlich deutliche Veränderungen im Metabolismus von DNA, Nukleotiden, Kohlenhydraten, Cofaktoren und Vitaminen sowie in den Kategorien „Transport- und Bindungsproteine“ und „Glycan-Biosynthese und -Metabolismus“ festgestellt. Der quantitative Vergleich von WT und Mutanten offenbarte zudem, dass deutlich mehr statistisch signifikant veränderte Proteine in Δ*phpP* als in Δ*stkP* auftraten. Darüber hinaus

zeigten die Ergebnisse, dass der Funktionsverlust von PhpP eine erhöhte Abundanz von Proteinen im Phosphat-Aufnahmesystem Pst innerhalb der Pneumokokken verursacht. Des Weiteren verdeutlichten die quantitativen Proteomdaten, dass StkP und PhpP im Zusammenhang mit der Regulation der Zweikomponentensysteme ComDE, LiaRS, CiaRH und VicRK stehen.

Jüngste Studien des Pneumokokken-StkP/PhpP-Paares zeigten, dass beide Proteine eine wesentliche Rolle beim Zellwachstum, der Zellteilung und -trennung einnehmen. Wachstumsanalysen und die phänotypische Charakterisierung der Mutanten durch Elektronenmikroskopie, die im Rahmen dieser Arbeit durchgeführt wurden, zeigten, dass die Mutanten Δ*phpP* und Δ*stkP* deutlich unterschiedliche Wachstumseigenschaften, eine abnormale Zellteilung und Zelltrennung aufwiesen. Diese morphologischen Effekte ließen sich jedoch nicht auf Veränderungen der Proteinzusammensetzung und -abundanz auf globaler Ebene zurückführen. Von daher war die eingehende Analyse des Phosphoproteoms unabdingbar, um weitere Hinweise zu PhpP und StkP und ihren Einfluss auf die Zellteilung und Peptidoglykansynthese durch Modifikation der an diesen Mechanismen beteiligten Proteine zu liefern. Um einen detaillierteren Einblick in die Aktivität und die Substrate von PhpP und StkP zu erhalten, wurde eine Anreicherung der phosphoryltierten Peptide mit Hilfe von Titandioxid durchgeführt. Zudem wurde der Versuchsansatz mit einer Spektrenbibliotheks basierten Datenauswertung zur Verbesserung der Phosphopeptididentifizierung kombiniert. Die Anwendung eines angepassten Arbeitsablaufs für die Phosphoproteomanalyse bei Pneumokokken und die Nutzung einer neu konstruierten umfassenden Spektrenbibliothek, die eine besonders hohe Anzahl von Phosphopeptiden (504) enthält, verbesserten die zuverlässige und reproduzierbare Identifizierung von phosphorylierten Proteinen in dieser Arbeit erheblich.

Schließlich konnten bereits aus anderen Studien, mit anderen experimentellen Verfahren nachgewiesenen StkP- und PhpP- Substrate mit entsprechenden Phosphorylierungsstellen identifiziert und bestätigt werden. In Anbetracht des Einflusses von StkP auf die Zellteilung und Zelltrennung konnte eine Reihe von Proteinen detektiert werden, die an der Zellwandsynthese und Zellteilung beteiligt sind und offensichtlich durch StkP phosphoryliert werden. Im Vergleich zu StkP ist die physiologische Funktion und Bedeutung der co-exprimierten Phosphatase PhpP nur wenig erforscht. Insbesondere die Liste der bisher unbekannten potentiellen Substrate von PhpP konnte im Rahmen dieser Arbeit erheblich erweitert werden. Zu den neuen potentiellen Substraten von PhpP zählen unter anderem fünf Proteine mit direkter Beteiligung an der Zellteilung (DivIVA, GpsB) und der Peptidoglykan-Biosynthese (MltG, MreC, MacP).

Alles in allem stellt diese Arbeit ein komplexes und umfassendes Protein-Repositorium mit hoher Proteomabdeckung von *S. pneumoniae* D39, einschließlich der Identifizierung bisher unbekannter Serin/Threonin/Tyrosin-Phosphorylierungsstellen zur Verfügung. Dies kann zur Unterstützung verschiedener Forschungsinteressen innerhalb der wissenschaftlichen Gemeinschaft beitragen und die Untersuchung jenes wichtigen humanpathogenen Erregers vorantreiben.

3. INTRODUCTION

3.1. *STREPTOCOCCUS PNEUMONIAE*

3.1.1. HISTORICAL AND GENERAL ASPECTS

Streptococcus pneumoniae, the pneumococcus, is a Gram-positive bacterium that can survive under both aerobic and anaerobic conditions. Moreover, *S. pneumoniae* is an important human respiratory pathogen. It can colonize various niches in the human body and causes several severe and invasive infections like pneumonia, septicemia, otitis media and meningitis (Musher 2004).
The first one recognizing pneumococci in infected sputum and lung tissue was probably the German-Swiss Scientist Edwin Klebs in 1875 (Gray and Musher 2008). Five years afterwards, in 1880, the pneumococcus was isolated for the first time from saliva independently from each other by Louis Pasteur in France and in the same year by George M. Sternberg in the United States of America (Austrian 1999; Pasteur 1881; Pasteur et al. 1881; Sternberg et al. 1881). Later on, Friedländer (Friedländer 1883), Talamon (Talamon 1883) and Fraenkel (Fraenkel 1884) found out that *S. pneumoniae* is the causative agent of pneumonia in patients. For this reason, in 1886 the described bacterium was called *Pneumococcus* by Albert Fraenkel. In the same year, the official name became *Diplococcus pneumoniae* due to the suggestion of the Austrian bacteriologist Anton Weichselbaum. The reclassification in 1974 included the observation that pneumococci form chains in liquid media and resulted in the still official name *Streptococcus pneumoniae* (Gray and Musher 2008). Typically, pneumococci are lancet-shaped, occur in pairs (diplococci) and form short chains. Furthermore, they are characterized by an α-hemolytic, catalase- and oxidase-negative phenotype (Bridy-Pappas et al. 2005; Brown 1919). In laboratory practice pneumococci are grown at 37°C in either ambient air or in an atmosphere of 5 – 10% CO_2. *S. pneumoniae* is classified into the phylum Firmicutes, belongs to the class Bacilli, the order Lactobacillales, the family Streptococcaceae within the genus *Streptococcus* and the species *S. pneumoniae* (Facklam 2002). Based on the characteristic architecture of the polysaccharide capsule and the serologic properties, pneumococci are divided into to date 98 known different serotypes summarized in 48 serogroups with shared serologic properties (Geno et al. 2017; Geno et al. 2015). The pneumococcal capsular polysaccharides are amongst others highly important for the protection of bacteria against phagocytic killing and clearance from the host. They shield the bacterial cell surface from interactions with components of the host immune system by hindering the activation and deposition of complement factors or the recognition of antigens by specific host-derived antibodies on the cell surface (Hyams et al. 2010; Abeyta et al. 2003). During the investigation of smooth (encapsulated) and rough (non-encapsulated) pneumococcal strains by Griffith in 1928 it

could be shown that genetic information transfer in bacteria is possible through the process of transformation (Griffith 1928). 16 years later, the scientists Avery, MacLeod and McCarty proved that deoxyribonucleic acid (DNA) act as the carrier of the genetic material (Avery et al. 1944). In the focus of their studies was a clinical isolate from 1916, the pneumococcal serotype 2 strain D39 (NCTC 7466). The pneumococcal strain D39 was successfully sequenced in 2007 (Lanie et al. 2007) and became a well-established laboratory strain, which is often used in pneumonia, meningitis and sepsis models (Oggioni et al. 2004; Holmes et al. 2001; Winter et al. 1997). All in all, the pneumococcus continues to be a challenging pathogenic organism to treat successfully in the 21st century.

3.1.2. DISEASES, TREATMENT AND PREVENTION

Streptococcus pneumoniae is part of the commensal flora of the human host, which is its natural habitat. The pneumococcus is able to colonize the human upper respiratory tract and can reside asymptomatically in the nasopharynx. In general, every human individual is colonized at least once a life with pneumococci. Around 27 to 65 percent of children and less than ten percent of adults are carriers of pneumococci (Weiser et al. 2018). The carriage state harbors the potential for transmission of *S. pneumoniae* within a population by person-to-person contact through airborne droplets and rises the risk of pneumococcal diseases (Mehr and Wood 2012; Bogaert et al. 2004). The pneumococcus has emerged as a serious opportunistic human pathogen that can transmigrate from the nasopharynx into the major organs, blood and the nervous system, causing severe and invasive infections like pneumonia, otitis media, bacteremia and meningitis (Ramirez et al. 2015; Kadioglu et al. 2008; Bogaert et al. 2004; Mitchell 2000). The occurrence of invasive pneumococcal disease is increased in young children, in elderly, debilitated and immunosuppressed individuals (Song et al. 2013; Welte et al. 2012). According to the World Health Organization (WHO) in 2015 pneumonia led to death of estimated 920,136 children under the age of five, this corresponds roughly to 16% of all deaths of children under five years old (World Health Organization (WHO) 2016). Besides the age and health status of an individual, risk factors for serious pneumococcal infections are e.g. viral co-infections, an increased consumption of carbohydrates, the exposure to tobacco smoke in the household, the socio-economic condition of communities often connected with missing vaccination (Weiser et al. 2018; Siemens et al. 2017; Spratt et al. 2004).

With the beginning of the first half of the 20th century, antibiotics like penicillin have been a therapeutic intervention strategy for pneumococci and other bacteria. Until 1960 penicillin treatment remained an efficient method to control pneumococcal diseases, but then the first case of penicillin-nonsusceptibility arose for pneumococci. Alternative antibiotics e.g., macrolide, fluoroquinolone, tetracycline, rifampicin, chloramphenicol and others replaced penicillin for a

while until the emerge of pneumococcal resistance for a multitude of these kind of antibiotics (Wyres et al. 2013; Ferrándiz et al. 2005; Kupronis et al. 2003; Widdowson et al. 2000). The key to prevention of human individuals from severe infectious pneumococcal diseases is vaccination. In consideration of the fact, that the polysaccharide capsule of pneumococci is highly immunogenic vaccine development has focused on the application of immunogenic proteins and carbohydrates found on the pneumococcal surface as antigens (Daniels et al. 2016; Hyams et al. 2010; MacLeod et al. 1945). Therefore, scientists have made effort to include first six capsular variants in the vaccine, thus, forming a hexavalent vaccine followed by a 12-valent vaccine in the 1970s increasing to a 17-valent vaccine formulation (Austrian et al. 1976). A striking development in 1983 was the introduction of a 23-valent pneumococcal polysaccharide vaccine (PPSV-23, Pneumovax23). Pneumovax23 is recommended especially for adults older than 65 years and children older than two years, who have an increased risk for pneumococcal diseases (Centers for Disease Control and Prevention (CDC) 2019; Grabenstein and Manoff 2012; Fedson et al. 2011). Nevertheless, these polysaccharide vaccines are ineffective for children under the age of two, which is besides elderly individuals the most vulnerable group in nowadays society.

To overcome this issue, the development of conjugate vaccines was in the focus of research. To do so, carbohydrate moieties of polysaccharide capsular antigens were conjugated with a protein moiety from a non-toxic variant of the diphtheria toxin (CMR197). The new conjugated vaccine PCV7 (Prevnar 7), including serotypes 4, 6B, 9V, 14, 18C, 19F, 23F, licensed in 2000, was reported to generate a T-cell-dependent immune response in children (Paradiso 2012; Oosterhuis-Kafeja et al. 2007). Another conjugated vaccine was introduced in 2003. PCV10 (Synflorix) includes three additional serotypes, 1, 5 and 7F. Nowadays, the conjugated vaccine PCV13 (Prevnar 13), including serotypes of PCV10 and 3, 6A and 19A, is recommended for young children and also for elderly individuals older than 65 years (Centers for Disease Control and Prevention (CDC) 2019). Although several vaccines are available against different pneumococcal serotypes, not all serotypes are covered by vaccination. Moreover, the emergence of antimicrobial resistance during bacterial infections has become a central public health concern worldwide. Pneumococci adapt rapidly to stress and starvation conditions in their ever-dynamic-surrounding, additionally they are able to overcome host defense mechanisms and antibiotic treatment (Kohler et al. 2016; Rabes et al. 2016; Saleh et al. 2013; Koppe et al. 2012). Furthermore, the pneumococcus has become increasingly resistant to most of the commonly applied clinical drugs such as *beta*-lactam antibiotics and macrolides (Gladstone et al. 2019; Peyrani et al. 2019; Schulz and Hammerschmidt 2013). In addition to that, pneumococci can express numerous specific virulence factors which raise their pathogenicity by complex mechanisms (Loughran et al. 2019; Subramanian et al. 2019; Doran et al. 2016; Gamez and Hammerschmidt 2012; Voss et al. 2012; Kadioglu et al. 2008; Bogaert et al. 2004). For this reason, it is indispensable to develop novel antimicrobial drugs against pneumococci and their resistant strains, that are not based on the

pneumococcal polysaccharide capsule composition but on other virulence factors like specific proteins, e.g. choline-binding proteins or lipoproteins, to ensure effective treatments of pneumococcal infections in the future (Voß et al. 2018; Kohler et al. 2016; Pérez-Dorado et al. 2012). Hence, basic research of protein regulation in pneumococci is of great relevance to decipher the molecular and cellular mechanisms that underlie pathogenesis and virulence. Beyond that, knowledge about protein abundance in *S. pneumoniae* may provide an extensive source of information for the selection of new targets for vaccine and antibiotic development.

3.2. EUKARYOTIC-TYPE SERINE/THREONINE PROTEIN KINASES (ESTKS) AND PHOSPHATASES (ESTPS) IN BACTERIA

In eukaryotic as well as in prokaryotic organisms' phosphorylation/dephosphorylation cascades play a key role in protein regulation. This reversible post-translational modification enables the translation of extracellular signals into cellular responses ensuring the adaptation to a steadily changing environment. Thus, phosphorylation can rapidly and reversibly modify the physico-chemical properties of proteins resulting in changes in their enzymatic activity, cellular localization, oligomeric state, half-life and interaction with other proteins (Barák 2014; Kobir et al. 2011). Two families of enzymes regulate the phosphorylation state of proteins in a cell: Protein kinases mediate phosphorylation most commonly on serine (Ser), threonine (Thr), tyrosine (Tyr), arginine (Arg), histidine (His), and aspartate (Asp) side chains while phosphatases reverse protein phosphorylation. Kinases act as molecular switches being in either an "off," inactive or an "on," active state (Huse and Kuriyan 2002). Protein phosphorylation is a crucial component of various signal transduction pathways modulating the activity of target substrates either directly by causing conformational changes of proteins or indirectly by regulating protein-protein interactions (Pereira et al. 2011).

The most abundant signaling systems in bacteria are two-component regulatory systems consisting of a histidine kinase coupled to a cognate response regulator (Gómez-Mejia et al. 2017; Jung et al. 2012). For a long time, it was assumed that Ser/Thr/Tyr as well as Arg phosphorylation occur exclusively in eukaryotes and do not exist in bacterial species. Many studies refuted this assumption and demonstrated the presence of a large number of different protein kinases in bacteria that were classified into five types: His kinases, Tyr kinases, Arg kinases, Hanks-type Ser/Thr kinases (STKs) (also commonly named eukaryotic-like STKs), and atypical Ser kinases (Mijakovic et al. 2016). Hanks and his co-workers defined and described the major family of Ser/Thr/Tyr protein kinases found in eukaryotes in 1988 (Hanks et al. 1988). Three years later, the first bacterial STK, Pkn1, from the Gram-negative soil bacterium *Myxococcus xanthus* was discovered and characterized by Munoz-Dorato et *al.* (Muñoz-Dorado et al. 1991). Pkn1 reveals significant structural similarities with eukaryotic STKs and plays a crucial role in early

developmental events in *M. xanthus*. In 1994 Atsushi et al. described a eukaryotic-type protein kinase in Streptomyces species, that phosphorylates the AfsR protein, which is involved in processes of secondary metabolism (Atsushi et al. 1994). In the following years, numerous studies proved the presence of eukaryotic-like kinases in bacteria, e.g. PrkD in *Bacillus anthracis*, PknB in *Streptococcus mutans*, PpkA in *Pneudomonas aeruginosa*, Stk1 in *Staphylococcus aureus* (Arora et al. 2012; Banu et al. 2010; Lomas-Lopez et al. 2007; Mougous et al. 2007; Mukhopadhyay et al. 1999). Nowadays, increasing attention is being paid especially to bacterial Ser/Thr kinases, that share structural homologies with eukaryotic STKs and seem to play a similar important role as in eukaryotes. Hanks-type STKs occur either in the membrane or in the cytoplasm and can be autophosphorylated. Based on sequence homology of the kinase domains, they are grouped into one superfamily. Moreover, these kind of kinases are characterized by a catalytic domain with 12 conserved subdomains, that fold a common two-lobed catalytic core structure (Hanks and Hunter 1995; Hanks et al. 1988). The catalytic active site is located in a cleft between the two lobes (Kornev and Taylor 2010). While the N-terminal lobe functions primarily in binding and orientation of the phospho-donor ATP molecule, the C-terminal lobe binds the target substrate initiating the transfer of the phosphate group. Bacterial and eukaryotic kinases reveal a remarkable structural conservation of the catalytic domain. The catalytic domain is characterized by the occurrence of specific conserved motifs and 12 almost unvarying residues that are directly or indirectly involved in the arrangement of the phosphate donor ATP molecule and the protein substrate for catalysis (Hanks and Hunter 1995). Besides the catalytic domain, most STKs in bacteria have additional domains like penicillin-binding and Ser/Thr kinase-associated repeats (PASTA) or forkhead-associated domains, that mediate the binding of ligands and/or protein-protein interactions. One specific class of membrane-associated STKs, that commonly possesses the extracellular PASTA domain was not detected in eukaryotes. In general, Gram-positive bacteria have at least one membrane-associated STK, composed of a cytoplasmic catalytic domain linked to a transmembrane segment and an extracellular domain, that contains a varying number of PASTA motifs. These PASTA motifs have been shown to interact with the peptidoglycan, furthermore, it has been demonstrated, that STKs containing PASTA domains play a crucial role in bacterial cell division and morphogenesis (Janczarek et al. 2018; Pereira et al. 2011; Pérez et al. 2008; Yeats et al. 2002). However, previous described phylostratigraphic analyses provide evidence that Hanks-type STKs found in Eukarya, Bacteria and Archaea have a common evolutionary origin in the lineage leading to the last universal common ancestor. This was supported by the fact, that researchers could not find any evidence of horizontal transfer of genes coding for Hanks-type kinases from Eukarya to Bacteria (Stancik et al. 2018).

Apart from eukaryotic-type STKs (ESTKs) less is known about the role of the cognate phosphatases (STPs) in complex regulatory mechanisms in bacteria. Only a few bacterial STPs have been described and biochemically characterized so far. This might be due to the assumption

that the number of STPs present in bacterial cells is smaller compared to STKs and therefore they did not come into the focus of research for a long time. Moreover, the necessity of dedicated phosphatases was not immediately appreciated in bacteria since phosphohistidine residues as well as aspartyl-phosphate residues within two-component systems and phosphorelay signal transduction are subjected to relatively rapid hydrolysis. Therefore, the need of specific phosphatases to reverse phosphorylation was not expected to be crucial in bacterial species (Sickmann and Meyer 2001; Hoch 2000; Zhang 1996; Stock et al. 1990). But, phosphorylated Ser/Thr and Tyr residues are not that labile and for this reason the involvement of dedicated phosphatases quenching signaling cascades was considered in more recent investigations (Sajid et al. 2015; Shi et al. 2014; Pereira et al. 2011; Alber 2009). Archaea and bacteria have homologs of four eukaryotic protein phosphatase superfamilies: phosphoprotein phosphatases (PPPs), metallo-dependent protein phosphatases (PPMs), protein Tyr phosphatases and Asp-based phosphatases (Uhrig et al. 2013; Shi 2009). Eukaryotic-like STPs are categorized into two structurally different phosphatase families: PPPs and PPMs. In general, members of the PPP family have been defined as Ser/Thr phosphatases but it was also demonstrated that they can dephosphorylate phosphohistidine and phosphotyrosine residues (Barford 1995). An example of a PPP family member is the phosphatase PrpE of *B. subtilis*, which exclusively reverses phosphorylation of tyrosine residues *in vitro* (Hinc et al. 2006; Iwanicki et al. 2002). Most of the other phosphatases belonging into the same family have a dual-specificity and dephosphorylate Tyr residues as well as Ser/Thr residues (Pereira et al. 2011; Lai and Le Moual 2005; Missiakas and Raina 1997). The majority of yet identified and biochemically described STPs is classified into the family of PPMs. Members of this family dephosphorylate Ser-P and Thr-P of target substrates. These STPs are either Mg^{2+}- or Mn^{2+}-dependent enzymes sharing a common conserved catalytic domain with the eukaryotic protein Ser/Thr phosphatase 2C family (PP2C) that contains 11 to 13 signature motifs with eight conserved amino acids residues (Kennelly 2014; Shi 2009; Kennelly 2002; Bork et al. 1996). STPs of the PPM family are present in both, Gram-negative and Gram-positive bacteria. Typically, one STP of this family is dedicated to a cognate STK, often encoded by genes in the same operon, e.g. the STP Stp1 and the STK Stk1 in *S. aureus* or the phosphatase PhpP of *S. pneumoniae* and the cognate kinase StkP (Beltramini et al. 2009; Osaki et al. 2009). However, in certain bacterial species there are discrepancies regarding the numbers of STKs and STPs. In *M. tuberculosis* 11 STKs were identified to date but only one STP. The physiological relevance of this phenomena is still not quite clear, but it is suggested that at least in *M. tuberculosis* the STP is required for complex regulation (Wright and Ulijasz 2014; Av-Gay and Everett 2000).

All in all, it was shown that eukaryotic-like Ser/Thr protein kinases (ESTKs) as well as Ser/Thr phosphatases (ESTPs) are present in a broad range of bacterial species operating in various parallel or overlapping signaling networks thereby constituting an important signaling mechanism for the

regulation of different cellular functions (Janczarek et al. 2018; Zhang et al. 2017; Shi et al. 2014; Wright and Ulijasz 2014).

3.2.1. THE PNEUMOCOCCAL EUKARYOTIC-TYPE SERINE/THREONINE PROTEIN KINASE STKP AND PHOSPHATASE PHPP

The pneumococcus has only one gene encoding a eukaryotic-like phosphatase, *phpP*, located upstream of the *stkP* gene, which encodes the only annotated ESTK named StkP (Nováková et al. 2005; Echenique et al. 2004). The pneumococcal PhpP and StkP proteins are in the focus of this work. Both proteins are expected to constitute a functional signaling *in vivo* and likely belong to the same complex (Osaki et al. 2009). In the last two decades research primarily focused on StkP, which has been extensively investigated and its participation in the regulation of various cellular processes has been reported. StkP is a conserved transmembrane protein with a cytoplasmic kinase domain and repeated PASTA domains in their extracellular region. Therefore, StkP is classified into the distinct group of ESTKs which are involved in the regulation of cell cycle and cell division in many Gram-positive bacteria (Manuse et al. 2016; Dworkin 2015; Pereira et al. 2011; Jones and Dyson 2006; Yeats et al. 2002). Furthermore, it was already demonstrated that StkP supports virulence and its presence is relevant for successful lung infection and bloodstream invasion (Piñas et al. 2018; Herbert et al. 2015; Echenique et al. 2004). In addition to that, it has been reported, that StkP is involved in the regulation of pilus expression and modulates adherence to eukaryotic cells (Grangeasse 2016; Herbert et al. 2015; Nováková et al. 2005; Echenique et al. 2004). Moreover, StkP is essential for the resistance of pneumococci to various stress conditions as well as competence development. In a previous published transcriptome analysis it was demonstrated that StkP affects the transcription of several genes encoding proteins which participate in the process of cell wall metabolism, pyrimidine biosynthesis, DNA repair, iron uptake and oxidative stress response (Sasková et al. 2007). Although StkP was initially proposed to have only a pleiotropic role in the pneumococcus by influencing processes like gene transcription, competence or even virulence, nowadays there is a scientific consensus that it is a crucial regulator of pneumococcal cell division. (Beilharz et al. 2012; Fleurie et al. 2012; Sasková et al. 2007; Echenique et al. 2004). StkP coordinates the particular steps of the cell division process and is mainly involved in septum assembly and/or closure, spatial localization of peptidoglycan synthesis sites, and the final separation of the two daughter cells (Grangeasse 2016; Fleurie et al. 2012).

In contrast to the pneumococcal kinase StkP, the physiological role of the co-expressed phosphatase PhpP remains poorly understood. Up to date, only a few cognate ESTPs have been investigated in more detail. Nevertheless, for some of them it has been proved that they are essential for bacterial survival. Thus, for a long time, scientists were not able to generate ESTP mutants in *Streptococcus pyogenes*, *Streptococcus agalactiae* or *Bacillus anthracis*, only ESTK or

ESTK-ESTP double mutants could be successfully constructed (Agarwal et al. 2011; Burnside et al. 2010; Alber 2009; Jin and Pancholi 2006). On the other hand, there are studies reporting that ESTP knockout mutant strains were viable and the phosphatases are involved in virulence, cell segregation and cell wall metabolism (Sajid et al. 2015; Banu et al. 2010; Burnside et al. 2010; Beltramini et al. 2009; Rajagopal et al. 2003).

In 2011 Agarwal et *al.* described the first generated streptococcal ESTP mutant in *S. pyogenes*. Subsequent investigation of this mutant has among others shown that the ESTP influenced the expression of several surface proteins. Moreover, it acts as an essential regulator of group A streptococcal virulence (Agarwal et al. 2011). Later on, the characterization of the first PhpP mutant derived from the encapsulated *S. pneumoniae* D39 strain revealed that PhpP is not essential for growth or survival of pneumococci (Agarwal et al. 2012). Another successfully constructed *phpP* deletion mutant generated in the background of a non-encapsulated *S. pneumoniae* Rx1 strain by Ulrych et *al.* (2016) resulted in the discovery of a novel PhpP substrate, the putative RNA binding protein Jag. The same study towards the characterization of PhpP led to the suggestion, that PhpP and StkP cooperatively regulate cell division in the pneumococcus. Additionally, it is known that the pneumococcal phosphatase PhpP dephosphorylates its cognate kinase StkP. Furthermore, PhpP is categorized into the group of PP2C-type Mn^{2+}-dependent enzymes, containing 11 conserved signature motifs. *In vitro* essays demonstrated that mutations of the highly conserved residues D192 and D231, which are involved in metal binding, resulted in a complete suppression of PhpP activity (Nováková et al. 2005; Bork et al. 1996). PhpP is localized in the cytoplasm of pneumococcal cells. Localization studies with GFP fused PhpP showed an enrichment of the protein in the midcell. Still, the localization of PhpP to cell division sites was shown to be dependent of the presence of active StkP (Ulrych et al. 2016; Beilharz et al. 2012).

3.2.2. SERINE/THREONINE PHOSPHORYLATION AND PNEUMOCOCCAL CELL DIVISION AND MORPHOGENESIS

A characteristic of the pneumococcus is its diplo-ovococcal cell shape and its protective polysaccharide capsule, which is essential for pneumococcal virulence. Recent investigations have shown that *S. pneumoniae* possesses phosphorylation-dependent regulatory mechanisms aimed at controlling cell division as well as the concealment of the newborn cells by the capsule. Crucial for the synthesis and transport of the polysaccharide polymer is the Tyr-kinase CpsD. The Ser/Thr kinase StkP primarily participates in the regulation of pneumococcal cell division and morphogenesis (Grangeasse 2016). The majority of bacterial species yields two genetically and morphologically identical daughter cells through cell division. This process of binary fission has also been observed in the pneumococcus. Cell division in pneumococci is carried out along the successive parallel planes which are perpendicular to the cells' long axis. Therefore, the cell center

needs to be determined followed by the positioning of the division machinery (divisome) at mid-cell. An important role during cell division plays the highly conserved tubulin-like protein FtsZ that also belongs to the divisome. FtsZ forms a contractile ring (Z-ring) leading to two newborn cells. (Massidda et al. 2013; Sham et al. 2012). Within this process, cell elongation is not due to lateral insertion of peptidoglycan. The peptidoglycan synthesis takes plays at mid-cell and thus leads to the formation of the two new cell halves of the two daughter cells (Wheeler et al. 2011). However, the regulation and coordination of the essential process of cell morphogenesis and the duplication of the genetic information is not yet completely deciphered. Nonetheless, it has been demonstrated that the membrane protein StkP localizes at the division septa of the pneumococcal cells. Its extracellular domain consisting of four PASTA motifs is able to bind peptidoglycan (Morlot et al. 2013; Sasková et al. 2007; Yeats et al. 2002). Moreover, the kinase activity of StkP as well as its extracellular and cytoplasmic domains are generally essential for cell division in pneumococci. Pneumococcal strains with *stkP* mutations revealed disrupted cell wall synthesis and displayed either round or elongated morphologies including multiple, often delocalized and non-functional cell division septa in which sites of peptidoglycan synthesis and StkP are mislocalized as well (Zucchini et al. 2018; Fleurie et al. 2014b; Beilharz et al. 2012). Regarding its role in pneumococcal cell division it was already reported that several proteins participating in cell wall synthesis and cell division are phosphorylated by StkP. Importantly the cell division proteins DivIVA and MapZ, both required for cell elongation and the positioning of the division sites at mid-cell, were proved to be targets for StkP dependent phosphorylation *in vitro* and *in vivo* (Fleurie et al. 2014b; Holečková et al. 2014; Nováková et al. 2010). The same was observed for the phosphoglucosamine mutase GlmM. GlmM catalyzes essential steps in the biosynthetic pathway resulting in the formation of peptidoglycan precursors (Nováková et al. 2005). Furthermore, it has been demonstrated that FtsZ and its regulator FtsA are both phosphorylated by StkP (Beilharz et al. 2012; Giefing et al. 2010). Another promising observation includes the finding that the cell wall biosynthesis enzyme MurC which is together with GlmM involved in the peptidoglycan synthesis was found to be phosphorylated by StkP as well. (Falk and Weisblum 2013). Nevertheless, FtsZ, FtsA and MurC have been shown to be substrates of StkP *in vitro*; but their phosphorylation by StkP *in vivo* has not yet been confirmed. Since ESTKs like the pneumococcal StkP are essential for the regulation of proper cell division and peptidoglycan synthesis, it has also been reported that deletions of ESTPs in several bacterial species also affected normal cell division as well as bacterial growth. For instance, the deletion of the phosphatase PppL in *Streptococcus mutans* resulted in abnormal cell shapes and diminished growth compared to the wild-type strain. These observations reflected the effects of the deletion of its cognate kinase PknB (Banu et al. 2010). With this in mind and in consideration of the recent findings of Ulrych et *al.* 2016 (see 3.2.1.) it can be suggested that the pneumococcal phosphatase PhpP and StkP cooperatively regulate cell division of *S. pneumoniae*.

3.3. PROTEOMICS AND PHOSPHOPROTEOMICS

“Proteomics" comprises a research field in natural sciences focused on large-scale studies of proteomes. The term “proteome” was first used in 1994 by Wasinger and co-workers, including Marc Wilkins (Wasinger et al. 1995). Marc Wilkins has coined the portmanteau word “proteome”. It is a blend of the words “protein” and “genome” defined as "the entire protein complement expressed by a genome, or cell or tissue type" (Wilkins et al. 1996). In contrast to the definite genome of an organism, the proteome is not constant, moreover, it is an entity of proteins that can vary in size, properties and post-translational modifications with time and distinct requirements, or stresses, that an organism or a cell undergoes (Anderson et al. 2016). However, the proteome remains a product of a genome, to some degree, reflecting the underlying transcriptome. The term “proteomics” was characterized in 1998 by Anderson and Anderson as "the use of quantitative protein-level measurements of gene expression to characterize biological processes (e.g., disease processes and drug effects) and decipher the mechanisms of gene expression control” (Anderson and Anderson 1998). In brief, it describes the comprehensive analyses of proteomes (van Oudenhove and Devreese 2013). Proteomics implements the investigation of protein identifications, protein expression patterns, protein production rates, degradation and steady-state abundances, furthermore, protein modifications, the movement of proteins between subcellular compartments, their involvement in metabolic pathways and protein interactions. Therefore, proteomics is an interdisciplinary domain that can provide crucial information of important biological processes within cells, tissues and organisms. In the end, proteomics can be practically applied to investigate the dynamics of important proteins during host-pathogen interaction and disease development while it also allows to uncover the role and molecular structure of proteins or protein groups during pathogenesis.

In 1975 Klose, O'Farrell and Scheele have introduced independently the two-dimensional polyacrylamide gel electrophoresis technique (2D-PAGE), that immediately became a popular tool to separate and analyze complex protein mixtures (Klose 1975; O'Farrell 1975; Scheele 1975). This method to investigate proteomes is based on the combination of two orthogonal separation procedures. In the first dimension, proteins are separated by their isoelectric point and in the second dimension, proteins are further separated by their electrophoretic mobility due to their molecular weight using a sodium dodecyl sulfate-polyacrylamide gel electrophoresis (SDS-PAGE). Subsequently, proteins can be visualized and quantified by different staining procedures, such as Coomassie, silver, or fluorescence staining. Thus, protein expression patterns of multiple conditions can be compared to each other. With the introduction of matrix-assisted laser desorption/ionization time-of-flight mass spectrometry (MALDI-TOF-MS) in 1985 by Karas and co-workers, the traditional qualitative and quantitative large-scale analysis of proteomes was realized in the combination of 2D-PAGE and MALDI-TOF-MS (Karas et al. 1985). Finally, the

development of soft techniques that are capable of ionizing peptides or proteins such as MALDI and later on electrospray ionization (ESI) (Fenn et al. 1989) revolutionized the field of MS based proteomics. Still, the early developed techniques possess a limited dynamic range and only high abundant proteins within a proteomic sample could be detected (Gygi et al. 2000). Rapidly, it was realized that the analysis of complex protein mixtures would require effective separation of the compounds in the sample prior to highly effective fragmentation methods. In 1992, Hunt and colleagues published the first scientific manuscript applying liquid chromatography coupled to a tandem mass spectrometer (LC-MS/MS) as a further tool for proteomic investigations (Hunt et al. 1992). This straight-forward technique with higher sensitivity has meanwhile become the most prominent application within proteomic analyses. The huge advances in LC-MS/MS methodologies paved the way for deeper insights into dynamic post-translational modifications like reversible protein phosphorylation at serine, threonine and tyrosine which have crucial regulatory and signaling functions in eukaryotes as well as prokaryotes.

Nowadays, phosphoproteomics is getting more and more attention within the scientific community (Pagano and Arsenault 2019; Yagüe et al. 2019). Phosphoproteomics comprises the analysis of a complete set of phosphorylation sites present in a cell. Modern mass spectrometry offers numerous advantages for the investigation of protein phosphorylation, enabling qualitative and also quantitative, sensitive and site-specific detection of phosphorylated peptides and proteins on a large scale (Needham et al. 2019). Large datasets reporting the identification and localization of phosphosites have been created for various organisms, including pathogenic bacteria.

Due to the fact that modified proteins occur usually at low abundance, enrichment processes for a specific post-translational modification are typically carried out prior to MS measurement (Semanjski and Macek 2016). If only a particular phosphorylated amino acid is in the spotlight of the analysis, immunoprecipitation is suitable for phosphopeptide enrichment. This method entails the application of antibodies raised against phosphorylated amino acids binding and isolating the specific peptide. For large-scale phosphopeptide enrichment, the most common methods comprise the use of metals like iron (IMAC = immobilized metal affinity chromatography) (Villén and Gygi 2008) or metal oxides like titanium dioxide as stationary phases (Larsen et al. 2005). All in all, there are nine amino acids, Ser, Thr, Tyr, His, Lys, Arg, Asp, Glu and Cys, that can be modified by four different types of phosphate protein linkages, however, most of all studies have the focused on phosphorylation events at Ser, Thr and Tyr. These phosphorylations have been extensively described and characterized during the last years and have been associated with crucial regulatory and cellular signaling functions, especially in eukaryotes (Pawson and Scott 2005). For instance, the reference human phosphoproteome harbors more than 119,800 Ser/Thr/Tyr phosphorylation sites (Ochoa et al. 2020). The phosphoproteome of *Arabidopsis thaliana*, the model organism in plant sciences includes at least 56,800 Ser/Thr/Tyr phosphorylation sites (Durek et al. 2010). Phosphorylation at Ser/Thr/Tyr also occurs in many essential bacterial proteins as well.

Nevertheless, the characterization of phosphorylated proteins in bacteria remains a challenging analytical task since many of the phosphorylated proteins are low in abundance. Highly efficient enrichment procedures and sensitive mass spectrometry are essential to decipher bacterial phosphoproteomes. To date, MS based Ser/Thr/Tyr phosphoproteomic studies have been reported for more than 38 bacterial species, i.e. *Bacillus subtilis* (Macek et al. 2007)*, Escherichia coli* (Potel et al. 2018; Soares et al. 2013; Macek et al. 2008), *Streptococcus pneumoniae* (Hirschfeld et al. 2019; Sun et al. 2010)*, Staphylococcus aureus* (Junker et al. 2018a), *Acinetobacter baumanii* (Soares et al. 2014) and *Mycobacterium tuberculosis* (Verma et al. 2017). Thus, the phosphoproteomes of more than 24 species of eubacteria and also some species of archaea, for example *Halobacterium salinarum* (Aivaliotis et al. 2009) and *Methanohalophilus portucalensis* (Wu et al. 2016) have been described. The largest bacterial phosphoproteomes have been assigned to *Mycobacterium tuberculosis* and *Escherichia coli*. Over 500 Ser/Thr/Tyr phosphorylation sites from more than 300 proteins have been reported so far for the causative agent of pulmonary tuberculosis (Yagüe et al. 2019; Fortuin et al. 2015; Prisic et al. 2010). For the Gram-negative model organism *E. coli,* more than 1,400 Ser/Thr/Tyr phosphorylation sites assigned to more than 600 different proteins have been described (Potel et al. 2018). Furthermore, the MS-based phosphoproteomic analysis of *S. pneumoniae* that was performed within the framework of this study resulted in the detection of 692 Ser/Thr/Tyr phosphorylation sites belonging to 332 pneumococcal proteins, all included in a comprehensive spectral library for this important human pathogen (Hirschfeld et al. 2019).

The ever developing LC-MS/MS instrumentations and methodologies as well as phosphopeptide enrichment strategies will contribute to more extensive and accurate studies of large Ser/Thr/Tyr phosphopeptide and phosphoprotein pools, mainly in eukaryotes, but also in bacteria. Finally, the comprehensive analysis of bacterial phosphoproteomes might revolutionize the understanding of bacterial physiology.

3.3.1. CHALLENGES IN DECIPHERING BACTERIAL PHOSPHOPROTEOMES

Traditional phosphoproteomics applied in bacteriology before 2007 relied on 2D-gel separation of bacterial proteomes, ^{32}P-radiolabelling or immunodetection, and detection of phosphoproteins by low-resolution mass spectrometry, which impeded the identification of various phosphorylation sites. Studies based on these methodologies did not support the argument that among others many essential bacterial proteins are indeed phosphorylated. In recent years, high-resolution mass spectrometry coupled to gel-free analysis led to the generation of site-specific Ser/Thr/Tyr phosphoproteomes for many bacterial organisms, on average, reporting around one hundred phosphorylation sites for each species (Yagüe et al. 2019). Nonetheless, the major challenges in phosphoproteomics remain the in general particularly low stoichiometry and high complexity of

phosphorylation, a limited dynamic range of detection methods accessible, and quantitative difficulties (Ge and Shan 2011; Mann et al. 2002). This is again aggravated by the fact that the number of phosphoproteins and phosphorylation sites reported for bacterial species is extreme lower than in eukaryotes. However, a high-throughput analysis of a phosphoproteome applying a state-of-the-art detection technique should incorporate an enrichment of phosphoproteins or peptides, the detection and identification of phosphopeptides and the localization of the phosphorylation sites. Due to low levels of Ser/Thr/Tyr phosphorylation in bacteria, most bacterial Ser/Thr/Tyr phosphoproteomic studies start with large protein amounts (milligrams) obtained from bacterial liquid cultures during the vegetative growth phase, in the end detecting only a relatively low number of phosphopeptides. The aim of many described proteomic studies in bacteriology is the identification of as much phosphosites as possible, still, every study should provide reliable and reproducible results which can be underpinned embedding biological or technical replicates. Therefore, the reproducible growth of bacteria represents the first important step within every proteomic investigation especially regarding bacterial physiology. It has to be ensured that for all biological replicates for the same analysis the bacterial cultures underlie the same conditions. Otherwise, differences in protein composition and phosphorylation patterns might occur and increase the variance between the samples resulting in a less accurate analysis lacking statistical significance (Lithgow et al. 2017). A common feature of bacterial phosphoproteome studies is the relatively low conservation on phosphosite level. It suffices to change a single parameter in the growth conditions, and in the same bacterium yet undetected phosphorylation sites can appear, while some of the already detected ones can be lost (Pagano and Arsenault 2019; Kobir et al. 2011). This could be caused by phosphorylation mediated regulation mechanisms evolving to cope with different environmental niches. Another possible reason might be, that most of the published phosphoproteomes are incomplete because of the loss of low-occupancy phosphosites due to technical imperfections of the analysis. Besides the bacterial cultivation, phosphorylation analyses of complex protein mixtures and global phosphoproteomics consist of certain fundamental sample preparation steps prior to LC-MS/MS measurement: 1st cell lysis; 2nd fractionation of the lysate (optional); 3rd proteolysis; 4th fractionation of complex peptide mixture (optional) and 5th enrichment of phosphopeptides (Ozlu et al. 2010). At acidic and physiological pH conditions phospho groups on proteins are chemically stable, thus, dephosphorylation of a phosphoprotein would occur only in the presence of phosphatases. To minimize phosphatase activity all sample preparation steps should be carried out on ice. In addition to that, the usage of a mixture of phosphatase inhibitors is recommended to avoid dephosphorylation. Furthermore, phosphopeptides are usually under-represented compared to their unphosphorylated counterpart. So, it might be necessary to fractionate highly complex mixtures, such as whole cell lysates before the enrichment of the phosphorylated species. Another

prefractionation can be performed on peptide level using an additional liquid or affinity chromatography, i.e. strong cation exchange chromatography (SCX), strong anion exchange chromatography (SAX) or hydrophilic interaction liquid chromatography (HILIC) (Macek et al. 2009; Nühse et al. 2004). Beside the fact that fractionation steps provide better separation of complex samples allowing a more comprehensive analysis, there is sample loss during every additional step, moreover, an increased amount of single fractions demands multiple MS runs and extra measurement time. Another crucial step in the phosphoproteomic workflow is the enrichment of phosphorylated peptides. Currently the most commonly applied enrichment strategies for large-scale bacterial phosphoproteomic studies are affinity based techniques such as IMAC or metal oxide affinity chromatography (MOAC) including titanium dioxide (TiO_2) (Olsen and Macek 2009; Villén and Gygi 2008). Since most protocols for phosphopeptide enrichment and detection based on TiO_2 chromatography and high resolution MS require immense amounts of staring material there is urgent need for modified protocols that enable in-depth detection and quantification of phosphorylation sites from significantly lower amounts of bacterial material therewith saving preparation time, preventing sample loss through extensive fractionation and finally saving MS measurement time as well.

MS will remain the method of choice for phosphoproteomic investigations due to its versatility and speed. Applying tandem mass spectrometry (MS/MS) it is possible to obtain distinct information concerning phosphopeptides within a sub second timescale. It can be confirmed whether a protein/peptide is phosphorylated or not, a phosphorylated peptide can be identified and the site of modification can be determined, additionally quantitative information about phosphorylated peptides can be gathered. Nevertheless, analyzing phosphopeptides by MS creates further challenges. The ionization/detection efficiencies of phosphopeptides are lower in comparison to unphosphorylated peptides especially when using MALDI in combination with 4-hydroxy-α-cyanocinnamic acid as the MALDI matrix (Ozlu et al. 2010; Steen et al. 2005). Applying electrospray ionization (ESI), the issue of decreased flyability of phosphopeptides is still discussed, although several studies have already demonstrated that liquid chromatography (LC) and ionization conditions can be optimized to prevent a bias against phosphorylated peptides (Semanjski and Macek 2016; Steen et al. 2006). Another critical step involving the risk of phosphopeptide loss is the sample loading onto the reversed-phase column, for desalting and/or LC/MS analysis. Even if HPLC-solution conditions can be adapted and optimized to increase the hydrophobicity of phosphopeptides relative to their unphosphorylated cognates, there is a relative higher loss of phosphopeptides during the loading process. It is still the case that peptides with high hydrophobicity are not retained on reversed-phase columns under normal conditions. Therefore, it is quite difficult to analyze highly hydrophilic phosphopeptides by LC-MS/MS. Last but not least, the MS analysis of phosphopeptides is compromised by the fragmentation properties upon collision-induced dissociation (CID) in tandem MS. With the application of CID, phosphoric

acid is easily lost resulting in an energetically favorable α, β- unsaturated carbonyl group (Ozlu et al. 2010). This does not hamper the localization of the former phosphorylation site because characteristic dehydroalanine or dehydro-2-amino butyric acid residues are formed at the phosphorylation sites. But, it is often the case that the loss of phosphoric acid is predominant and additional fragmentation of sequence revealing peptide bonds remains a secondary process and is thus significantly suppressed. This is mainly the case for ion trap mass analyzers (Kim et al. 2016; Jünger and Aebersold 2014). Finally, the identification of phosphopeptides in shotgun proteomics is once more hampered by the limited predictability of fragment patterns necessary for peptide-to-spectrum-matching during classical database search. Identifications through classical database search relies on matches of predicted ion series derived from genomic data considering general fragmentation rules to query spectra of the experimental MS data. This process is time consuming and requires immense computational power and rigorous control regarding sensitivity and accuracy. Previous studies of bacterial phosphoproteomes have reported that the application of spectral libraries results in enhanced sensitivity and reproducibility (Junker et al. 2018b). The inclusion of spectral library searching in the phosphoproteomic workflow is extremely beneficial because major qualitative and quantitative information of fragment spectra are considered within the analysis. During spectral library searching experimental MS spectra are compared to already detected and reliably annotated spectra, that have been collected as applicable spectral libraries. Anyhow, searching against a spectral library entails that an a priori built high quality spectral library is available (Wiese et al. 2014). If this is the case, spectral library based data search has the huge advantage of increased speed of analysis through less calculation power. Moreover, the depth of spectrum-spectrum matching also maintenances the mapping of query spectra, that are not suitable for classical database searching e.g. because of high background noise (Lam 2011). All in all, recent large-scale phosphoproteomics experiments call for appropriate bioinformatics support, which is fundamental at numerous stages of those investigations: identification of phosphopeptides, validation of phosphorylation site assignments, data repositories, phosphorylation motif prediction, and phosphorylation site prediction. Still, the majority of phosphosite databases and phosphosite prediction tools gears towards eukaryotes, therefore it remains a quite challenging task especially for researchers in bacteriology to investigate and untangle phosphoproteomes of prokaryotic organisms.

3.4. OBJECTIVE OF THE THESIS

This thesis presents a global and comprehensive LC-MS/MS based study of the proteome and especially the phosphoproteome of the non-encapsulated *S. pneumoniae* strain D39. Within this study it was of particular interest to capture precise information about the impact of the kinase/phosphatase-couple StkP/PhpP on pneumococcal physiology. An aim was to achieve a global view on processes influenced by the absence of StkP or PhpP in pneumococci. Moreover, the main focus was set on the elucidation of the pneumococcal phosphoproteome, that paved the way for the identification of yet unknown potential targets and target sites of StkP and PhpP. Therefore, suitable strategies and techniques for proteome and phosphoproteome analyses had to be applied and adapted. The generated data will provide an extensive source of information for advanced investigations in terms of new possible targets and target sites of StkP and PhpP.

4. MATERIALS

4.1. REAGENTS AND CHEMICALS

Table 4-1: Reagents and chemicals used in this work

Reagent/Chemical	Manufacturer
Acetic acid	Carl Roth GmbH + Co. KG, Karlsruhe, Germany
Acetonitrile LC-MS grade	VWR International, Radnor, PA, USA
Acetonitrile with 0.1% acetic acid	Carl Roth GmbH + Co. KG, Karlsruhe, Germany
Adenine	Carl Roth GmbH + Co. KG, Karlsruhe, Germany
Agarose	Thermo Fisher Scientific, Waltham, MA, USA
Ammoniumbicarbonate	Carl Roth GmbH + Co. KG, Karlsruhe, Germany
Ammonium hydroxide solution	Fluka analytical, Sigma-Aldrich Chemie GmbH, Darmstadt, Germany
Ammonium sulphate	Carl Roth GmbH + Co. KG, Karlsruhe, Germany
L-Arginine HCl, Arg-10, 13C,15N	Silantes GmbH, Munich, Germany
BSA Fraction V	Thermo Fisher Scientific, Waltham, MA, USA
Bromphenol Blue sodium salt, for electrophoresis	Sigma Aldrich Chemie GmbH, Steinheim, Germany
Choline chloride	Sigma Aldrich Chemie GmbH, Steinheim, Germany
Columbia agar with sheep blood plus	OXOID, Wesel, Germany
cOmplete Tablets, Mini EDTA-free, EASYpack	F. Hoffmann-La Roche AG, Basel, Switzerland
Coomassie Brilliant Blue G-250	Sigma Aldrich Chemie GmbH, Steinheim, Germany
1,4-Dithiothreitol (DTT)	Sigma Aldrich Chemie GmbH, Steinheim, Germany
3,4-Dihydroxybenzoic acid	Sigma Aldrich Chemie GmbH, Steinheim, Germany
DreamTaq™ Polymerase Buffer	Thermo Fisher Scientific, Waltham, MA, USA
α-D(+)-Glucose monohydrate	Carl Roth GmbH + Co. KG, Karlsruhe, Germany

Reagent/Chemical	Manufacturer
β-Glycerophosphate disodium salt hydrate	Sigma Aldrich Chemie GmbH, Steinheim, Germany
EDTA disodium salt dihydrate	AppliChem GmbH, Darmstadt, Germany
Ethanol	Carl Roth GmbH + Co. KG, Karlsruhe, Germany
Gene rulerTM 1 kb DNA Ladder	Thermo Fisher Scientific, Waltham, MA, USA
Gibco RPMI 1640 Medium, no glutamine, no phenol red	Thermo Fisher Scientific, Waltham, MA, USA
Gibco SILAC RPMI 1640 Flex Media, no glucose, no phenol red	Thermo Fisher Scientific, Waltham, MA, USA
D(+)-Glucose, monohydrate	Carl Roth GmbH + Co. KG, Karlsruhe, Germany
Octyl β-d-glucopyranoside	Sigma Aldrich Chemie GmbH, Steinheim, Germany
L-Glutamine	Fluka analytical, Sigma-Aldrich Chemie GmbH, Darmstadt, Germany
Glutaraldehyde 25%	Carl Roth GmbH + Co. KG, Karlsruhe, Germany
Glycerol, anhydrous	Carl Roth GmbH + Co. KG, Karlsruhe, Germany
Glycine	Carl Roth GmbH + Co. KG, Karlsruhe, Germany
HEPES	Carl Roth GmbH + Co. KG, Karlsruhe, Germany
Hydrochloric acid	Merck KGaA, Darmstadt, Germany
Iodoacetamide (IAA)	Sigma Aldrich Chemie GmbH, Steinheim, Germany
LB-(Luria Bertani) agar	Carl Roth GmbH + Co. KG, Karlsruhe, Germany
L-Lysine HCl, Lys-8, ^{13}C,^{15}N	Silantes GmbH, Munich, Germany
Methanol	Merck KGaA, Darmstadt, Germany
2-Mercaptoethanol	Carl Roth GmbH + Co. KG, Karlsruhe, Germany
Nuclease Mix	GE Healthcare Europe GmbH, Freiburg, Germany
PageRuler Prestained Protein Ladder	Thermo Fisher Scientific, Waltham, MA, USA
Paraformaldehyde	Carl Roth GmbH + Co. KG, Karlsruhe, Germany

Reagent/Chemical	Manufacturer
Phosphoric acid	Carl Roth GmbH + Co. KG, Karlsruhe, Germany
Potassium chloride	Carl Roth GmbH + Co. KG, Karlsruhe, Germany
Potassium dihydrogen phosphate	Carl Roth GmbH + Co. KG, Karlsruhe, Germany
Roti-Nanoquant	Carl Roth GmbH + Co. KG, Karlsruhe, Germany
Sodium bicarbonate	Sigma Aldrich Chemie GmbH, Steinheim, Germany
Sodium chloride	Carl Roth GmbH + Co. KG, Karlsruhe, Germany
Sodium dihydrogen phosphate monohydrate	Sigma Aldrich Chemie GmbH, Steinheim, Germany
Sodium dodecyl sulfate (SDS)	Sigma Aldrich Chemie GmbH, Steinheim, Germany
Sodium fluoride	Sigma Aldrich Chemie GmbH, Steinheim, Germany
di-Sodium hydrogen phosphate	Sigma Aldrich Chemie GmbH, Steinheim, Germany
Sodium hydroxide	Carl Roth GmbH + Co. KG, Karlsruhe, Germany
Sodium orthovanadate	Sigma Aldrich Chemie GmbH, Steinheim, Germany
Sodium pyrophosphate tetrabasic	Sigma Aldrich Chemie GmbH, Steinheim, Germany
Thiourea	Sigma Aldrich Chemie GmbH, Steinheim, Germany
Titanium dioxide beads, Titansphere TiO	GL Science Inc., Tokyo, Japan
Todd-Hewitt-Bouillon	Carl Roth GmbH + Co. KG, Karlsruhe, Germany
Trichlormethane/Chloroform	Carl Roth GmbH + Co. KG, Karlsruhe, Germany
Triethylammonium bicarbonate buffer (TEAB)	Fluka analytical, Sigma-Aldrich Chemie GmbH, Darmstadt, Germany
Trifluoroacetic acids	Carl Roth GmbH + Co. KG, Karlsruhe, Germany
Tris	Carl Roth GmbH + Co. KG, Karlsruhe, Germany
Trypsin Resuspension buffer	Promega GmbH, Mannheim, Germany

Reagent/Chemical	Manufacturer
Uracil	AppliChem GmbH, Darmstadt, Germany
Urea	Merck KGaA, Darmstadt, Germany
Water with 0.1% acetic acid, LC-MS grade	Carl Roth GmbH + Co. KG, Karlsruhe, Germany
Yeast extract	Carl Roth GmbH + Co. KG, Karlsruhe, Germany

4.2. CULTURE MEDIA USED FOR CULTIVATION OF MICROORGANISMS

Table 4-2: Culture media used for the cultivation of *S. pneumoniae* and *E. coli*

Culture media	Composition/Source
Blood agar plates	23 g/l Pepton, 5 g/l NaCl, 14 g/l Agar, 65 ml/l, Sheep blood, pH 7.4 (Oxoid, Wesel, Germany)
THY	36.4 g/l Todd Hewitt Broth, 0.5% yeast extract
RPMI *modi*	RPMI 1640 Medium (GE Healthcare Bio-Sciences, Freiburg, Germany), 30.52 mM glucose, 2.05 mM glutamine, 0.65 mM uracil, 0.27 mM adenine, 1.1 mM glycine, 0.24 mM choline chloride, 1.7 mM NaH_2PO_4·H2O, 3.8 mM Na_2HPO_4, and 27 mM $NaHCO_3$, 20 mM HEPES
SILAC RPMI *modi*	SILAC RPMI 1640 Flex Medium (Life Technologies, Darmstadt, Germany), 30.52 mM glucose, 2.05 mM glutamine, 0.65 mM uracil, 0.27 mM adenine, 1.1 mM glycine, 0.24 mM choline chloride, 1.7 mM NaH_2PO_4·H2O, 3.8 mM Na_2HPO_4, and 27 mM $NaHCO_3$, 20 mM HEPES, 11.11 mM glucose, heavy labeled arginine (Arg-10:HCl, 200 mg/l), lysine (Lys-8:HCl, 40 mg/l)
LB	1% Bacto-Trypton, 0.5% yeast extract, 0.5% NaCl, pH 7.5
LB agar plates	1% Bacto-Trypton, 0.5% yeast extract, 0.5% NaCl, 1.5% Agar, pH 7.5

4.3. ANTIBIOTICS

Table 4-3: Final concentrations of antibiotics used for selection of microorganisms

Antibiotic	*E.coli* [µg/ml]	*S. pneumoniae* [µg/ml]	Source
Ampicillin	100	-	AppliChem GmbH, Darmstadt, Germany
Erythromycin	-	5	Sigma Aldrich Chemie GmbH, Steinheim, Germany
Kanamycin	50	50	Serva, Heidelberg, Germany

4.4. ENZYMES

The commercially acquired enzymes were used with the respective buffers according to the manufacturer.

Table 4-4: Enzymes

Enzymes	Source
Pfu-DNA-Polymerase, recombinant	Department of Molecular Genetics and Infection Biology, *E. coli* clone E162*
Taq-DNA-Polymerase, recombinant	Department of Molecular Genetics and Infection Biology, *E. coli* clone E175*
DreamTaq DNA Polymerase	Thermo Fisher Scientific, Waltham, MA, USA
T4-DNA-Ligase	New England BioLabs GmbH, Frankfurt a. M., Germany
Lysozyme	Sigma Aldrich Chemie GmbH, Steinheim, Germany
Trypsin	Promega GmbH, Mannheim, Germany
Lysyl Endopeptidase (LysC)	Wako Chemicals GmbH, Neuss, Germany

* Numbering from the internal lists of the Department of Molecular Genetics and Infection Biology, Interfaculty Institute of Genetics and Functional Genomics, Center for Functional Genomcis of Microbes, University of Greifswald

4.5. CONSUMABLES

Table 4-5: Consumables

Consumable	Manufacturer
C18, Aeris PEPTIDE 3.6 µm xB	phenomenex, Aschaffenburg, Germany
Cotton swabs	A. Hartenstein GmbH, Würzburg, Germany
Cuvettes	Sarstedt AG & Co., Nümbrecht,Germany
Fused Silica Capillaries 360 µm	Postnova Analytics GmbH, Landsberg, Germany
Quartz beads 0.10-0.11 mm	Sartorius AG, Göttingen, Germany
Glass inserts	VWR International GmbH, Darmstadt, Germany
Glass vials	VWR International GmbH, Darmstadt, Germany
iRT Kit	Biognosys AG, Schlieren, Switzerland

Consumable	Manufacturer
Low binding microcentrifuge tubes (1.7 ml, 2.0 ml)	Sorenson BioScience, Inc., Salt Lake City, USA
Parafilm	Bemis Company, Inc., Oshkosh, USA
Pasteur pipettes	Carl Roth GmbH + Co. KG, Karlsruhe, Germany
Pipette tips (10 µl, 200 µl, 1000 µl, 5000 ml)	Sarstedt AG & Co., Nümbrecht, Germany
Precast Midi Protein Gel, 4-20% Criterion TGX	Bio-Rad Laboratories GmbH, Munich, Germany
0.22 µm Rotilabo-syringe filters, CME, sterile	Carl Roth GmbH + Co. KG, Karlsruhe, Germany
Serological pipettes (5 ml, 10 ml, 25 ml)	TPP Techno Plastic Products AG, Trasadingen, Switzerland
Screw cap, 8mm	VWR International, Radnor, PA, USA
Screw Cap Micro Tube	Sarstedt AG & Co., Nümbrecht, Germany
StageTips	Thermo Fisher Scientific, Waltham, MA, USA
Tubes (15 ml, 50 ml)	Sarstedt AG & Co., Nümbrecht, Germany
ZipTip pipette tips	Merck KGaA, Darmstadt, Germany

4.6. EQUIPMENT

Table 4-6: Equipment

Equipment	Manufacturer
Allegra X-15R Centrifuge	Beckman Coulter, Brea, CA, USA
Analytical balance 510	KERN & SOHN GmbH, Balingen, Germany
Analytical balance ABJ-NM/ABS-N	KERN & SOHN GmbH, Balingen, Germany
Analytical balance PRECISION Plus	OHAUS Europe GmbH, Greifensee, Switzerland
Analytical balance Sartorius Basic	Sartorius AG, Göttingen, Germany
Automatic pipette Pipetus	Hirschmann Laborgeräte GmbH & Co. KG, Eberstadt, Germany
Bench-top centrifuge Micro Star 17R	VWR International GmbH, Darmstadt, Germany
Bench-top centrifuge, Megafuge 1.0R	Heraeus Instruments GmbH, Hanau, Germany
BioPhotometer plus	Eppendorf AG, Hamburg, Germany
Bunsen burner	WLD-TEC GmbH (Wartewig), Göttingen, Germany
Clean Bench Hera Safe	Thermo Fisher Scientific, Waltham, MA, USA

Equipment	Manufacturer
CO_2 incubator Heracell 150	Thermo Fisher Scientific, Waltham, MA, USA
Electrophoretic power supply PowerPac	Bio-Rad Laboratories GmbH, Munich, Germany
Heating plate, MR 3001	Heidolph Instruments GmbH & Co.KG, Schwabach, Germany
Heraeus Biofuge Primo R Centrifuge	Thermo Fisher Scientific, Waltham, MA, USA
Liquid chromatography system EASY-nLC 1000	Thermo Fisher Scientific, Waltham, MA, USA
Liquid chromatography system EASY-nLC II	Thermo Fisher Scientific, Waltham, MA, USA
Mass spectrometer Orbitrap Velos	Thermo Fisher Scientific, Waltham, MA, USA
Multi-Functional Tube Rotator, PTR-35	Grant Instruments Ltd, Great Britain
Homogenizer FastPrep-24	MP Biomedicals, Santa Ana, CA, USA
Homogenizer Precellys 24	Bertin, Montigny-le-Bretonneux, France
Orbital shaker Polymax 1040	Heidolph Instruments GmbH & CO. KG, Schwabach, Germany
Orbital shaker	VWR International GmbH, Darmstadt, Germany
Photometer Genesys 10S Vis	Thermo Fisher Scientific, Waltham, MA, USA
pH meter, FiveEasy pH/mV Bench Meter	Mettler-Toledo GmbH, Gießen, Germany
Scanner (gel documentation) ViewPix 700	Biostep, Burkhardtsdorf, Germany
SCX column Resource S, 1 ml	GE Healthcare Life Sciences, Freiburg, Germany
SDS-PAGE chambers Criterion™	Bio-Rad Laboratories GmbH, Munich, Germany
Thermo-cycler	Analytik Jena AG, Jena, Germany
ThermoMixer C	Eppendorf AG, Hamburg, Germany
Ultrasonic water bath Sonorex Super RK 102 H	BANDELIN electronic GmbH & Co. KG, Berlin, Germany
UV-Light Transilluminator TFX-20M	Vilber Lourmat GmbH, Eberhardzell, Germany
Vacuum centrifuge, Concentrator plus	Eppendorf AG, Hamburg, Germany
Vortex mixer VF2	IKA-Werke GmbH & CO. KG, Staufen, Germany
Water bath	GFL Gesellschaft für Labortechnik mbH, Burgwedel, Germany
ICP-MS 7500c	Agilent Technologies, Waldbrunn, Germany

4.7. SOFTWARE

Table 4-7: Software

Software; Version	Company; Reference
ClustVis	BIIT Research Group, Tartu, Estonia, (Metsalu and Vilo 2015)
Image Lab™ Software v 4.1	Bio-Rad Laboratories GmbH, Munich, Germany
Inkscape 0.92.2	
MaxQuant 1.6.1.0	MPI of Biochemistry; (Cox and Mann 2008)
MS-Viewer, ProteinProspector 5.24.0	UCSF Mass Spectrometry Facility ,The Regents of the University of California, USA
Paver 2.0	DECODON GmbH, Greifswald, Germany
Perseus 1.6.1.1	MPI of Biochemistry; (Tyanova et al. 2016)
RStudio 3.5.0	RStudio, Boston, MA, USA
Sorcerer - SEQUEST 4.0.4	Sage-N Research, Inc., Milpitas, CA, USA
Scaffold 4.4.7	Proteome Software, Inc., Portland, OR, USA
Trans Proteomic Pipeline (TPP) 5.1.0-rc1 Sysygy	Seattle Proteome Center (SPC); Deutsch *et al.* 2015
Xcalibur 2.2 SP1.48 Qual Browser	Thermo Fisher Scientific, Waltham, MA, USA

5. EXPERIMENTAL PROCEDURES

5.1. BACTERIAL STRAIN CONSTRUCTION

In this study the non-encapsulated pneumococcal serotype 2 strain D39 (D39Δ*cps*), the isogenic kinase (D39Δ*cps*Δ*stkP*) and phosphatase mutants (D39Δ*cps*Δ*phpP*) were analyzed. The initial strain D39Δ*cps* was constructed by Claudia Rennemeier as described in her PhD thesis (Claudia Rennemeier 2007). The kinase mutant D39Δ*cps*Δ*stkP* was constructed by Angelika Hohmann during her diploma thesis (Hohmann 2012) and Nadine Gotzmann prepared the phosphatase mutant D39Δ*cps*Δ*phpP* as well during her diploma thesis (Gotzmann 2013). Both mutants are available in the strain collection of the laboratory of Prof. Sven Hammerschmidt in the Interfaculty Institute of Genetics and Functional Genomics. Kinase and phosphatase mutant were checked for correctness before starting the experiments. D39Δ*cps*Δ*stkP* was verified through PCR with specific primers and D39Δ*cps*Δ*phpP* was reconstructed in this work as described in the diploma thesis (Gotzmann 2013) and below.

5.1.1. STRAINS, PLASMIDS, PRIMERS

Table 5-1: Strains, plasmids and oligonucleotides used in this work

Strain, plasmid, or primer	Resistance or sequence	Source or reference
***E.coli* DH5α**	None	Betheseda Research Labs, Gaithersburg, USA
S. pneumoniae		
TIGR4	None	(Tettelin et al. 2001)
D39Δ*cps*	Km^R	(Rennemeier et al. 2007)
D39Δ*cps stkP*::erm^R	Km^R, Erm^R	(Hohmann 2012)
D39Δ*cps*Δ*phpP*::erm^R	Km^R, Erm^R	(Gotzmann 2013), this study
Plasmids		
pGEM®-T Easy	Amp^R	Promega
pGXT	Amp^R	(Chen et al. 2009)
pET28TEV	Km^R	(Saleh et al. 2013)
pGEM®-T Easy-ChS-Erm	Amp^R, Erm^R	(Hohmann 2012)
pGXT Erm^R	Amp^R, Erm^R	(Gotzmann 2013)
pGEM®-T Easy-*stkP*	Amp^R	(Hohmann 2012)
pGEM®-T Easy Δ*stkP*	Amp^R	(Hohmann 2012)
pET28c Erm^R-loxP	Amp^R, Erm^R	This study

Strain, plasmid, or primer	Resistance or sequence	Source or reference
pGEM®-T Easy Erm^R-loxP	Amp^R, Erm^R	This study
pGEM-T Easy *stkP*::ErmR	Amp^R, Erm^R	(Hohmann 2012)
pGXT-*phpP*	Amp^R	This study
pGXT*phpP*::Erm^R	Amp^R, Erm^R	This study
Primer		
stkPStartForw	5'-CGCAAGATATCGGATTAGGAAGG-3'	
stkPEndRev	5'-TCATAATATCACGGACCGCATTGG-3'	
stkPStartRev	5'-AAGCGCATGCCTTGCCGATTTGGATCATTC-3'	
stkPEndForw	5'-GCGCGCATGCATCTACAAACCTAAAACAAC-3'	
ChS-Erm-F	5'-GCGCGCGCGGATCCCTGCAGTTGGCTTACCGTTCGTATAGC-3'	
ChS-Erm-R	5'-GCGCGCGGATCCAAGCTTTACCGTTCGTATAATGTATGCTATACGAAGTTATCCCAGTCTTTCGACTGAGCC-3'	
lox66_Erm_forw	5'-TACCGTTCGTATAGCATACATTATACGAAGTTATACGGTTCGTGTTCGTGCTG-3'	
lox71_Erm_rev	5'-ACCGTTCGTATAATGTATGCTATACGAAGTTATGTAGGCGCTAGGGACCTC-3'	
lox66_forw	5'-GGGGGGGGGGGGGGCCCGGGTACCGTTCGTATAGCATACAT-3'	
lox71_rev	5'-GACAAAAAAAAAAAAGATATCTACCGTTCGTATAATGTATGC-3'	
pGEM_rev	5'-GACAAAAAAAAAAAAGATATCCCATATGGTCGACCTGCAG-3'	
PhpPStartForw	5´-GGGAAAACAGCCCATATAGC-3'	
PhpPEndRev	5´-TCCCCGTCATAAGGGATATG-3'	
PhpPEndForw	5´-AAGGAAGCTTCATTACGGTTGCCCTTGTTT-3'	
PhpPStartRev	5´-AAGGGCTAGCTTGTTCGTTTCTGACCAACAT-3'	
ermforw	5´-GCGCGCCTGCAGACGGTTCGTGTTCGTGCTG-3'	
ermrev	5´-GCGCGCCTGCAGCGTAGGCGCTAGGGACCTC-3'	

5.1.2. CONSTRUCTION OF D39Δ*CPS*Δ*STKP* MUTANT

The kinase mutant D39Δ*cps*Δ*stkP* was constructed by Angelika Hohmann as described in her diploma thesis (Hohmann 2012). In brief, for the construction of the *stkP* mutant in D39Δ*cps*, a DNA fragment consisting of the *S. pneumoniae* TIGR4 *stkP* gene (sp_1732) and its up- and downstream flanking regions were amplified by PCR from genomic DNA using primers stkPStartForw and stkPEndRev (Table 5-1). The purified PCR product was cloned into pGEM-T Easy. The resulting plasmid pGEM-T Easy-*stkP* (pGstkP1) was transformed in chemically competent *E. coli* DH5α cells and positive mutants were selected using blue/white screening and verified by PCR. pGstkP1 was subsequently cleaved with *Bgl*II and purified. In parallel, an erythromycin resistance gene cassette containing loxP-sites was cloned into pGEM-T Easy, cleaved with *Nco*I and *Sac*I

and cloned into pET28c. Afterwards, the antibiotic-cassette was amplified with the primers pGEM_rev and lox66_forw and cloned into the *Xcm*I cleaved vector pGXT. The erythromycin-cassette was excised with BamHI and ligated into the *Bgl*II cleaved pGstkP1 plasmid. The recombinant plasmid pGstkP1::*erm* harboring the disrupted *stkP* gene was transformed into *E. coli* DH5α. Positive colonies were selected on ampicillin and finally on erythromycin. The D39Δ*cps*Δ*stkP* mutant was obtained after transformation of D39Δ*cps* with pGstkP1::*erm*. Transformants were verified for the correct integration of the antibiotic resistance cassette into the *stkP* gene region.

5.1.3. RECONSTRUCTION OF D39Δ*CPS*Δ*PHPP* MUTANT

The original phosphatase mutant D39Δ*cps*Δ*phpP* was prepared by Nadine Gotzmann during her diploma thesis (Gotzmann 2013). Due to the fact that the strain was not growing on the selective antibiotic erythromycin anymore and that the colony PCR control with specific primers revealed a signal for the *phpP* gene in the DNA from bacteria of the D39Δ*cps*Δ*phpP* cryo storage tubes, the phosphatase mutant was reconstructed in this work and replaced in the strain collection of Prof. Sven Hammerschmidts laboratory.

5.1.3.1. PLASMID CONSTRUCTION FOR D39Δ*CPS*Δ*PHPP* MUTANT

For the reconstruction of the pneumococcal phosphatase mutant in D39Δ*cps* WT strain, a DNA fragment consisting of the spd_1543 gene was amplified by PCR from chromosomal DNA using the specific primers PhpPStartForw and PhpPEndRev. The purified PCR product was cloned into pGXT and *E. coli* DH5α chemically competent cells were transformed with the resulting plasmid. The recombinant plasmid pGXT harboring the desired DNA insert was purified and used as template for an inverse PCR reaction with primer pair PhpPStartForw and PhpPEndRev. The deleted gene sequence was replaced by an erythromycin gene cassette, amplified by PCR from vector pET28c-ErmR-loxP using primer ermforw and ermrev. The final recombinant plasmid was used to transform and mutagenize pneumococci. The deletion of *phpP* was verified by PCR.

5.1.3.2. TRANSFORMATION OF *E. COLI* AND *S. PNEUMONIAE*

Chemocompetent *E. coli DH5α* cells and plasmid aliquots were thawed on ice. Plasmid DNA concentration was estimated by measuring the absorbance at 260 nm using the Nanodrop Photometer. Around 300 ng of plasmid DNA were added to *E. coli* cell aliquots followed by incubation on ice for 30 min. Afterwards, a heat shock was applied by immersing the samples for 45 sec at 42 °C in a thermo-mixer. Then, cells were immediately placed on ice for 2 min. Five volumes of pre-warmed LB medium were added and cells were incubated in a thermo-shaker at 900 rpm for 45 min. For the selection of positive transformants, cells were spread on agar plates

containing appropriate antibiotics. Plates were incubated overnight at 37 °C and afterwards stored at 4 °C.

For the transformation of pneumococci, bacteria were spread on blood-agar plates and incubated for 6 – 8 hours at 37 °C in an atmosphere of 5% CO_2. In the next step, bacteria were cultured overnight onto fresh blood agar plates containing the selective antibiotics. Afterwards, pneumococci were transferred to pre-warmed THY medium and cultered until they reached an $OD_{600\ nm}$ of 0.2 - 0.25. An aliquot of 200 µl was mixed with 1 -2 µg DNA and incubated for 10 min on ice. After an incubation of 30 min in a 30 °C waterbath, bacteria were cultivated for 2 hours at 37 °C in the waterbath. The selection of positive transformants was carried out on blood agar plates containing a high concentration of the selective antibiotics.

5.1.3.3. Isolation of plasmid-DNA from bacteria

Plasmid DNA from *E. coli* was isolated from 10 ml of an overnight culture using DNA Purification System Wizard (Promega, USA) according to the manufacturer's instructions.

For the isolation of plasmid DNA from pneumococci, bacteria from 7 ml of pneumococcal liquid culture in THY medium ($OD_{600\ nm}$ of 0.25 - 0.4) were harvested by centrifugation. Bacterial cells were washed twice with 1x PBS (18.25 mM NaCl, 931.90 mM KCl, 246.45 mM Na_2HPO_4, 1.42 M KH_2PO_4; pH 7.4) and resuspended in 80 µl sterile *Aq. Dest*. Cell lysis was performed for 8 min at 96 °C. After another centrifugation step, the supernatant was used for the transformation of *E. coli DH5α*. The verification of positive transformants was done by PCR.

5.1.3.4. Polymerase Chain Reaction (PCR)

In the polymerase chain reaction (PCR) (Saiki et al. 1988), the amplification of DNA fragments was carried out using specific oligonucleotides (Table 5-1). PCR was performed in cloning protocols for amplification of the target sequences using genomic DNA of *S. pneumoniae* TIGR4 as template for subsequent cloning into expression vectors. For the amplification of DNA either the Taq-DNA-polymerase or Pfu-DNA-polymerase (3'-5' exonuclease activity) was used.

Table 5-2: Buffers used in PCR

Buffer	Composition/Source
10× ThermoPol™ Reaction Buffer	200 mM Tris-HCl, 100 mM $(NH_4)2S0_4$, 100 mM KCl, 20 mM $MgS0_4$, 1% Triton® X-100, pH 8.8
10× PfuUltra HF Reaction Buffer	Agilent Technologies, Waldbronn, Germany
dNTPs	Promega GmbH, Mannheim, Germany

Table 5-3: Standard PCR reaction mixture

Component	Volume [µl]
Reaction buffer (10×)	5
dNTPs (10 mM)	1
$MgCl_2$ (25 mM)	1
Oligonucleotide, fwd (20 pmol)	1
Oligonucleotide, rev (20 pmol)	1
DNA (~ 100 ng)	1
DNA Polymerase	1
A. dest	39

Table 5-4: Reaction conditions for amplification

Parameter	Temperature/Time	
Start	98 °C, 3 min	
Denaturation	94 °C, 10 sec	
Annealing	55 °C, 30 sec	30 cycles
Elongation	72 °C, 1 kb/min	
Final Extension	72 °C, 3 min	
Cooling	7 °C	

5.1.3.5. AGAROSE-GEL ELECTROPHORESIS

Agarose gel electrophoresis was performed to separate nucleic acids based on their size. The separation of DNA was performed by using 0.8% agarose gels at a voltage of 80-90 V. For visualization of the nucleic acids, agarose was supplemented with the fluorescent dye HDGreen™. The GeneRuler™ 1 kb DNA ladder (Table 4-1) was used as a DNA marker.

5.2. STRAIN MAINTENANCE

Pneumococci were grown on Columbia blood agar plates for 6 - 8 hours at 37 °C in an atmosphere of 5% CO_2. Bacteria were cultured onto a fresh blood agar plate containing the selective antibiotics kanamycin [50 µg/ml] and erythromycin [5 µg/ml] and incubated for approximately 8 - 9 hours at 37 °C and 5% CO_2. Colonies from the blood agar plate were collected with a cotton swab and transferred into cryo storage tubes containing THY with 20% (v/v) glycerol. The bacteria were stored at -80 °C for long-term storage.

5.3. CULTIVATION OF PNEUMOCOCCI

Pneumococci from long term storage at -80°C were transferred to Columbia blood agar plates and incubated for 6 - 8 hours at 37°C in an atmosphere of 5% CO_2. Afterwards, bacteria were cultured onto fresh blood agar plates containing the selective antibiotics kanamycin [50 µg/ml] and erythromycin [5 µg/ml] and incubated for approximately 8 - 9 hours at 37 °C and 5% CO_2. Pneumococcal liquid cultures were prepared in modified RPMI 1640 medium (Schulz et al. 2014) or THY medium and incubated at 37 °C in a water bath without agitation in 50 ml conical tubes. For label-free quantification (LFQ) experiments RPMI *modi* medium without L-glutamine, phenol red supplemented with additional nutritive substances according to Schulz et al. 2014, was used. For SILAC-based proteome quantification, bacteria were cultivated in SILAC RPMI medium

adding the heavy labeled amino acids arginine and lysine. Liquid cultures were inoculated to starting optical densities ($OD_{600\,nm}$) between 0.05 and 0.06 and grown to exponential growth phase at $OD_{600\,nm}$ 0.3 - 0.35. In order to reach almost complete incorporation (five to six generation times) of heavy labeled amino acids in SILAC standards, two subsequent pre-cultures were grown before inoculating the main cultures. To verify the incorporation rate a MS analysis was executed as described in Hoyer *et al.* 2018 (Hoyer et al. 2018). All experiments were carried out in three independent biological replicates.

Table 5-5: Media used for *S. pneumoniae* cultivation

Medium	Composition/Source
THY	36.4 g/l Todd Hewitt Broth, 0.5% yeast extract
RPMI *modi*	RPMI 1640 Medium (GE Healthcare Bio-Sciences, Freiburg, Germany), 30.52 mM glucose, 2.05 mM glutamine, 0.65 mM uracil, 0.27 mM adenine, 1.1 mM glycine, 0.24 mM choline chloride, 1.7 mM $NaH_2PO_4 \cdot H_2O$, 3.8 mM Na_2HPO_4, and 27 mM $NaHCO_3$, 20 mM HEPES
SILAC RPMI *modi*	SILAC RPMI 1640 Flex Medium (Life Technologies, Darmstadt, Germany), 30.52 mM glucose, 2.05 mM glutamine, 0.65 mM uracil, 0.27 mM adenine, 1.1 mM glycine, 0.24 mM choline chloride, 1.7 mM $NaH_2PO_4 \cdot H_2O$, 3.8 mM Na_2HPO_4, and 27 mM $NaHCO_3$, 20 mM HEPES, 11.11 mM glucose, heavy labeled arginine (Arg-10:HCl, 200 mg/l), lysine (Lys-8:HCl, 40 mg/l)

5.4. ELECTRON MICROSCOPIC ANALYSIS

The morphology of the non-encapsulated D39 strain (WT), the isogenic kinase (Δ*stkP*) and phosphatase mutants (Δ*phpP*) was analyzed by field emission scanning and transmission electron microscopy (FESEM, TEM). After cultivation and fixation of pneumococci, the samples were sent to Prof. Dr. Manfred Rohde (HZI Braunschweig) for further processing and analysis by FESEM. Therefore, pneumococci were grown until exponential phase in RPMI *modi* medium or rather in THY medium and fixed with 5% formaldehyde (v/v) and 2% glutaraldehyde (v/v) in growth medium and kept at 7 °C.

5.4.1. FIELD EMISSION SCANNING ELECTRON MICROSCOPY (FESEM)

The fixed samples were washed twice with TE buffer (20 mM tris, 2 mM ethylene-diamine-tetraacetic acid (EDTA), pH 6.9). Bacterial cells were attached onto poly-L-lysine coated cover slips (12 mm in diameter) for 15 minutes, fixed with 1% (v/v) glutaraldehyde in TE buffer, washed twice with TE buffer and dehydrated with an increasing concentration of acetone (10, 30, 50, 70, 90, 100% (v/v)) on ice for 15 minutes each. Samples in 100% acetone were handled at room temperature and transferred one more time to 100% acetone. Afterwards, samples were subjected

to critical-point drying with liquid CO_2 (CPD 030, Bal-Tec). Dried samples were mounted with carbon adhesive tape onto aluminium stubs and coated with an approximately 8 nm thick gold-palladium film by sputter coating (SCD 500 Bal-Tec) before examination in a field emission scanning electron microscope (Zeiss Merlin) using the Everhart-Thornley SE-detector alone or coupled to the Inlens SE-detector in a 75:25 ratio at an acceleration voltage of 5 kV.

5.4.2. EMBEDDING IN LRWHITE RESIN AND TRANSMISSION ELECTRON MICROSCOPY (TEM)

Fixed bacteria were centrifuged and the resulting cell sediment was mixed with an equal volume of 1.75% (w/v) water agar. After solidification the agar was cut into small cubes and dehydrated with an increasing concentration of ethanol in 30 minutes (10, 30, 50% (v/v)) steps on ice. Samples were incubated in 70% ethanol with 2% uranyl acetate overnight. Samples were dehydrated with 90% and 100% ethanol. This step was repeated twice before the samples were infiltrated with one part 100% ethanol and one part LRWhite resin (London resin Company) overnight. Next, samples were infiltrated with one part 100% ethanol and two parts LRWhite resin for 24 hours and subsequently infiltrated with pure LRWhite resin with two exchanges over two days. Then 1 µl starter was added to 10 ml LRWhite resin, stirred and resin was transferred into 0.5 ml gelatin capsules. After polymerization for four days at 50 °C, ultrathin sections were cut with a diamond knife. Sections were counter-stained with 4% aqueous uranyl acetate (w/v) for one minute. Samples were imaged using a Zeiss TEM 910 transmission electron microscope at an acceleration voltage of 80 kV at calibrated magnifications. Images were recorded digitally at calibrated magnifications with a Slow-Scan CCD-Camera (ProScan, 1024 x 1024) with ITEM-Software (Olympus Soft Imaging Solutions).

5.5. SAMPLE PREPARATION FOR GLOBAL IDENTIFICATION AND LABEL-FREE QUANTIFICATION USING GELC-MS/MS

To address the global impact and physiological relevance of StkP and PhpP the WT, Δ*stkP*, Δ*phpP* a qualitative and quantitative global proteome analysis using one-dimensional sodium dodecyl sulfate-polyacrylamide gel electrophoresis followed by liquid chromatography-tandem mass spectrometry (GeLC-MS/MS) was performed.

5.5.1. CELL HARVEST AND CELL DISRUPTION

For classical proteome analysis applying a label-free quantification strategy, pneumococci grown in THY medium were harvested in the exponential growth phase at $OD_{600\,nm}$ 0.4 - 0.45 and in the stationary growth phase at $OD_{600\,nm}$ 2.1 - 2.5. Bacteria grown in RPMI *modi* medium were

harvested in the exponential growth phase at $OD_{600\,nm}$ 0.3 - 0.35 and two hours after reaching the stationary growth phase at $OD_{600\,nm}$ 0.75 - 1.1. Pneumococci were harvested by centrifugation (4,500 x g, 10 min, 4 °C) and washed three times with ice cold 1x PBS supplemented with 1% (w/v) choline chloride and 1x cOmplete protease inhibitor cocktail according to the manufacturer's protocol. The bacterial sediments were suspended in 750 µl Tris-EDTA buffer. Bacterial cell disruption was performed by bead beating with a Precellys homogenizer (6,000 rpm, 9 x 30 sec, 4 °C). Glass beads and cell debris were removed by subsequent centrifugation steps (5,000 x g, 15 min, 4 °C; 10,000 x g, 45 min, 4 °C).

Table 5-6: Buffers and substances used for cell harvest and cell disruption

Buffer/substance	Composition/source	Resolvent
1× PBS (phosphate buffered saline)	137 mM NaCl, 2.7 mM KCl, 80 mM Na_2HPO_4, 1.8 mM KH_2PO_4, pH 7.4	*A. dest*
cOmplete™, EDTA-free Protease Inhibitor Cocktail	F. Hoffmann-La Roche AG, Basel, Switzerland	PBS
Tris-EDTA	50 mM tris-HCl, 10 mM EDTA, pH 7.4	*A. dest*

5.5.2. DETERMINATION OF PROTEIN CONCENTRATION

The determination of protein concentrations was carried out with the Bradford assay (Bradford 1976) using Roti-Nanoquant according to the manufacturer's protocol. In brief, an appropriate sample volume was filled up to 200 µl with *Aq. dest* and mixed in a cuvette with 800 µl 1x Roti-Nanoquant solution. The absorbance of the samples was measured after an incubation time of 5 minutes at 590 nm and 450 nm against *Aq. dest*. The BSA calibration curve with known protein concentration (1 – 40 µg/µl) was measured in parallel. By means of the calibration curve the protein concentration of the samples could be ascertained using the quotient of the sample values measured at 590 nm and 450 nm. All measurements were conducted in triplicates and samples were diluted appropriately to fit into the range of the standard curve.

5.5.3. SDS-POLYACRYLAMIDE GEL ELECTROPHORESIS

The sodium dodecyl sulfate polyacrylamide gel electrophoresis (SDS-PAGE) (Laemmli 1970) is used to separate proteins according to their molecular weights. In this study the electrophoresis was performed using the Criterion™ (BioRad) system with 4 – 20 % gradient TGX™ precast separation gel (BioRad).

Table 5-7: Solutions, substances and buffers used for SDS-PAGE

Solution/substance/buffer	Composition/source	Resolvent
2× Laemmli sample buffer	100 mM Tris-HCl, 4% SDS, 20% glycerine, 4% 2- mercaptoethanol, 0.05% bromophenol blue, pH 6.8	*A. dest*
10x SDS running buffer	0.23 M Tris, 1.92 M glycine, 1% SDS	*A. dest*
Fixing solution	40% ethanol, 10% acetic acid	*A. dest*
Coomassie stock solution	5% Coomassie Brilliant Blue G-20	*A. dest*
Colloidal Coomassie stock solution	2% Coomassie Brilliant Blue dye stock solution, 10% ammonium sulphate, 1.2% phosphoric acid (75%)	*A. dest*
Colloidal Coomassie stain	80% Colloidal Coomassie stock solution, 20% methanol	

Samples in 30 µl 2x Laemmli sample buffer were loaded into the gel wells. Loaded gels were placed into the electrophoresis cell, which was filled up with 1x SDS running buffer. Electrophoresis was performed at constant voltage of 150 V for approximately 1 hour at room temperature. After electrophoresis, proteins were fixed in 25 ml fixing solution for at least 30 min. All incubation steps took place on an orbital shaker. After removing the fixing solution, gels were washed in *Aq. dest* and dyed with 25 ml colloidal Coomassie stain overnight. Gels were then washed with *Aq. dest* to reduce background color. The gel was documented using a scanner and stored until further processing at 4 °C.

5.5.4. *IN-GEL* PROTEIN DIGESTION

Table 5-8: Solutions used for *in-gel* protein digestion

Solution	Composition/source	Resolvent
Washing solution	200 mM ammonium bicarbonite, 30% acetonitrile (HPLC grade)	
Trypsin	2 ng/µl Sequencing Grade Modified Trypsin	ASTM type1 water

For the qualitative and quantitative analysis of the pneumococcal proteome, samples were fractionated by electrophoresis as described above. The resulting gel lanes were subdevided into 10 pieces. The protein bands were cut using a scalpel into approximately 2 x 2 mm pieces and transferred into low protein binding tubes (Bonn et al. 2014). Gel pieces in tubes were washed at least three times with 700 µl of the washing solution at 37 °C for 15 min with shaking (1100 rpm) to remove salt and non-proteinogenous contaminants. After the last washing step, the solution was

discarded and the gel pieces were dried in a vacuum centrifuge at 30 °C. The dried gel pieces were rehydrated with an aqueous solution of trypsin and incubated for 15 min at room temperature. Then, any excess of trypsin solution was removed and the gel pieces in tubes were incubated overnight at 37 °C, placing the reaction tubes upside down. Afterwards, the resulting peptides were eluted in ASTM type1 water (approximately 20 µl) and therefore incubated in an ultrasonic bath for 15 min. Tubes were centrifuged for 30 sec at 10000 x g and the supernatant containing the peptides was transferred into MS sample vials with glass inserts. To assure equal sample volumes, the peptide mixture was dried in a vacuum centrifuge and then resolved in 10 µl water with 0.1% acetic acid (LC-MS grade). The samples were stored at -80 °C until LC-MS/MS measurement.

5.6. SAMPLE PREPARATION FOR PHOSPHOPROTEOME ANALYSIS

5.6.1. CELL HARVEST AND CELL DISRUPTION

Table 5-9: Buffers and solutions used for cell harvest and cell disruption

Buffer/solution	Composition/source	Resolvent
1× PBS (phosphate buffered saline)	137 mM NaCl, 2.7 mM KCl, 80 mM Na_2HPO_4, 1.8 mM KH_2PO_4, pH 7.4	*A. dest*
cOmplete™, EDTA-free Protease Inhibitor Cocktail	F. Hoffmann-La Roche AG, Basel, Switzerland	PBS
Tris-HCl buffer	50 mM tris-HCl, pH 7.4	*A. dest*
Phosphatase inhibitors	10 mM sodium fluoride, 5 mM sodium vanadate, 5 mM glycerol pyrophosphate, 5 mM sodium pyrophosphate	Tris-HCl
Nuclease mix	Nuclease mix, GE Healthcare, Freiburg, Germany	
Octyl β-d-glucopyranoside	Octyl β-d-glucopyranoside, Sigma Aldrich Chemie GmbH, Steinheim, Germany	

For phosphoproteome experiments, pneumococci were harvested at mid-exponential growth phase by centrifugation as described in 5.5.1. and washed three times with ice cold PBS, pH 7.4 containing 0.1% choline chloride and a protease inhibitor cocktail. Harvested bacteria were resuspended in 50 mM tris-HCl buffer, pH 7.4, supplemented with phosphatase inhibitors and disrupted as described for the GeLC-MS/MS proteome samples. Afterwards, the suspension was treated with 1 × Nuclease Mix for 20 min at RT and with 1% Octyl β-d-glucopyranoside before cell debris and glass beads were removed by two centrifugation steps (5,000 x g, 15 min, 4 °C; 10,000 x g, 45 min, 4 °C).

5.6.2. DETERMINATION OF PROTEIN CONCENTRATION AND PROTEIN PRECIPITATION

The protein concentration was determined as described in 5.5.2. to ensure the precipitation of 50 mg protein for each sample for the classical phospho-analysis protocol and 5 mg for the modified SCX-free workflow. To remove interfering agents such as lipids, nucleic acids from the protein samples an acetone precipitation or a methanol/chloroform precipitation was performed.

For the acetone precipitation protein samples were transferred into new tubes and six volumes of pre-chilled (-20 °C) acetone were added. The protein-acetone mixture was mixed thoroughly and frozen at -20 °C. The precipitation was proceeded for at least 8 hours up to overnight. After precipitation the samples were centrifuged for 30 min with 13000 x g at 4 °C. The tubes were inverted carefully to decant the acetone without disturbing the protein pellet. For drying, the pellet was left for 15 - 20 min under the clean bench.

For the methanol/chloroform precipitation, the samples were mixed with four volumes of methanol and briefly mixed using a vortexer. Then 1 volume of chloroform was added and the samples were briefly mixed by vortexing. Afterwards, the samples were mixed with three volumes of ASTM type 1 water and centrifuged for 5 min at 1000 x g. The aqueous phase was discarded and the samples were mixed with four volumes of methanol and again centrifuged for 5 min at 1000 x g. The methanol was removed and the precipitated proteins were dried for approximately 25 - 30 min.

5.6.3. *IN-SOLUTION* DIGESTION OF PROTEINS

Table 5-10: Buffers and solutions used for *in-solution* digestion of proteins

Buffer/solution	Composition/concentration	Resolvent
Tris-HCl	10 mM tris-HCl, pH 8.0	
Ammoniumbicarbonate	50 mM NH_4HCO_3	ASTM type 1 water
1,4-Dithiothreitol (DTT)	1 M DTT	ASTM type 1 water
Iodoacetamide (IAA)	550 mM IAA, 50 mM ammoniumbicarbonate	
Denaturation buffer	6 M Urea/ 2 M Thiourea, 10 mM Tris-HCl, pH 8.0	
Reduction buffer	1M DTT, 50 mM ammoniumbicarbonate	
Alkylation byffer	550 mM IAA, 50 mM ammoniumbicarbonate	
LysC	2 ng/µl Lysyl Endopeptidase, Mass Spectrometry Grade	ASTM type 1 water
Trypsin	1 ng/µl Sequencing Grade Modified Trypsin	ASTM type 1 water

The precipitated protein pellets were dissolved in as low volume of denaturation buffer as possible (5 mg protein in 100 µl buffer; 50 mg protein in 1 ml buffer). In the next step reduction buffer was added to final concentration of 1 mM DTT and the samples were incubated at room temperature for one hour shaking in the dark. Afterwards, the samples were mixed with alkylation buffer to a final concentration of 5.5 mM IAA and incubated one hour at room temperature shaking in the dark. During these steps the pH was checked and if necessary adjusted to 8.0 with 1M NaOH or 1M HCl. Per 100 µg protein 1 µg endoproteinase LysC was added and the protein samples were digested for 6 hours at room temperature on a shaker. For the tryptic digestion the samples were diluted with four volumes of ASTM type 1 water and the pH was adjusted again before 1 µg trypsin per 100 µg protein was added. The digestion was performed overnight at room temperature on a shaker.

5.6.4. SCX PRE-FRACTIONATION OF PHOSPHOPROTEOME SAMPLES

Table 5-11: Solutions used for SCX pre-fractionation

Solution	Composition/source	Resolvent
SCX solvent A	5 mM potassium dihydrogen phosphate, 30% acetonitrile, pH 2.7	*A. dest*
SCX solvent B	5 mM potassium dihydrogen phosphate, 30% acetonitrile, 350 mM potassium chloride, pH 2.7	*A. dest*

For the classical analysis of phosphorylated peptides, 50 mg protein were prepared for phosphopeptide enrichment by using strong cation exchange (SCX) chromatography and titanium dioxide beads according to Olsen and Macek (2009) (Olsen and Macek 2009). The digested protein mixture was acidified to pH 2.7 with trifluoroacetic acid, incubated 15 min at room temperature and centrifuged (15 min, 1000 x g) to remove any precipitate that might be formed. The supernatant was load onto an equilibrated 1 ml SCX column in SCX solvent A at a flow rate of 1 ml/min. The flow-through was collected. The bound peptides were eluted with a linear gradient of 0 - 30% of SCX solvent B in 30 min at a flow rate of 1 ml/min. 2 ml fractions were collected. After the sample run, the SCX column was washed with five column volumes of 100% SCX solvent B.

5.6.5. ENRICHMENT OF PHOSPHOPEPTIDES WITH TITANIUM DIOXIDE BEADS

The classical workflow for the phosphoproteome analysis includes a sample fractionation with strong cation exchange (SCX) chromatography, which requires an amount of 50 mg protein per sample. To decrease the amount of necessary cell material, a modified protocol without an SCX prefractionation was applied.

Table 5-12: Solutions and substances used for phosphor-peptide enrichment with titanium dioxide beads

Solution/substances	Composition/source	Resolvent
Titanspere beads (TiO)	Titansphere beads (Titanium dioxide) 10 µm, GL Sciences	Loading solution
Loading solution	30 mg/ml 2,5 dihydrobenzoic acid (DHB), 80% acetonitrile in ASTM type 1 water	
Washing solution I	30% acetonitrile, 3% trifluoroacetic acid, in ASTM type 1 water	
Washing solution II	80% acetonitrile, 0.1% trifluoroacetic acid, in ASTM type 1 water	
Elution solution	40% of ammonium hydroxide solution (aq. NH_3 (25%)) in 60% acetonitrile, pH > 10.5	
Solution A	1% acetonitrile, 0.5% trifluoroacetic acid	ASTM type 1 water

For the classical phosphopeptide enrichment approach (Olsen and Macek 2009), resulting SCX fractions with low peptide amounts were pooled. Each sample, including the flow-through, was incubated with TiO beads separately (5 mg TiO beads per sample). The beads were resuspended in a required volume of loading solution (50 µl per 5 mg beads) and incubated 10 min at room temperature, shaking. Aliquots containing 5 mg of TiO beads slurry were added to each sample. After an incubation time of 30 min in an orbital shaker in the dark at room temperature, the samples were centrifuged (10000 x g) and the supernatant was discarded. The beads were washed with 1 ml Washing solution I for 10 min in the shaker and centrifuged 2 min (10000 x g). The supernatant was removed and the beads were washed 10 min with Wash solution II followed by 2 min centrifugation with 10000 x g and the removal of the supernatant. The beads were resuspended in 50 µl Washing solution II and the slurry was transferred to prepared C_8 mircocolumns (3 x 1 mm^2 pieces of Empore C_8 material were placed into a 200 µl pipette tip) and centrifuged with 1000 x g. The flowthrough was discarded. Each sample was eluted three times with 100 µl of Elution solution with maximum 1000 x g. Finally, the eluates were dried in the vacuum centrifuge to 5 µl and acidified with Solution A.

In case of the modified, SCX free workflow, the digested protein mixture was acidified to pH 2.7 with trifluoroacetic acid, incubated 15 min at room temperature and centrifuged (15 min, 1000 x g) to remove any precipitate that might be formed. The supernatant was repetitively incubated with TiO beads to collect nine enrichment fractions. Therefore, beads were suspended in a required volume (50 µl per 5 mg beads) of loading solution and incubated for 10 min at room temperature

in an orbital shaker in the dark. Afterwards, TiO beads were added to each sample. Following bead to peptide ratios were used for the enrichment:

5 mg TiO_2 beads/1 mg protein → **fraction 1**

3 mg TiO_2 beads/1 mg protein → **fraction 2**

1 mg TiO_2 beads/1 mg protein → **fraction 3**

This procedure was repeated twice. After incubation for 15 min in an orbital shaker (in the dark, room temperature), the samples were centrifuged (10,000 x g, 2 min, room temperature) and the supernatant was discarded. The beads were washed twice with each Washing solution and eluted three times using C_8-microcolumns as described above.

5.7. MASS SPECTROMETRIC ANALYSIS

All proteomic samples were analyzed by reversed phase liquid chromatography (LC) electrospray ionization (ESI) MS/MS using an LTQ Orbitrap Velos (Thermo Fisher Scientific). In-house self-packed nano-LC columns (100 µm x 20 cm) containing reverse-phase C_{18} material (3.6 µm, Aeris, phenomenex) were used to perform LC with an Easy-nLC1000 system (Thermo Fisher Scientific). The peptides were loaded with solvent A (0.1% acetic acid (v/v)). Subsequently, the peptides were eluted by a non-linear binary gradient of 80 minutes from 5% to 99% solvent B (0.1% acetic acid (v/v), 99.9% ACN (v/v)) in solvent A at a constant flow rate of 300 nl/min. After injection of non-enriched proteomic samples into the mass spectrometer, a full scan was recorded in the Orbitrap (m/z 300 - 1,700) with a resolution of 30,000 at 400 m/z. The twenty most abundant precursor ions were consecutively isolated in the linear ion trap and fragmented via collision-induced dissociation (CID). Unassigned charge states as well as singly charged ions were rejected and the lock mass correction was enabled. Selected ions were fragmented with 35% normalized collision energy (NCE) and analyzed in data-dependent MS/MS in the linear trap quadrupole (LTQ).
During the measurement of the phosphopeptide-enriched samples a full scan with a resolution of 60,000 at 400 m/z was recorded in the Orbitrap (m/z 300 - 2,000). The twenty most abundant precursor ions were fragmented via CID and recorded in the LTQ analyzer. Lock mass correction, wideband activation and multistage activation at -97.98, -48.99, -32.70 and -24.49 Th were enabled.

5.8. DATABASE SEARCH AND LABEL-FREE QUANTIFICATION

For classical database search, spectra were searched separately for each strain with MaxQuant (1.6.1.0, Max Planck Institute of Biochemistry, (Cox and Mann 2008)) and its implemented search engine Andromeda (Cox et al. 2011) against the *S. pneumoniae* D39 database from UniProt (2017)

containing 1,918 proteins. Parameters for precursor mass deviation were set to 4.5 ppm and 0.5 Da for fragment mass tolerance. A false discovery rate (FDR) of 0.01 on protein, peptide and spectra level was applied as well as a minimum peptide length of seven amino acids and two unique peptides per protein. Full tryptic specificity with a maximum of two missed cleavage sites was applied. Variable modifications were oxidation on methionine (M) and N-terminal acetylation (Protein N-term). The label-free quantification option LFQ was activated (min. ratio count set to two) as well as the option "match between runs" for the biological replicates of each strain. Furthermore, MaxQuant's generic contamination list was included.

For shot gun proteomic data analyses the software Perseus 1.6.1.1 (Tyanova et al. 2016) was used. The data from MaxQuant output files were filtered for contaminations, reverse and only identified by site hits (Supplementary material - Electronic appendix: Perseus). The quantification of comparative proteome analysis of D39Δ*cps* wild-type and mutants was based on MaxQuant's LFQ intensities (Cox et al. 2014). Proteins were considered for quantification if an LFQ value was present in all three biological replicates of each strain. Data were normalized over the median in Microsoft Excel. Statistical evaluation of quantified proteins was performed using RStudio (version 3.5.0) and the SAM (Significance analysis of microarrays (Tusher et al. 2001)) script by Michael Seo (https://github.com/MikeJSeo/SAM) with the implemented two-class unpaired test, which is analogous to a t-test between subjects. The input data tables can be found in the Supplementary material - Electronic appendix: SAM. Differentially expressed proteins with a minimum fold change of two and a q-value ≤ 0.01 were considered as significantly regulated. The results were visualized in Voronoi tree maps (Bernhardt et al. 2013) using the software Paver 2.0 (DECODON) as previously described in Hoyer *et al.* 2018 (Hoyer et al. 2018).

5.9. CONSTRUCTION OF A SPECTRAL LIBRARY AND SPECTRAL LIBRARY SEARCH FOR PHOSPHOPROTEOMICS

For generation of the combined spectral library 908 .raw files of *S. pneumoniae* samples available from a defined set of experiments were considered (Supplementary material - Electronic appendix: - Overview of data sets and raw files). First, all samples were searched against the *S. pneumoniae* D39 database from UniProt (1,918 proteins, 2017) with Sorcerer – SEQUEST 4.0.4 (SageN). For the respective parameter files, precursor mass tolerance was set to 10 ppm and fragment mass tolerance was set to 1.0005 Da (CID). Full tryptic specificity with a maximum of two missed cleavage sites was considered as well as variable modifications like oxidation on methionine, carbamidomethylation on cysteine and phosphorylation on serine (S), threonine (T) and tyrosine (Y). For SILAC samples an additional search with static modifications on lysine (Lys $C_{13}N_{15}$ (K), 8.014199 amu) and arginine (Arg $C_{13}N_{15}$ (R), 10.008269 amu) was done. For further processing of

the MS/MS data in .mzXML and .pep.XML format from the Sorcerer output the Trans Proteomic Pipeline (TPP, 5.1.0-rc1 Sysygy, 2017) was applied.

Spectral library creation was performed according to Schubert *et al.* (2015) (Schubert et al. 2015) with slight modifications. Briefly, spectra and their particular identifications retrieved from all files were linked together and entries from all datasets were combined to interact.pep.XML files (InteractParser) (Figure 5-1A). Afterwards, the PeptideProphet algorithm was applied to calculate the false discovery rate (FDR) of the merged searches on peptide level.

The following settings were used:

- ➔ minimum peptide sequence length: seven amino acids
- ➔ use accurate mass binning, using: ppm
- ➔ use decoy hits to pin down the negative distribution
- ➔ ignore charge states: 1^+ and higher than 4^+.

Then spectra containing no phosphorylated amino acids were imported to build a raw spectral library if they had a calculated probability of at least 0.99. In parallel a raw library containing spectra with S/T/Y phosphorylated amino acids and with a probability of at least 0.95 was built. Within this step, spectra assigned to the same peptide ion identification were merged and a single, representative "consensus" spectrum for a particular "peptide species" was generated. Consensus spectra of phosphorylated peptides were then subjected to manual validation and only spectra conformed five out of six quality criteria were considered for the library.

Following filter criteria were used for manual review of spectra:

1. Identified fragments should not be within clusters of masses.
2. No more than three dominating unassigned peaks (u) should be in a spectrum.
3. Fragment intensities should be sufficiently above the signal to noise threshold (S/N).
4. Peptide fragments should be detected with and without phosphorylation ($-PO_3$).
5. At least three fragments should be detected post-phosphosite.
6. The phosphosite itself (Ph) should be identified within a spectrum.

The illustration in Figure 5-1B exemplifies the listed filter criteria for manual validation. The whole procedure of data processing and validation was repeated to build two raw libraries with the spectra of the SILAC samples which contain the heavy labeled amino acids lysine and arginine. Overall, four raw libraries were built: 1^{st}: including non-phosphorylated spectra; 2^{nd}: including non-phosphorylated spectra of SILAC samples; 3^{rd}: including phosphorylated spectra; 4^{th}: including phosphorylated spectra of SILAC samples. Afterwards, the four raw libraries were combined and filtered for contaminations and reverse hits. The final spectral library for phosphorylation-centered searches was then extended with the same number of spectra as decoy

hits generated by a random mass shift of the precursor and shuffling the peptide sequence (Yen et al. 2011). Finally, phospho-enriched samples of D39Δ*cps*, D39Δ*cps*Δ*stkP* and D39Δ*cps*Δ*phpP* were searched against the combined spectral library using SpectraST (Supplementary material - Electronic appendix: Spectral library *S. pneumoniae* D39) Search results were combined to interact.pep.xml files and filtered for probability of at least 0.95.

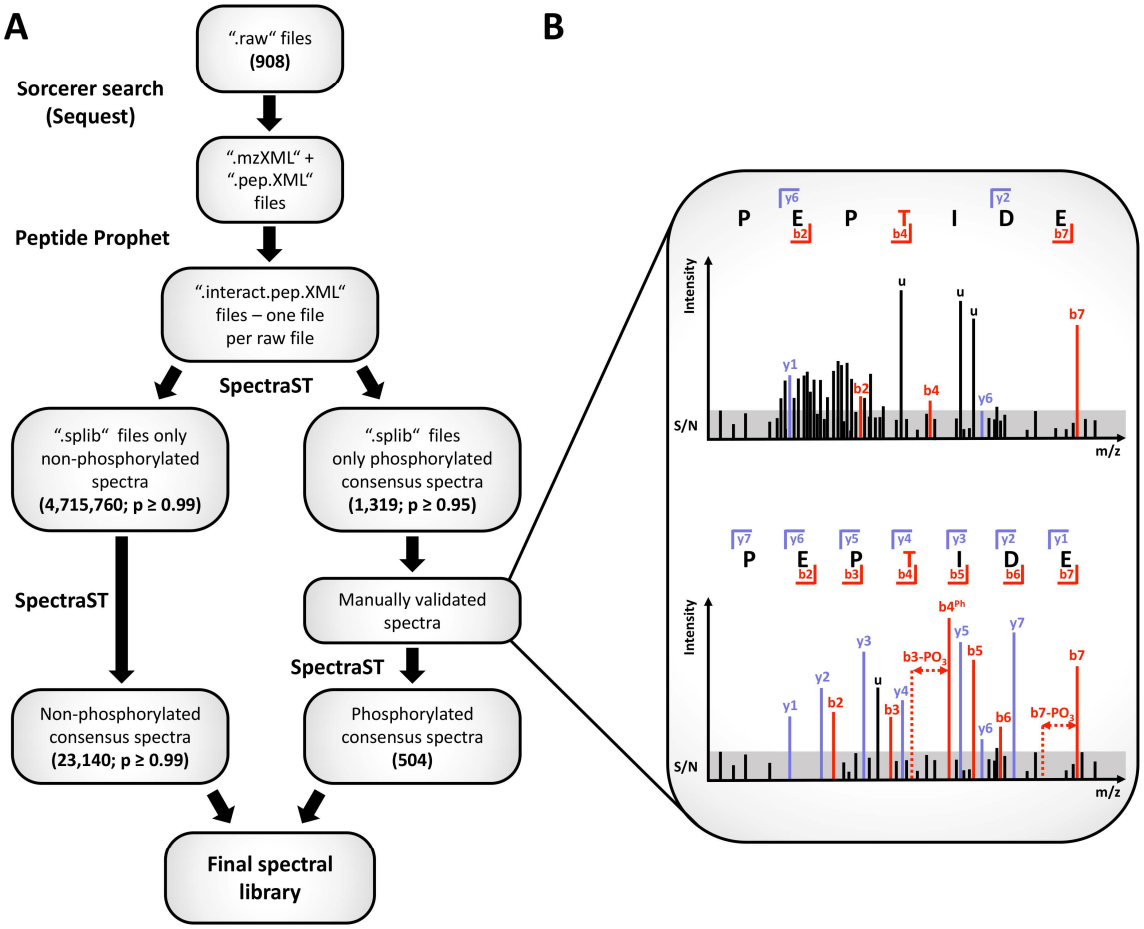

Figure 5-1: Workflow for spectral library creation (Hirschfeld et al. 2019). The particular data-processing steps of the spectral library generation are depicted in part A of the figure. All spectra belonging to the phospho-library were validated manually. Illustration B represents a discarded (upper spectrum) and a kept spectrum (lower spectrum) according to the applied filter criteria. For unambiguous spectrum identification, five of the six listed criteria had to be fulfilled (see main text). In the upper spectrum, peak clusters, unassigned peaks (u) as well as identified peaks not sufficient above or even below the signal to noise ratio (S/N) are visible (b4, y6). Additionally, no fragment ion series, no fragments with neutral losses or the phosphorylation site are assigned. In contrast to that, the lower spectrum displays a complete fragment ion series, identification of the fragment including the phosphorylation site and fragments with a neutral loss of phosphoric acid. Further, the signals of assigned fragment peaks are above the S/N range as well as only a limited number of unassigned peaks is visible.

6. RESULTS

6.1. GROWTH BEHAVIOR ANALYSIS OF *S. PNEUMONIAE* WT, KINASE AND PHOSPHATASE MUTANT

Eukaryotic-type kinases have been implicated in regulating cell division, correct septum progression and closure and thus bacterial growth in the pneumococcus and other pathogens (Fleurie et al. 2014b; Beilharz et al. 2012; Agarwal et al. 2011; Beltramini et al. 2009). As bacterial cell growth and division are closely linked, the strains were characterized by growth in the rich THY medium and modified chemically defined RPMI 1640 medium (RPMI *modi*).

Comparing the growth behavior of the WT and the mutant strains in THY medium, there are no significant differences visible (Figure 6-1). After a liquid pre-culture pneumococci grew immediately in exponential phase directly after inoculation of pre-warmed THY medium omitting a lag-phase in the main culture. Growth curves of all strains in THY medium were monitored for 360 minutes measuring the absorbance at 600 nm at different time points. The final OD_{600} was reached after 180 - 200 minutes in all strains. The WT strain grew to an OD_{600} of 2.514 ± 0.03, Δ*stkP* reached a maximal OD_{600} of 2.283 ± 0.06 and Δ*phpP* grew to an OD_{600} of 2.335 ± 0.09. Moreover, the growth of the different biological replicates was quite similar.

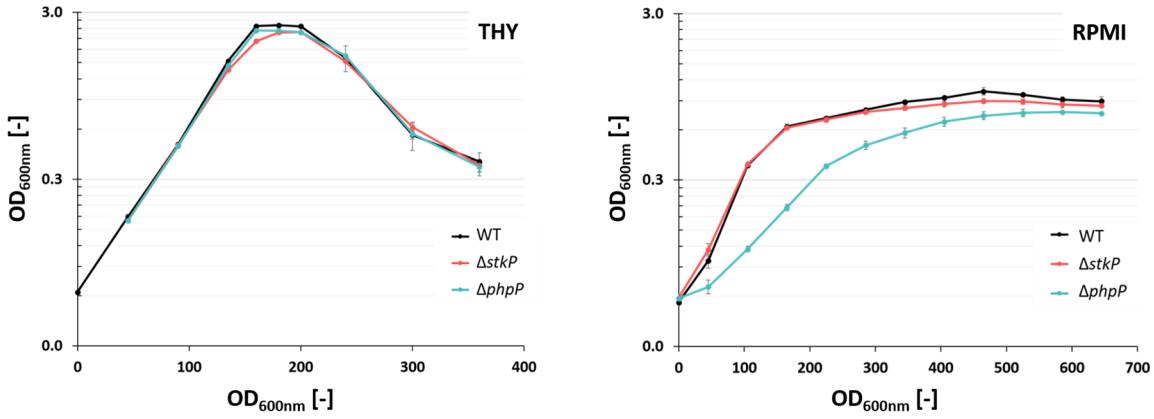

Figure 6-1: Growth of *S. pneumoniae* in THY and RPM *modi* medium after a liquid preculture. The growth analysis was always performed in the same manner, but every cultivation was prepared independent of each other. Three independent biological replicates for each strain were cultivated.

For the growth analysis of pneumococci in the chemically defined RPMI *modi* medium, the cultivation was prepared identical to the cultivation in THY medium. In the main culture pneumococci started growing in pre-warmed RPMI *modi* medium without a lag-phase. In general, growth curves of all strains showed a delayed growth in RPMI *modi* medium in comparison to the

complex THY medium. Therefore, the growth of pneumococci grown in RPMI *modi* medium was monitored over 645 minutes measuring the absorbance at 600 nm at different time points. Furthermore, pneumococci cultured in RPMI *modi* medium showed a later achievement of the stationary phase and a lower final optical density. Additionally, pneumococci grown in RPMI *modi* medium had a stable stationary phase for more than three hours, whereas pneumococci grown in THY medium immediately start to lyse after reaching the final optical density. However, growth of WT and Δ*stkP* was almost comparable in RPMI *modi* medium, whereas Δ*phpP* showed diminished growth in comparison to the WT and the kinase mutant and reached a lower final optical density. In the early exponential phase, the kinase mutant grew slightly faster than the WT. n the end, the WT strain grew to a final OD_{600} of 1.022 ± 0.05, Δ*stkP* reached a maximal OD_{600} of 0.894 ± 0.03 and Δ*phpP* grew to an OD_{600} of 0.768 ± 0.02.
All in all, the growth analysis of the pneumococcal WT, the kinase and the phosphatase mutant revealed a dissimilar growth behavior of the strains in the different cultivation media.

6.2. MORPHOLOGICAL CHARACTERIZATION OF *S. PNEUMONIAE* WT, KINASE AND PHOSPHATASE MUTANT BY ELECTRON MICROSCOPY

The analysis of cell morphology and cell division of pneumococci applying field emission scanning electron microscopy (FESEM) and transmission electron microscopy (TEM) revealed different phenotypes of the investigated strains cultivated in RPMI *modi* and THY medium.

The electron microscopic analysis of pneumococci cultivated in the chemically defined RPMI *modi* medium disposed remarkable differences in chain formation, cell separation and cell division septa morphology between WT, Δ*phpP* and Δ*stkP* (Figure 6-2). While cells of Δ*stkP* were more separated in comparison to the WT and were forming rarely only short chains, pneumococci of Δ*phpP* were forming aggregates. The cells of Δ*stkP* seemed to be perturbed in the progression of the septa during the cell division, often displaying elongated morphologies. The cell morphology of Δ*phpP* was unusual as well. Cell division was highly impaired, most of the pneumococcal cells were forming multiple asymmetric septa and were not properly separated. Furthermore, pictures derived from TEM analysis of Δ*phpP* revealed the DNA (light structure) to be delocalized and widely spread over the cell and not as dense as in WT cells.
Pneumococci grown in THY medium show less severe abnormalities in cell separation and cell shape in comparison to pneumococci grown in RPMI *modi* medium **(**Figure 6-2 and Figure 6-3**)**. Nevertheless, the electron microscopic pictures of pneumococci cultivated in THY medium generated from FESEM analysis show increased chain formation especially in the Δ*phpP* mutant but also in the Δ*stkP* mutant in comparison to the non-encapsulated WT **(**Figure 6-3**)**. Transmission electron microscopy pictures did not display conspicuous features of the pneumococcal cells.

Pneumococci of all strains were intact and not impaired in septum formation and septum progression and cell division. The shape of the pneumococcal cells was not affected as well. Furthermore, the DNA (light structure within the cells) appeared to be dense and it was localized in the center of each coccus displaying no obvious abnormalities.

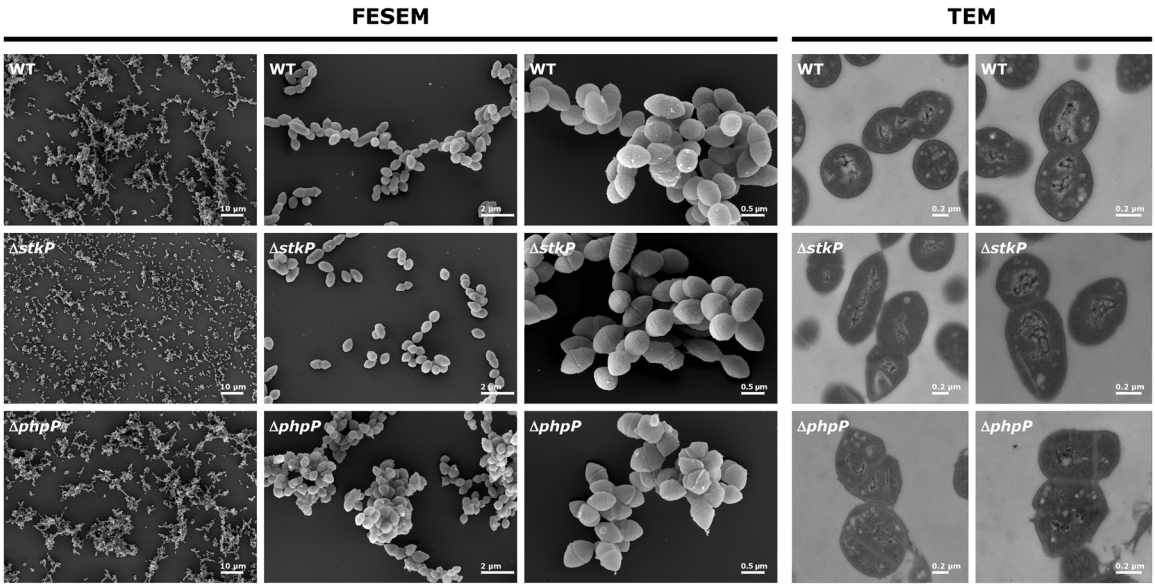

Figure 6-2: Microscopic analysis of WT, Δ*stkP* and Δ*phpP* morphology (Hirschfeld et al. 2019). The morphological characterization of all strains grown in RPMI *modi* medium by field emission scanning electron microscopy (FESEM) and transmission electron microscopy (TEM) pointed out that cell division and cell separation were abnormal in both mutants.

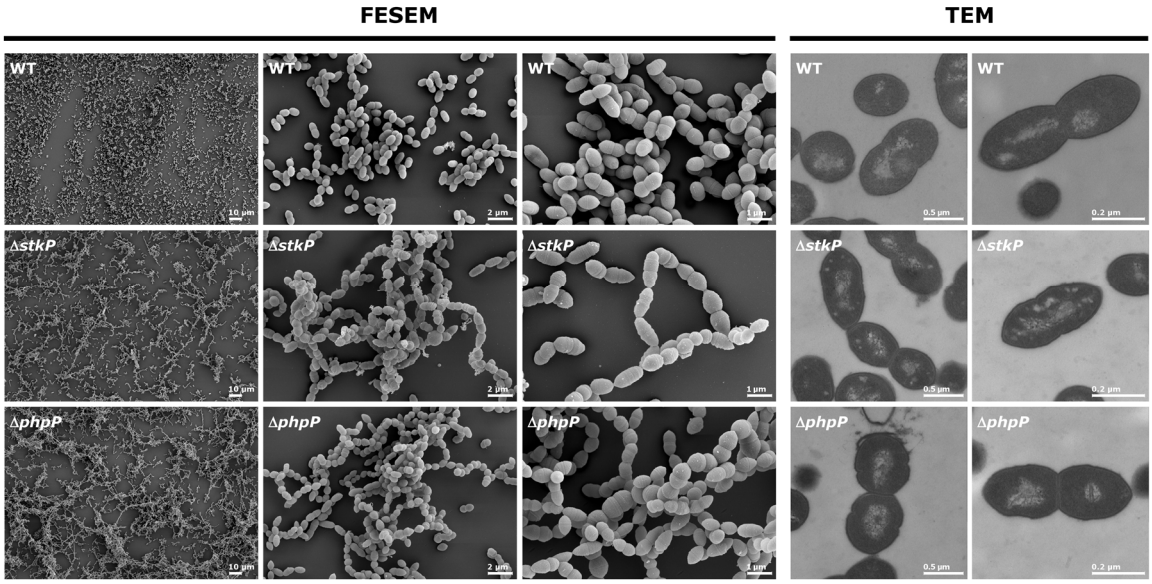

Figure 6-3: Microscopic analysis of WT, Δ*stkP* and Δ*phpP* morphology. The morphological characterization of all strains grown in THY medium by field emission scanning electron microscopy (FESEM) and transmission electron microscopy (TEM) indicated differences in chain formation in both mutants compared to the WT strain.

6.3. GLOBAL PROTEOME ANALYSIS OF WT, KINASE AND PHOSPHATASE MUTANT

In order to determine changes on proteome level in pneumococci deficient for StkP and PhpP, an in-gel digestion coupled with mass spectrometric analysis (GeLC-MS/MS) based qualitative and quantitative analysis was performed. Therefore, bacteria grown in THY medium and in RPMI *modi* medium were harvested in the exponential growth phase and in the stationary growth phase. Nevertheless, pneumococci cultivated in the chemically defined medium RPMI *modi* displayed a long-standing stationary growth phase in comparison to pneumococci grown in THY medium where cell lysis occurred right after reaching the maximal OD **(**Figure 6-1**)**. Since it is known that the outcome of a proteomic study is highly influenced by the sample preparation, it has to be ensured that all biological samples for the same analysis are harvested in the same state or at the same time-point. Otherwise, changes in the protein composition of biological samples might arise, which lead to an increase in the variance between the samples making a comparison less exact and less statistically significant. Due to the different growth behavior of pneumococci in THY and RPMI *modi* medium it was not possible to synchronize the time-points for sample harvest adequately over all experiments for a comparative proteome analysis. However, the approaches conducted in this work aimed at deciphering the influence of StkP and PhpP on cellular physiology through the determination of changes on proteome level in the pneumococcal mutants deficient for StkP or PhpP in comparison to the proteome of the WT strain. Hence, the proteomic investigations were performed separately with pneumococci cultured in two different media (THY and RPMI *modi*) and harvested in different growth phases. Thus, the focus was set on the comparison of each mutant to the WT separately in every condition.

6.3.1. QUALITATIVE PROTEOME ANALYSIS OF Δ*STKP*, Δ*PHPP* AND WT

The overall global proteome analysis executed in this work resulted in the high-confidence detection of 1348 pneumococcal proteins in total, identified with at least two unique peptides in a sample, representing 70 % of the annotated proteome of *S. pneumoniae* strain D39 (1,918 annotated proteins). Still, 570 annotated proteins remained not detected in this study (Figure 6-4). All in all, slightly more proteins were identified in pneumococci grown in RPMI *modi* medium (1,298 proteins) in comparison to the identification numbers of pneumococci cultivated in THY medium (1,250 proteins). Out of the 1,348 identified proteins, 98 proteins were exclusively identified in the strains cultivated in RPMI *modi* medium and 50 proteins were only identified using THY medium for pneumococcal growth. Moreover, there is no notable difference between the WT and the mutant strains comparing the pure protein identification numbers. Also the protein

identification numbers of each strain regarding the time-point of harvest, in this case exponential and stationary growth phase, are quite comparable.

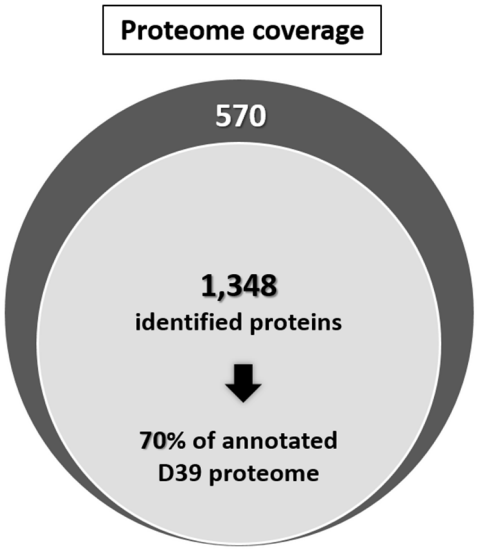

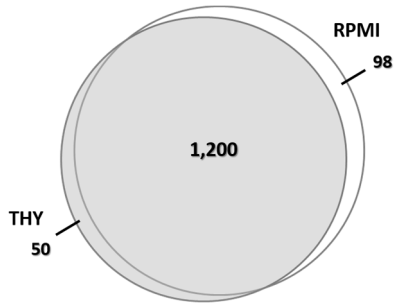

	Exponential phase			Stationary phase		
	WT	Δ*stkP*	Δ*phpP*	WT	Δ*stkP*	Δ*phpP*
RPMI	1,149	1,104	1,156	1,131	1,149	1,136
THY	1,132	1,080	1,174	1,113	1,035	1,154

Figure 6-4: Global identification results. Venn diagrams including identification numbers of pneumococcal proteins identified by LC-MS/MS analysis of samples derived from pneumococci cultivated in THY and RPMI *modi* medium. The corresponding table presents an overview of identification numbers assigned to the investigated pneumococcal strains, the cultivation medium used and the growth phase of bacterial cell harvest.

In order to define the distribution of identified proteins in WT, Δ*phpP* and Δ*stkP* in RPMI *modi* and THY medium as well as in the different growth phases of cell harvest, the overlap of identified proteins and single identifications in certain strains have been visualized in Venn diagrams (Figure 6-5). Under each condition 52 - 54% of the annotated pneumococcal proteins were identified commonly in the WT, the phosphatase and the kinase mutant strain. From samples of pneumococci cultivated in RPMI *modi* medium and harvested in exponential growth phase 1,245 proteins were detected. 83% of these proteins were found in all three strains. 1,231 proteins were detected in the samples of pneumococci harvested in the stationary growth phase. Out of these proteins, 85% were commonly identified in WT, Δ*phpP* and Δ*stkP*.

The distribution of protein identifications of samples derived from pneumococci grown in THY medium was almost comparable. 1,213 proteins were identified out of samples of pneumococci grown until exponential phase. 86% of them were present in all strains. In samples of pneumococci harvested in the stationary growth phase, 1,225 proteins were detected. Shared proteins comprised 81% among WT, Δ*phpP* and Δ*stkP*.

Altogether, the identification results using LC-MS/MS analysis did not display notable identification shifts in the distribution of proteins detected in the WT, the phosphatase mutant and the kinase mutant.

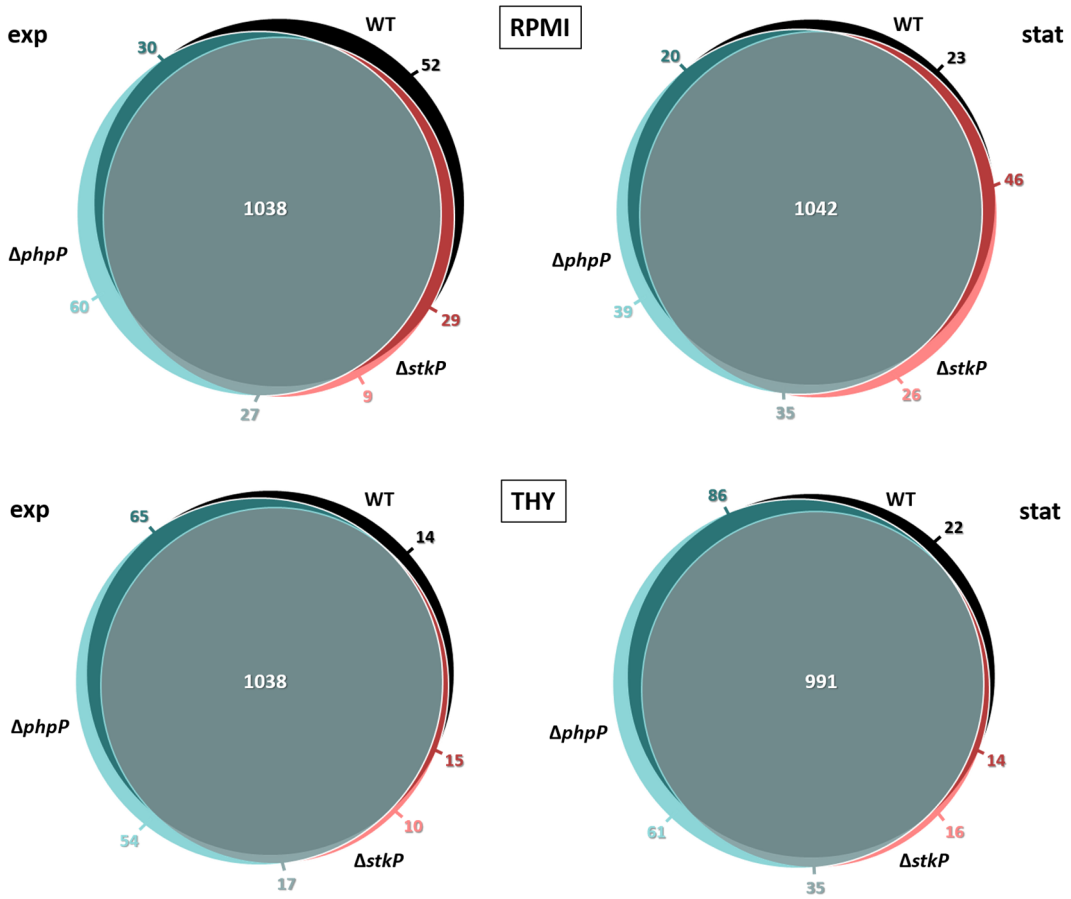

Figure 6-5: Overview of distribution of identified proteins in WT, Δ*phpP* and Δ*stkP*. Venn diagrams present the overlap of identified pneumococcal proteins in the investigated strains. The strain comparisons are arranged due to the different cultivation media and time-points of cell harvest.

6.3.2. Label-free quantitative proteome analysis of Δ*stkP*, Δ*phpP* mutants and WT

For the characterization of the impact of StkP and PhpP on the cellular physiology of pneumococci, a mass-spectrometry based label-free quantitative (LFQ) approach was performed. Thus, changes on proteome level in the mutants Δ*phpP* and Δ*stkP* in comparison to the WT strain were determined. The quantification was based on MaxQuant's LFQ intensities (Cox et al. 2014). Proteins with a calculated LFQ value in all three biological replicates of each strain were considered for quantification.

All in all, the quantification efficiency was in the range of 83-96%. A detailed overview of the protein identification and quantification numbers is given in Figure 6-6.

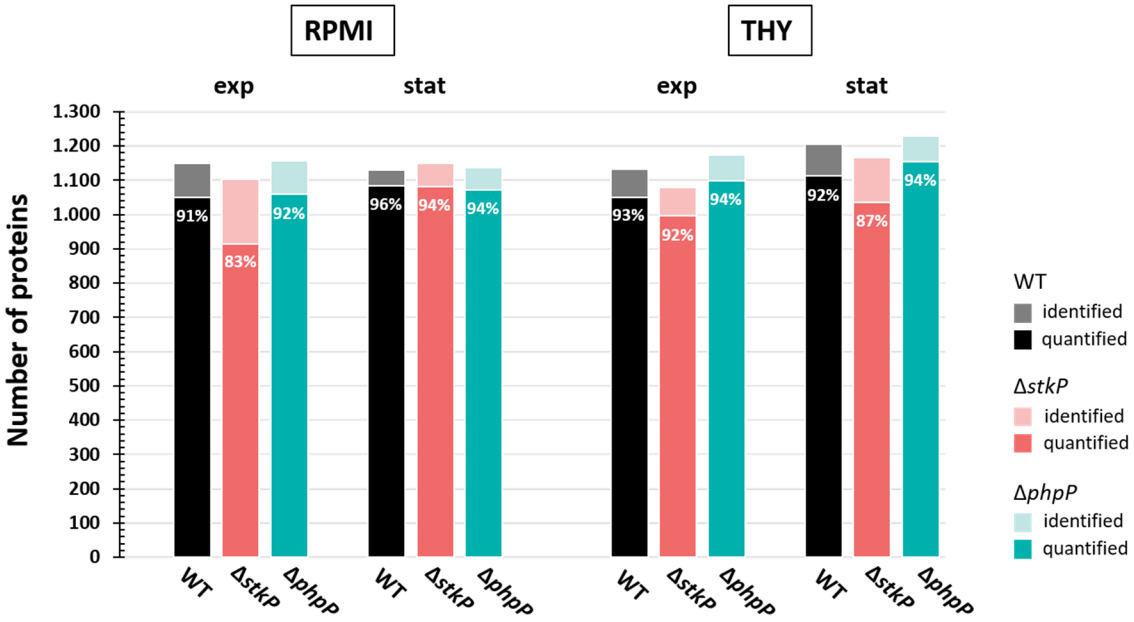

Figure 6-6: Global quantification results in WT, Δ*phpP* and Δ*stkP*. The graphs present the distribution of identified and quantified proteins within the analyzed strains grown in RPMI *modi* and THY medium harvested in exponential and stationary growth phase. The quantification efficiency is labeled within the graphs.

In order to evaluate the quality of the three independently generated biological replicates of the pneumococcal strains under the different growth conditions, a Principal component analysis (PCA) based on the quantitative data was examined (Figure 6-7). The PCA analysis revealed a clear separation of the WT strain and the mutant strains Δ*phpP* and Δ*stkP* on proteome level in each experiment. Clusters are formed by all three biological replicates. Moreover, the LFQ values of

the biological replicates correlate as well under the different conditions ($R^2 \geq 0.94$, Figure 10-1Figure 10-4) proving that the biological replicates are quite reproducible.

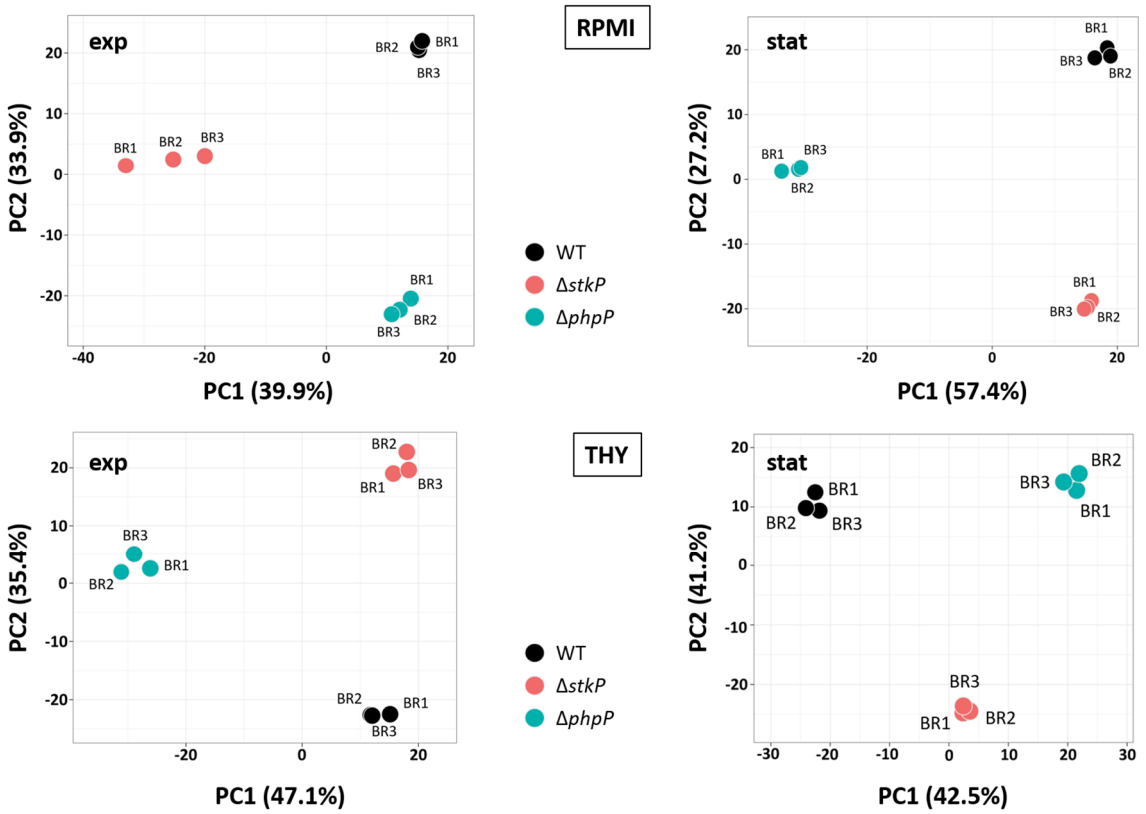

Figure 6-7: Principal component analysis (PCA). PCA plots of quantitative data generated from samples of *S. pneumoniae* strains cultivated in RPMI *modi* and THY medium and harvested in exponential and stationary phase. X and Y axis depict principal component 1 and principal component 2 that explain x% and y% of the total variance, respectively. N = 9 data points.

Within the LFQ analysis the mutants have been compared to the non-encapsulated wild type strain D39Δ*cps*. Differentially abundant proteins with a minimum fold change (FC) of two and a q-value ≤ 0.01 were considered as significantly altered in abundance in the mutants in comparison to the WT. Moreover, the significantly regulated proteins include “On” and “Off” proteins. So called “On” proteins are proteins that were exclusively identified with at least two unique peptides in three out of three biological replicates in the mutant strain but in none of the replicates of the WT strain.

Proteins exclusively identified with at least two unique peptides in three out of three biological replicates in the WT strain but in none of the replicates of the mutant strain are designated as "Off" proteins. For further information regarding the impact of StkP and PhpP on particular biological processes in the pneumococcus, all 1918 predicted proteins of *S. pneumoniae* D39 were classified into functional protein groups according to TIGRFAM (Haft et al. 2001) or KEGG-based

(Kanehisa and Goto 2000) annotation (Supplementary material - Electronic appendix: Annotation table - *Streptococcus pneumoniae* D39).

Altogether there was a higher number of significantly differentially abundant proteins detected in the phosphatase mutant Δ*phpP* in comparison to the kinase mutant Δ*stkP* in the samples derived from the cultivation in RPMI *modi* medium in both growth phases. In samples from pneumococci grown in THY medium and harvested in the exponential phase it was also the case that more changes were observed in Δ*phpP*/WT than in Δ*stkP*/WT (Figure 6-8). The number of significantly changed proteins in pneumococcal samples from the stationary phase in the THY cultivation approach was almost comparable between Δ*phpP*/WT and Δ*stkP*/WT.

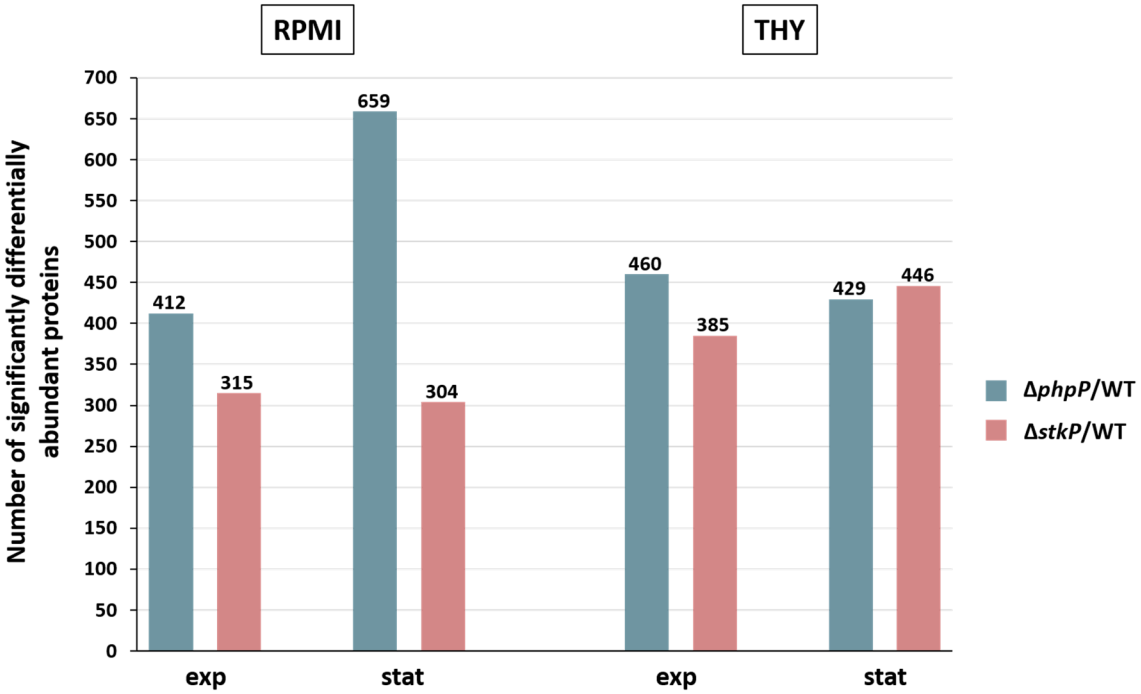

Figure 6-8: Comparison of quantity of significantly differentially abundant proteins within the analyzed pneumococcal strains. Within the analysis, the mutants were compared to the WT under the investigated growth conditions. Differentially abundant proteins with FC ≥ 2 and a q-value ≤ 0.01 were considered as significantly changed. The graphs visualize the number of significantly altered and "On/Off" proteins.

Proteins with significantly altered abundances were observed in almost every functional main group in both mutant strains in every condition (Figure 6-9). The quantitative functional comparative proteome analysis conducted in this work revealed notable changes especially in proteins belonging to the categories "Transport and binding proteins", "Transcription", "Protein synthesis and protein fate", "DNA and nucleotide metabolism" and "Central metabolism" in both mutants in comparison to the WT under each investigated condition. Moreover, slight differences were observed in the categories "Signal transduction", "Regulatory functions", "Energy

metabolism" and "Cellular processes". Furthermore, there is also a high percentage of significantly changed proteins with yet unknown functions. Nevertheless, there is no functional category with outstanding changes in the protein abundances under any condition in one of the mutants. The global quantitative proteome analysis rather revealed changes in proteins attached to a broad range of different cellular processes in the pneumococcal mutants deficient for StkP or PhpP in comparison to the WT strain.

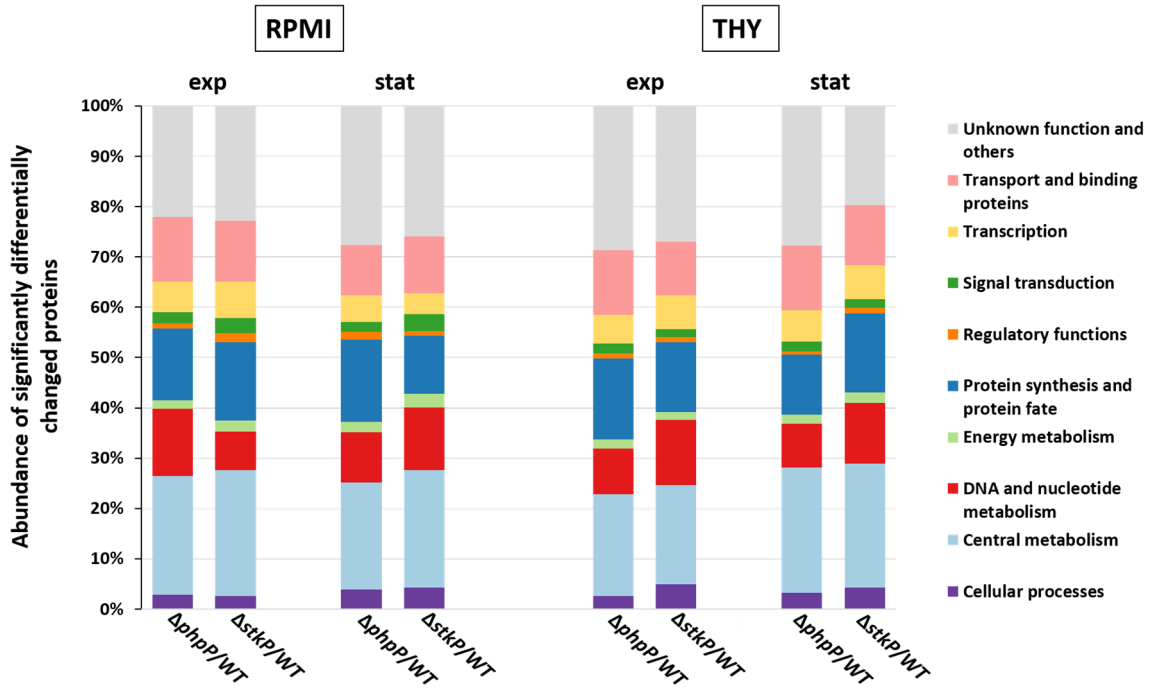

Figure 6-9: Distribution of significantly differentially abundant proteins within the analyzed pneumococcal strains. Within the analysis the mutants were compared to the WT under the investigated growth conditions. Differentially abundant proteins with FC ≥ 2 and a q-value ≤ 0.01 were considered as significantly changed. The graphs visualize the percentages of significantly altered proteins within the functional main categories.

For a more detailed view on differences in the proteome pattern of the kinase and the phosphatase mutant, Δ*stkP* and Δ*phpP*, all regulated proteins were clustered by a more specific functional annotation in Voronoi treemaps (Figure 6-10 and Figure 6-11; Supplementary material - Electronic appendix: Voronoi treemap collection). Within the treemap all tiles symbolize single proteins which are colored according to their abundance in a divergent color gradient. Proteins involved in the same biological process are clustered together. As already seen before, no distinct biological process is found to be remarkably changed entirely in the proteome of the Δ*phpP* or Δ*stkP* mutant in comparison to the WT. These data reflect the influence of StkP and PhpP in diverse cellular processes.

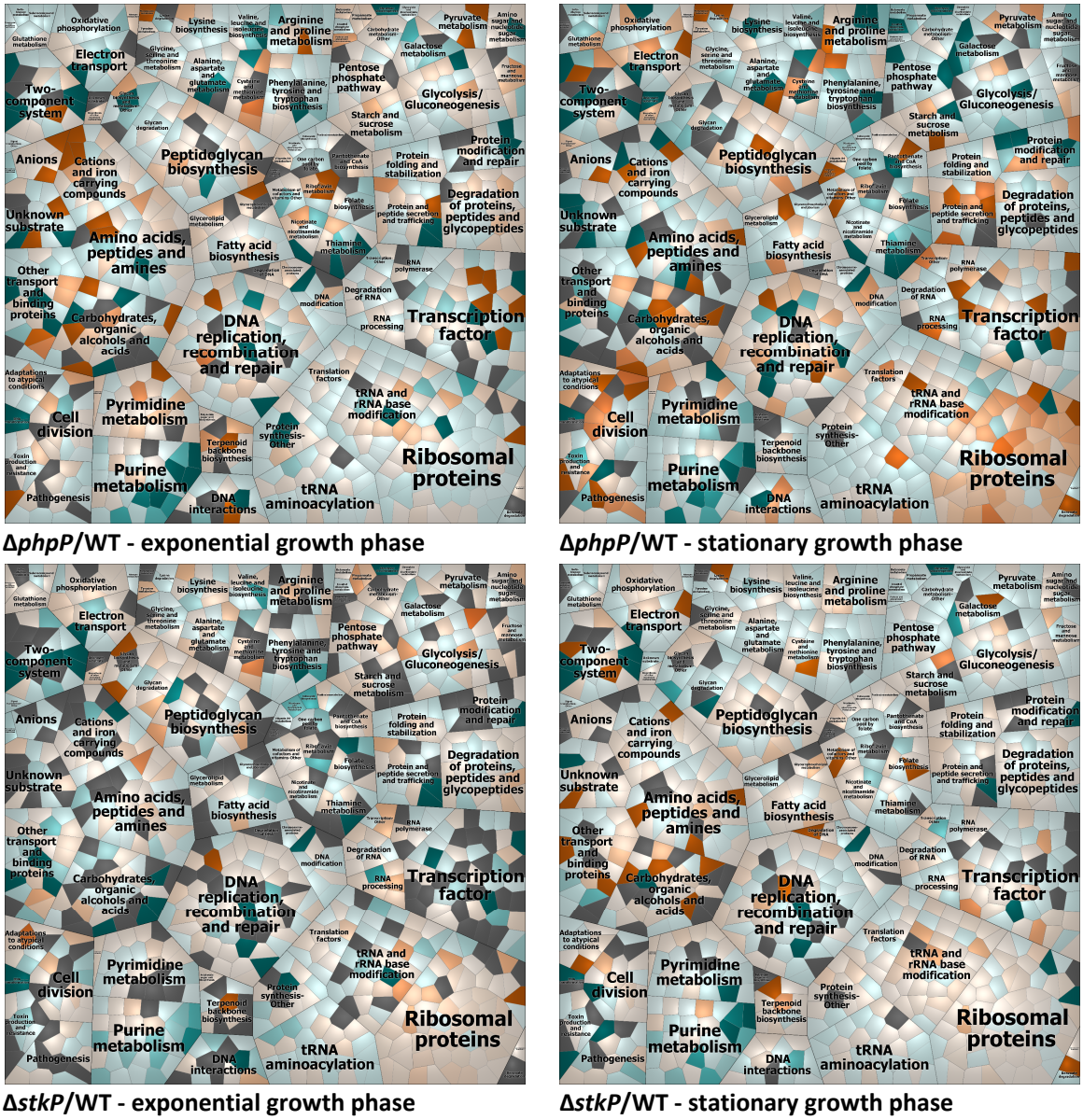

Figure 6-10: Comparison of protein abundances in Δ*phpP*/WT and Δ*stkP*/WT in samples derived from pneumococci grown in RPMI *modi* medium. Voronoi treemaps of the quantified proteome data of pneumococcal phosphatase and kinase mutant in comparison to WT assigned to specific functional sub roles. Within the treemap all tiles symbolize single proteins which are colored according to their abundance in a divergent color gradient. Turquoise cells indicate proteins that are less abundant or "Off" in the mutant in comparison to the WT whereas higher abundant or "On" proteins are illustrated in orange. Grey fields represent proteins that could not be quantified in the compared strains. Proteins involved in the same biological process are clustered together.

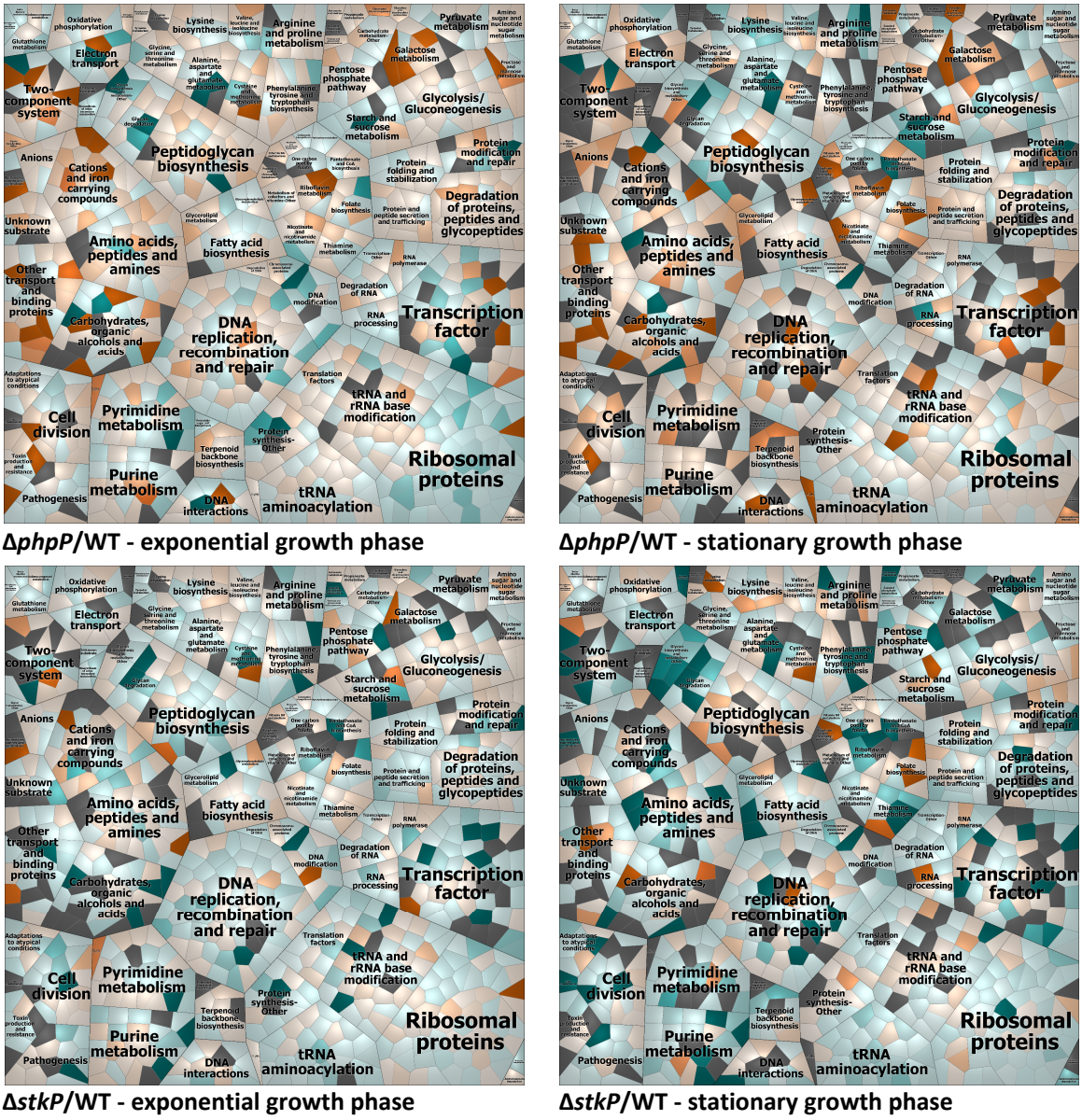

Figure 6-11: Comparison of protein abundances in Δ*phpP*/WT and Δ*stkP*/WT in samples derived from pneumococci grown in THY medium. Voronoi treemaps of the quantified proteome data of pneumococcal phosphatase and kinase mutant in comparison to WT assigned to specific functional sub roles. Within the treemap all tiles symbolize single proteins which are colored according to their abundance in a divergent color gradient. Turquoise cells indicate proteins that are less abundant or "Off" in the mutant in comparison to the WT whereas higher abundant or "On" proteins are illustrated in orange. Grey fields represent proteins that could not be quantified in the compared strains. Proteins involved in the same biological process are clustered together.

In samples cultivated in RPMI *modi* medium visible changes were detected in the cluster of proteins belonging to the purine metabolism. Lower abundant proteins were found in both growth phases in the kinase and in the phosphatase mutant in comparison to the WT. Furthermore, proteins with less abundance were detected in the category presenting the two-component systems in Δ*phpP*/WT or Δ*stkP*/WT, especially in the exponential growth phase but also in the stationary growth phase. Proteins within the cluster of anions and cations and iron carrying compounds were contrarily regulated in the mutants in RPMI *modi* medium in the exponential growth phase. While in Δ*phpP*/WT a prominent part of the proteins was higher in abundance, in Δ*stkP*/WT most of the proteins were less abundant or not changed. Furthermore, most of the ribosomal proteins were lower abundant in Δ*phpP*/WT in samples derived from the exponential growth phase. In the kinase mutant in Δ*stkP* most of the ribosomal proteins were less abundant in comparison to the WT. Ribosomal proteins are closely linked to bacterial growth. This goes along with the observations during the growth analysis of the strains (Figure 6-1). Pneumococci deficient for *phpP* grew consistently slower than the WT or the kinase mutant Δ*stkP*. In contrast to that, the kinase mutant Δ*stkP* grew slightly faster than the WT in the exponential growth phase. Pneumococci grown in THY medium did not show notable growth effects during the cultivation. Still, ribosomal proteins were less abundant in Δ*phpP*/WT in samples harvested in the exponential growth phase. In samples harvested in the stationary phase no explicit difference in the ribosomal protein pattern was observed in both mutants compared to the WT.

6.4. IN-DEPTH ANALYSIS OF *S. PNEUMONIAE* WT, KINASE AND PHOSPHATASE MUTANT IN CHEMICAL DEFINED MEDIUM

Previous studies have shown that eukaryotic-type Ser/Thr protein kinases (ESTKs) like the pneumococcal StkP as well as Ser/Thr phosphatases (ESTPs) such as PhpP function in diverse parallel or overlapping signaling networks. Moreover, it is known that both, StkP and PhpP play an essential role bacterial growth, cell division and cell separation. The global proteome analysis of the WT and the mutants Δ*stkP* and Δ*phpP* conducted in this work already demonstrated an influence of pneumococcal StkP and PhpP on a wide range of biological processes. However, morphological effects like impaired cell division and cell separation in the mutants observed through electron microscopy (Figure 6-2) could not be explained by changes in protein abundances on a global scale. Therefore, an in-depth analysis of the proteome and in the following part especially of the phosphoproteome was crucial to provide additional information of StkP and PhpP and their role in pneumococcal physiology.

Hence, when aiming to compare and characterize the mutants and the WT focusing on changes in protein abundances in distinct functional protein groups, it should be ensured that the most favorable growth conditions and time-point of cell harvest is chosen. Thus, it was considered that rich broth like THY medium provides optimal conditions during cultivation of pneumococci. There is an excess of nutrients and rarely accumulation of byproducts. Nevertheless, rich broth is an undefined medium. The amino acid source contains a variety of compounds but the exact composition is unknown. So, rich broth is ins general used for the cultivation and maintenance of bacteria kept in laboratory-culture collections. For the detailed characterization of the *S. pneumoniae* WT, kinase and phosphatase mutant strains the chemically defined RPMI 1640 medium supplemented with an extra of defined nutritive substances was used for bacterial liquid cultures. A medium with known quantities of all ingredients, which is further closer to cell culture media for bacterial infection approaches was found to be a suitable starting point for fundamental proteomic investigations which provide the basis for further research. In addition to that, the detailed analysis of changes in the proteome pattern of the mutants in comparison to the WT was performed with samples generated from pneumococci harvested in the exponential growth phase. In this growth phase the growth conditions should be optimal for bacteria, because of the sufficient availability of nutrients and less competition of bacterial cells. Indeed, within the exponential growth phase pneumococci of each strain reached high growth rates.

6.4.1. PROTEIN IDENTIFITATION AND LABEL-FREE QUANTITATIVE PROTEOMIC ANALYSIS OF Δ*STKP*, Δ*PHPP* MUTANTS AND WT

For the detailed characterization of changes in the proteome pattern of the kinase mutant Δ*stkP* and phosphatase mutant Δ*phpP* in comparison to the WT, an in depth examination of the data obtained from the label-free quantification approach using GeLC-MS/MS was done. For this analysis pneumococci of WT, and the mutants were cultivated in three independent biological replicates. on different days using always freshly prepared RPMI *modi* medium. Bacteria were harvested in the exponential growth phase and sample preparation was performed in parallel prior to LC-MS/MS analysis. The evaluation of the quality of the biological replicates for this analysis was depicted in 6.3.2. The square of the correlation coefficient, R^2, for the biological replicates of the WT was above 0.965, in case of Δ*stkP* ≥ 0.949 and for the biological replicates of Δ*phpP* ≥ 0.970 (Figure 10-1). That result proved that the variance between the biological replicates of each strain is quite low. Furthermore, the performed PCA analysis based on the quantitative data from the WT strain and the mutant strains Δ*phpP* and Δ*stkP* derived from samples of pneumococci grown in RPMI *modi* medium and harvested in the exponential growth phase sowed that the strains could be clearly distinguished on proteome level (see 6.3.2, Figure 6-7). For protein identification, at least two unique peptides must have been detected per protein. Proteins with attached LFQ values in three out of three biological replicates of each strain met the criteria for quantification. For comparative proteome analyses, statistical significance was assessed by a two-class unpaired test, analogous to a t-test between subjects.

All in all, 1,245 identified proteins were observed in this dataset (Figure 6-12A). Moreover, 1,070 proteins met the criteria for quantification, resulting in a quantification efficiency of 85.9%. Each mutant strain was compared to the WT strain in this approach. A remarkably higher number of proteins altered in abundance was found in the phosphatase mutant. In sum, 403 proteins were significantly changed in Δ*phpP*/WT and only 313 proteins in Δ*stkP*/WT (Figure 6-12B). These protein numbers consist of 156 higher abundant and 152 lower abundant detected proteins in Δ*phpP*/WT and additionally 46 “On” proteins and 49 “Off” proteins. “On” proteins were identified exclusively in Δ*phpP* with at least two unique peptides in three out of three replicates but not in the WT. On the other hand, “Off” proteins were identified only in the WT but in none of the replicates of the phosphatase mutant. In the comparison Δ*stkP*/WT 129 higher abundant and 132 lower abundant proteins were detected. Furthermore, seven additional “On” proteins and 45 “Off” proteins.

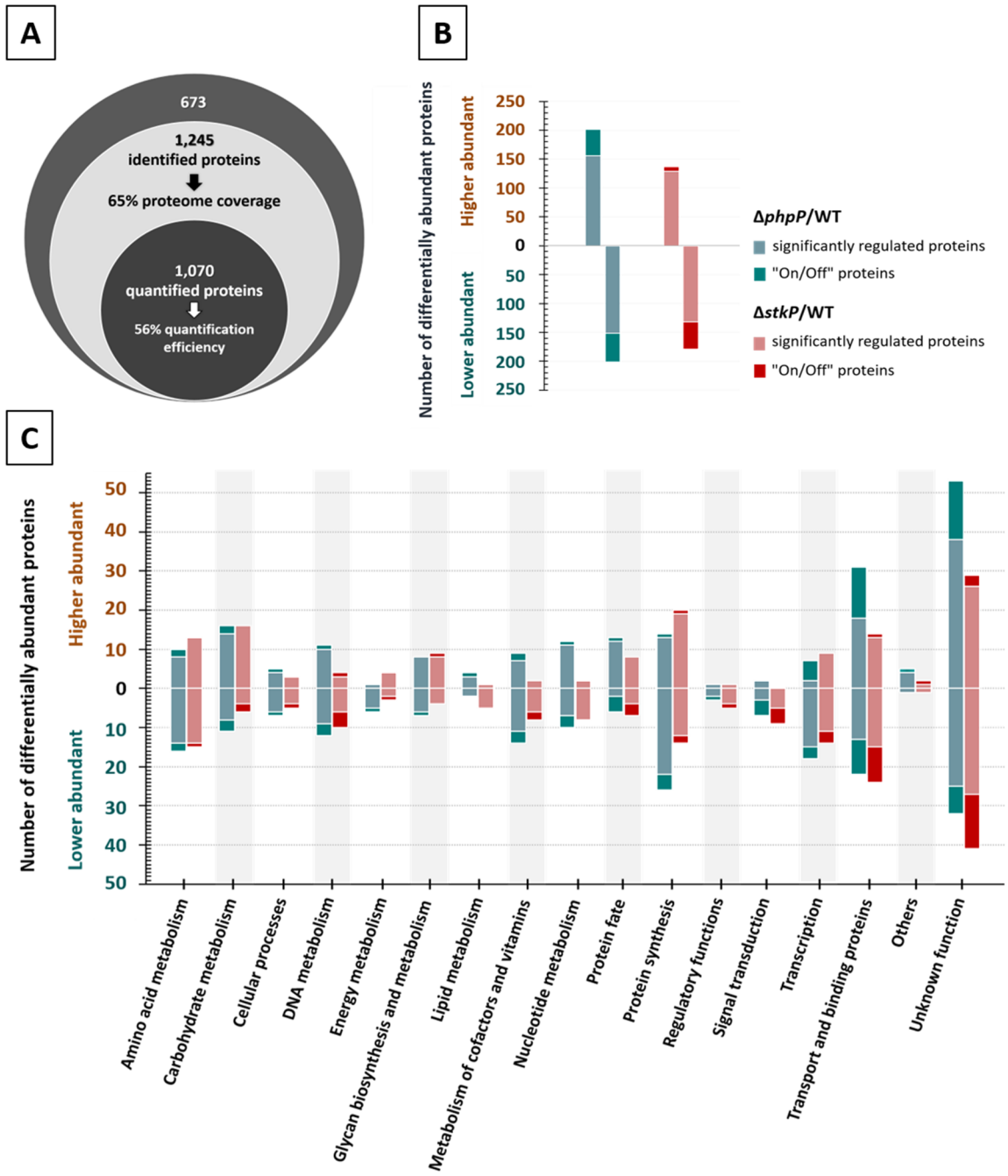

Figure 6-12: Protein identification and label-free quantification results of Δ*phpP*/WT and Δ*stkP*/WT in samples derived from pneumococci grown in RPMI *modi* medium (Hirschfeld et al. 2019). Part A provides an overview of identified and quantified protein numbers within the GeLC-MS/MS approach. A summary of proteins, that were significantly altered in abundance in Δ*phpP*/WT and Δ*stkP*/WT is depicted in part B. Part C sums up the absolute numbers of proteins belonging to the respective functional class and significantly quantified in at three out of three replicates of the mutants/WT. Proteins with significantly ($q \leq 0.01$) higher ratios ($\geq 2\times$) were considered for the analysis.

To obtain further knowledge of the influence of StkP and PhpP on particular biological processes in the pneumococcus, all 1918 predicted proteins of *S. pneumoniae* D39 were classified into

functional protein groups according to TIGRFAM (Haft et al. 2001) or KEGG-based (Aoki and Kanehisa 2005; Kanehisa and Goto 2000) annotation. As already seen before, in the overall global proteome analysis, proteins that were significantly altered in abundance were present in almost every functional group in the phosphatase mutant as well as in the kinase mutant (Figure 6-12C). In general notable changes in the proteome of the phosphatase mutant were particularly found in proteins classified into the functional categories "Transport and binding proteins", "Protein synthesis", "Amino acid metabolism" and "Carbohydrate metabolism", "DNA metabolism", "Metabolism of cofactors and vitamins" as well as "Transcription", "Protein fate" and "Glycan biosynthesis and metabolism". Changes in the proteome of the kinase mutant were observed also in proteins belonging to the categories "Transport and binding proteins", "Protein synthesis", "Amino acid metabolism" and "Carbohydrate metabolism", "Transcription", "DNA metabolism" as well as "Protein fate" and "Glycan biosynthesis and metabolism". Nevertheless, also during this examination there was no outstanding change in the abundance of the according to their main roles categorized proteins in a specific manner in both comparisons, Δ*phpP*/WT and Δ*stkP*/WT.

6.4.2. CHANGES IN SPECIFIC FUNCTIONAL PROTEIN CLUSTERS IN PNEUMOCOCCAL MUTANTS DEFICIENT FOR *STKP* AND *PHPP*

For a deeper insight into differences in the proteome pattern of *stkP* and *phpP* mutants all regulated proteins were clustered by an even more specific functional annotation in Voronoi treemaps (Figure 6-13 and Figure 6-14). Previous analysis was focussed on the main roles of the proteins. Here, proteins were assigned to their functional sub roles. These approach paved the way to uncover smaller, but more specified protein clusters that were influenced by the loss of function of pneumoococcal StkP and PhpP. As previously mentioned, notable changes in the protein were observed amongst others in the common category of "Transport and binding proteins. Within this group, remarkable differences in the protein abundance in the mutant strains in comparison to the WT were noticed especially in the cluster of proteins belonging to anions as well as cations and iron carrying compounds. Furthermore, it was shown that proteins involved in the nucleotide metabolism were affected primarily by the deletion of *phpP*. Now, more detailed, notable changes were observed in the pyrimidine and purine metabolism. A group that was not prominent regarding overall changes in protein abundances before, is the group of proteins which are involved in signal transduction. But interestingly a more detailed view showed that there are significant changes in protein abundances in the cluster "Two-component system".

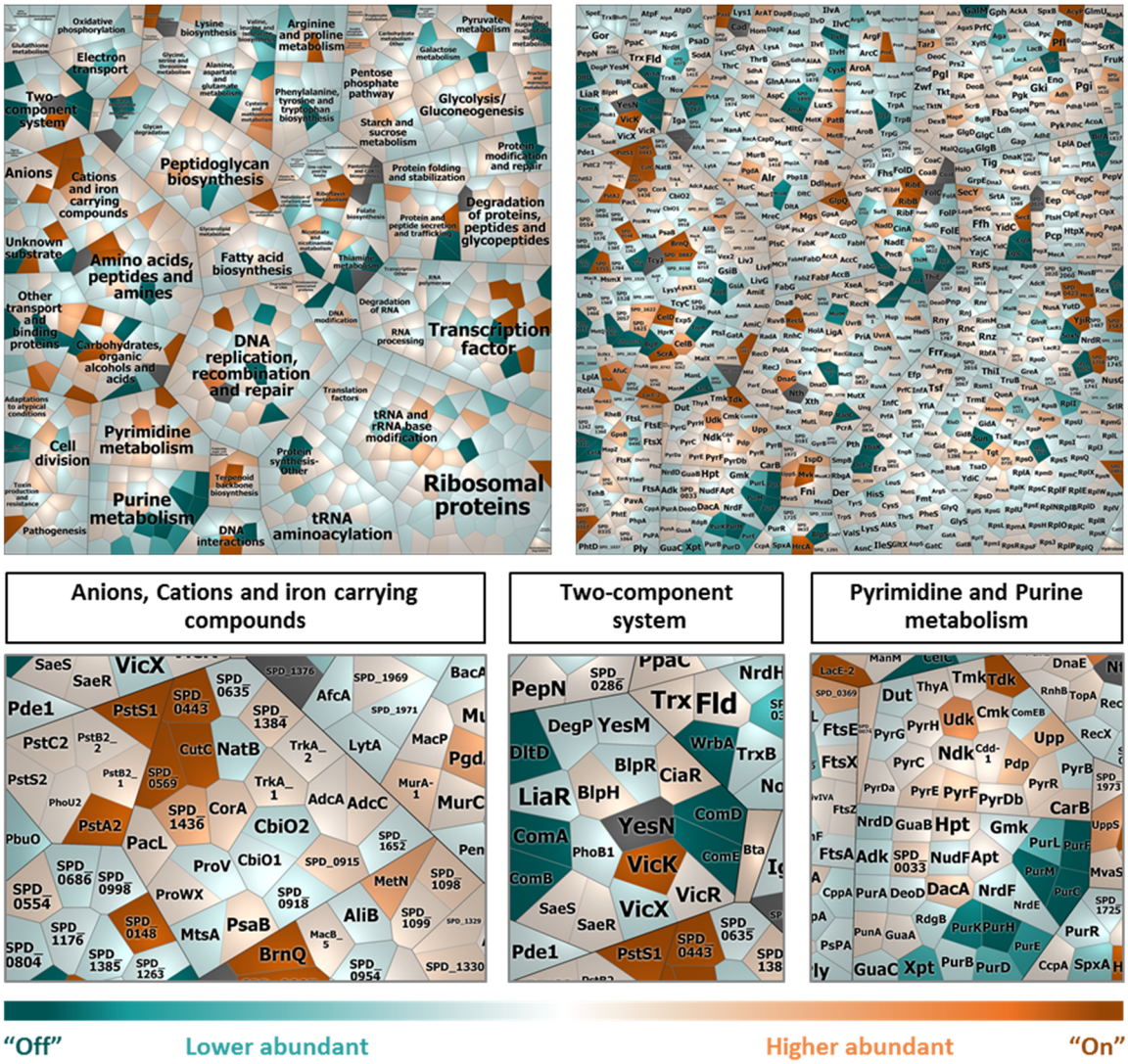

Figure 6-13: Comparison of protein abundances Δ*phpP*/WT. Voronoi treemap of the quantified proteome (1,070 proteins of the 1,918 theoretical proteins) of pneumococcal phosphatase mutant in comparison to WT assigned to specific functional sub roles. Within the treemap all tiles symbolize single proteins (quantified in Δ*phpP* and Δ*stkP*) which are colored according to their abundance in a divergent color gradient. Turquoise cells indicate proteins that are less abundant or "Off" in the mutant in comparison to the WT whereas higher abundant or "On" proteins are illustrated in orange. Grey fields represent proteins that could not be quantified in this comparison. Proteins involved in the same biological process are clustered together. For a deeper insight into changes of protein abundances in the cluster of anions, cations and iron carrying compounds, in two-component systems as well as in pyrimidine and purine metabolism, the protein level is enlarged under the overall treemaps.

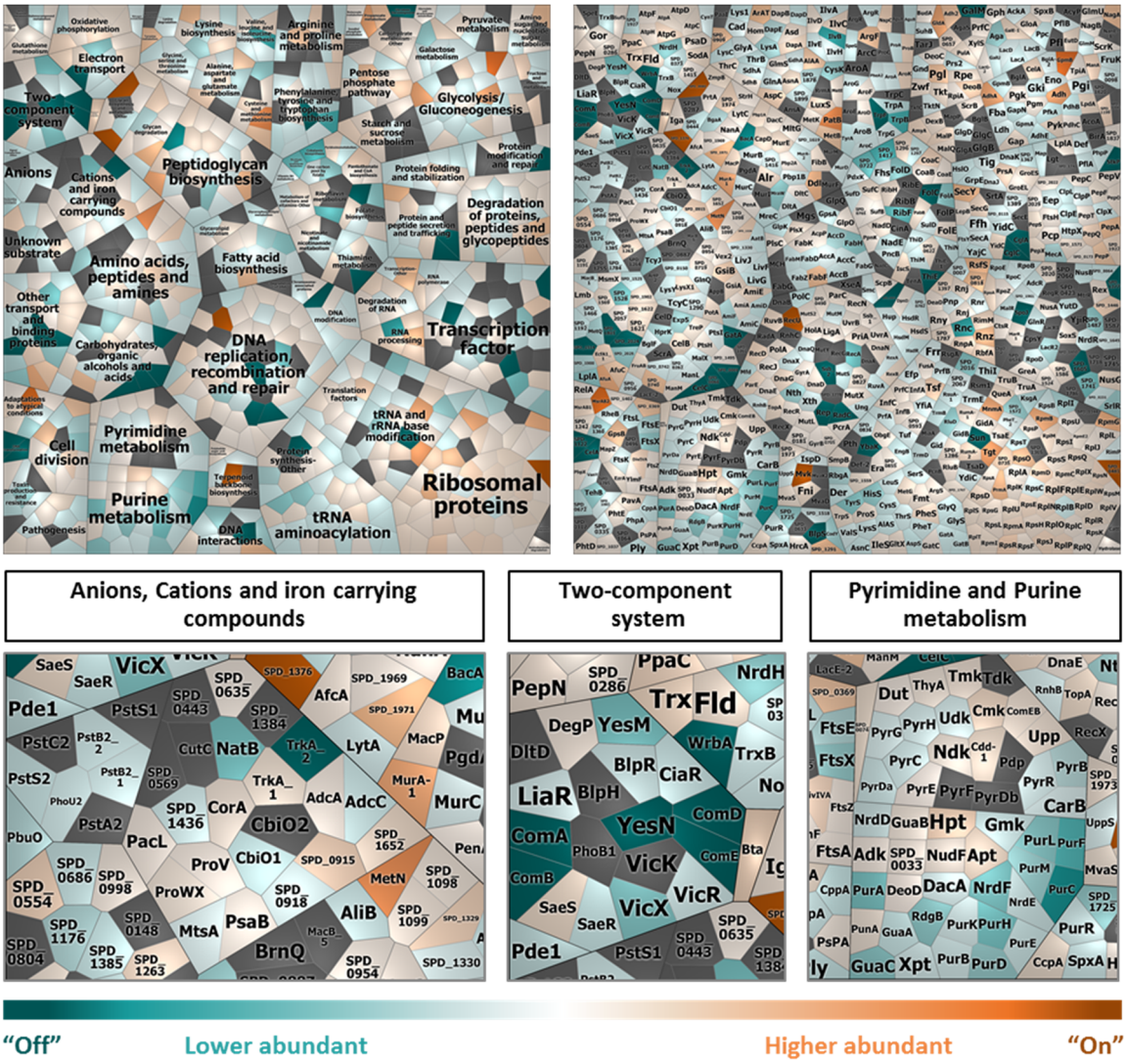

Figure 6-14: Comparison of protein abundances Δ*stkP*/WT. Voronoi treemap of the quantified proteome (1,070 proteins of the 1,918 theoretical proteins) of pneumococcal kinase mutant in comparison to WT assigned to specific functional sub roles. Within the treemap all tiles symbolize single proteins (quantified in Δ*stkP* and Δ*phpP*) which are colored according to their abundance in a divergent color gradient. Turquoise cells indicate proteins that are less abundant or "Off" in the mutant in comparison to the WT whereas higher abundant or "On" proteins are illustrated in orange. Grey fields represent proteins that could not be quantified in this comparison. Proteins involved in the same biological process are clustered together. For a deeper insight into changes of protein abundances in the cluster of anions, cations and iron carrying compounds, in two-component systems as well as in pyrimidine and purine metabolism, the protein level is enlarged under the overall treemaps.

6.4.2.1. PNEUMOCOCCAL PHOSPHATE UPTAKE SYSTEM PST IS AFFECTED BY *STKP* AND *PHPP* DELETION

In the previous analysis it was already shown, that notable changes in abundance were observed in proteins belonging to the category of "Transport and binding proteins". The in-depth observation of this category reavealed changes in the protein abundances especially when comparing the phosphatase mutant with the WT in the functional protein groups of "Anions and cations and iron carrying compounds". Among others, the ABC transporter complex PstSCAB, which is involved in phosphate import, showed a higher abundance in several proteins belonging to this mechanism in the phosphatase mutant Δ*phpP* whereas these proteins were less abundant in the kinase mutant Δ*stkP* compared to the WT (Figure 6-13 and Figure 6-14). In the pneumococcus there are two evolutionarily separated phosphate ABC pump transporters, Pst1 and Pst2, encoded. They function in adaptation to different Pi concentrations in the human host (Zheng et al. 2016; Moreno-Letelier et al. 2011; Lanie et al. 2007). In the pneumococcal chromosome the *pst*1-*pho*U1 and *pst*2-*pho*U2 operons are completely separated. All proteins included in the *pst*2 operon, namely PhoU2, PstA2, PstB2_1, PstB2_2, PstBC2 and PstS2 were identified and quantified in the phosphatase mutant Δ*phpP*. The phosphate import ATP-binding protein PstB2_1 (ATPase subunit 1) was significantly higher in abundance in Δ*phpP*/WT (FC 2.3) and the membrane channel protein PstA2, a putative phosphate ABC transporter, was identified only in the phosphatase mutant but not in the WT and not in the kinase mutant Δ*stkP*. The phosphate import ATP-binding protein PstB2_2 (ATPase subunit 2) (FC 1.5) and the putative phosphate ABC transporter proteins PstC2 (FC 1.8) and PstS2 (FC 1.6) were slightly more abundant in Δ*phpP*/WT, too. The phosphate-specific transport system accessory protein PhoU2 (FC 1.2) did not reveal a remarkable change in abundance. In the kinase mutant Δ*stkP* the putative phosphate-binding ABC transporter protein PstS2 was significantly less abundant compared to the WT (FC -2.3). PhoU2 (FC - 1.5), PstB2_1 (FC -1.4) and PstB2_2 (FC - 1.5) were also slightly less abundant in Δ*stkP*/WT. In case of the pneumococcal inorganic phosphate uptake system 1 just the phosphate-binding ABC transporter protein PstS1 was identified only in the phosphatase mutant but neither in the WT nor in the kinase mutant. Additional components of the *pst*1 operon were not detected in any of the strains.

Moreover, proteins, which do not directly participate in the phosphate homeostasis in the pneumococcus but that play a role in the regulation of the intracellular concentration of other cations were also affected: Within the adjacent cluster of cations and iron carrying compounds, the sodium/hydrogen exchange family protein SPD_0569 and the copper homeostasis protein CutC were detected exclusively in the phospatase mutant Δ*phpP* and not in the kinase mutant Δ*stkP* and in the WT. Furthermore, the magnesium transporter CorA , the zink ABC transporter AdcC, the potassium uptake protein TrkA (FC 2.03) and the cation-transporting ATPase SPD_1436 (FC 5.44) were significantly higher abundant in Δ*phpP*/WT, but not significantly changed in abundance in

Δ*stkP*/WT. Additionally, the iron-compound binding ABC transporter SPD_0915 (Δ*phpP*/WT FC 3.04; Δ*stkP*/WT FC 3.14) was significantly higher in abundance in both mutants.

6.4.2.2. SIGNIFICANT CHANGES IN PROTEIN ABUNDANCE IN PURINE AND PYRIMIDINE METABOLISM IN Δ*PHPP* AND Δ*STKP* MUTANTS

The global proteome analysis conducted before in this work showed that especially in the phosphatase mutant compared to the WT notable changes were visible in the abundance of proteins involved in the nucleotide metabolism of pneumococci. This group comprises proteins assigned to the purine and pyrimidine metabolism (Figure 6-13 and Figure 6-14). Another study presented that ESTKs and ESTKPs were important for the accurate balance of purine nucleotide pools and the regulation of purine biosynthesis (Rajagopal et al. 2005b). The data generated during this work displayed that the adenylosuccinate synthetase PurA was significantly less abundant in both mutants compared to the WT (Δ*phpP*/WT FC -2.6; Δ*stkP*/WT FC -7.4). PurA is the enzyme which catalyzes the first dedicated step in the biosynthesis of adenosine monophosphate (AMP) from inosine monophosphate (IMP). Other proteins that participate in the *de novo* purine biosynthesis (PurC, PurF, PurM) were less abundant in Δ*stkP*/WT (PurC FC -18.5; PurF FC -11.5; PurM FC -4.5) and "off" in the phosphatase mutant compared to the WT. PurE, the N5-carboxyaminoimidazole ribonucleotide mutase, was significantly lower in abundance in the phosphatase mutant Δ*phpP*/WT (FC -16.2). Among others, additional proteins belonging to the IMP *de novo* biosynthesis (PurB, PurD, PurH, PurK, PurL) were lower in abundance in Δ*phpP*/WT (PurB FC -1.89; PurD FC -10.73; PurH FC -36.06; PurK FC -24.61; PurL -10.72) likewise in Δ*stkP*/WT (PurB FC -1.37; PurD FC -4.48; PurH FC -7.94; PurK FC -2.85; PurL -6.25). The ribose-phosphate pyrophosphokinase SPD_0033, which plays a crucial role in the biosynthesis of the central metabolite phospho-*alpha*-D-ribosyl-1-pyrophosphate, was contrarily changed in abundance in Δ*phpP*/WT and Δ*stkP*/WT. The protein SPD_0033 was significantly more abundant in the phosphatase mutant (FC 2.9), but not significantly altered in abundance in the kinase mutant in comparison to the WT. NrdD, NrdE and NrdF, all of them are ribonucleoside-diphosphatase reductases, necessary for providing the precursors for the DNA synthesis, were significantly lower abundant in both mutants (Δ*phpP*/WT NrdD FC -3.74, NrdE FC -2.19, NrdF FC -2.19; Δ*stkP*/WT NrdD FC -2.99, NrdE FC -2.57, NrdF FC -7.34) same was observed for the guanosine monophosphate (GMP) reductase GuaC that catalyzes the irreversible NADPH-dependent deamination of GMP to IMP (Δ*phpP*/WT, FC -2.29; Δ*stkP*/WT FC -5.69). The diadenylate cyclase DacA, part of the cyclic-AMP biosynthetic process, was not remarkably changed in Δ*stkP*/WT (FC -1.2) but it was significantly more abundant in the phosphatase mutant Δ*phpP*/WT (FC 3.3).
An earlier published transcriptomic study pointed out that an ESTK deletion in a mutant of *Staphylococcus aureus* affected the expression of genes attached to regulons that participate in the

mechanism of purine and also of pyrimidine biosynthesis (Donat et al. 2009). As a result of the detailed proteome analysis of the pneumococcal mutants deficient for StkP or PhpP in comparison to the WT, significant changes in protein abundances were obvious in the functional cluster of pyrimidine metabolism (Figure 6-13 and Figure 6-14). Here it was especially the case for the *phpP* deletion mutant. The orotate phosphoribosyltransferase PurE and the orotidine 5'-phosphate decarboxylase PyrF, both part of the uridine monophosphate (UMP) *de novo* biosynthetic pathway, were significantly more abundant in Δ*phpP*/WT (FC PyrE 2.81; FC PyrF 3.55). Other significantly higher abundant proteins in Δ*phpP*/WT participating in the pyrimidine metabolism are: The uracil phosphoribosyl transferase Upp (FC 4.18), the pyrimidine-nucleoside phosphorylase Pdp (FC 4.07), the uridine kinase Udk (FC 8.4), the carbamoyl-phosphate synthase CarB (FC 2.49), the bifunctional protein PyrR (FC 2.38) and the cytidylate kinase Cmk (FC 2.53). Further, Tdk, a thymidine kinase, was identified in all biological replicates of Δ*phpP* but not in any of the WT. Regarding Δ*stkP*/WT these proteins were not notably changed in their abundance. Two other proteins involved in the UMP *de novo* biosynthesis (PyrDa and PyrB), were not altered in abundance in the phosphatase mutant but interestingly they were significantly less abundant in Δ*stkP*/WT (FC PyrDa -2.58; FC PyrB -3.51).

6.4.2.3. StkP and PhpP interact with pneumococcal two-component systems

Previously described proteome analyses of the mutants and the WT were performed on a global scale. Therewith, no proteins involved in the signal transduction in the pneumococcus were in the spotlight. However, in more detail the comparative proteome analysis of the deletion mutants Δ*phpP* and Δ*stkP* revealed variations of protein abundances in the pneumococcal two-component systems (Figure 6-13 and Figure 6-14).

Significant changes were observed in proteins belonging to the ComCDE and ComAB systems. For these two-component systems it was shown that they have critical functions regarding pneumococcal competence and interact under specific environmental conditions (Gómez-Mejia et al. 2017). In both mutants was the response regulator ComE significantly less abundant in comparison to the WT (Δ*phpP*/WT FC -231 and Δ*stkP*/WT FC -298.87). ComD, the putative sensor histidine kinase, was not detected in Δ*phpP* and Δ*stkP* but in the WT. Moreover, the competence factor transporting ATP-binding/permease protein ComA and the competence factor transport protein ComB were identified in each of the three bioreplicates of the WT with at least 15 unique peptides but in the kinase mutant and in the phosphatase mutant these proteins were not identified at all.

Another pneumococcal two-component system found to be influenced by the deletion of *phpP* and *stkP* was the LiaRS system. For the LiaRS two-component system it was also described that it is

involved in the competence process by responding to peptidoglycan cleavage by LytA, CbpD and LytC murein hydrolases (Gómez-Mejia et al. 2017; Eldholm et al. 2010). In the WT strain, the choline binding protein CbpD was reliable identified. In the mutants Δ*phpP* and Δ*stkP* CbpD was not detected at all. Furthermore, the autolysin/N-acetylmuramoyl-L-alanine amidase LytA was significantly lower abundant in both mutants compared to the WT (Δ*phpP*/WT, FC -2.96; Δ*stkP*/WT FC -2.91). The same was observed for the DNA-binding response regulator LiaR. LiaR was significantly less abundant in Δ*phpP*/WT (FC -2.42) and slightly less abundant in Δ*stkP*/WT (FC -1.3). The cognate sensor histidine kinase LiaS met the criteria for quantification in Δ*phpP*, but that was not the case for the WT and the kinase mutant.

A contrarily change of protein abundance in Δ*phpP*/WT and Δ*stkP*/WT was noticed with regard to the CiaRH (competence induction and altered cefotaxime susceptibility) system (Figure 6-13 and Figure 6-14). The DNA-binding response regulator CiaR was significantly less abundant in Δ*stkP*/WT (FC -2.95) but significantly more abundant in the phosphatase mutant Δ*phpP* compared to the WT (FC 2.97). CiaH, the corresponding sensor histidine kinase, was not detected in one of the strains. An already published study presented, that CiaR caused an upregulation of the virulence factor HtrA (DegP) (Stevens et al. 2011). In contrast to that, the proteomic data obtained during this work showed that the serine protease DegP was significantly lower in abundance in Δ*phpP*/WT (FC -2.41) and only slightly higher in abundance in Δ*stkP*/WT (FC 1.41).

VicRK (TCS02, WalRK) is another two-component system in the pneumococcus, which is involved in the regulation of competence. The VicX ancillary protein encoded in the *vicRK* operon was significantly lower in abundance in the kinase mutant Δ*stkP* in comparison to the WT (FC -6.71) and also in Δ*phpP*/WT it was less abundant (FC -1.92). While the sensory box sensor histidine kinase VicK was significantly more abundant in the phosphatase mutant (FC 44.03), there were no differences in the abundance of this protein observed in Δ*stkP*/WT. In addition to that, the DNA-binding response regulator VicR was only slightly more abundant in the phosphatase mutant (FC 1.08) but less abundant in the kinase mutant (FC -1.5) in comparison to the WT. Moreover, VicR is required for the positive regulation of a gene encoding a putative peptidoglycan hydrolase (PcsB, SPD_2043) that plays a critical role in cell wall biosynthesis and cell division in the pneumococcus. For PcsB it is already known that this protein interacts with the cell division complex FtsE/FtsX (Sham et al. 2011). PcsB was identified in each of the three strains within this approach. In the phosphatase mutant, PcsB was more abundant compared to the WT (FC 1.88), while no changes were seen in the comparison Δ*stkP*/WT. The cell division proteins FtsE (ATP-binding) and FtsX were significantly less abundant in Δ*stkP*/WT (FC FtsE -3.69; FC FtsX -4.77). Surprisingly, no significant changes in the abundance were observed for FtsE or FtsX in the Δ*phpP* mutant compared to the WT.

6.5. COMPARATIVE PHOSPHOPROTEOMIC ANALYSIS OF Δ*STKP*, Δ*PHPP* AND WT

The obtained LFQ results did not reveal remarkable changes in specific functional protein groups that might caused the strong phenotypic abnormalties presented in the pneumococcal kinase and phosphatase mutant strain. Therefore, it is reasonable to assume that StkP and PhpP are involved in the regulation of pneumococcal morphogenesis by modulating proteins attached to cell division and associated processes like peptidoglycan biosynthesis by balancing the phosphorylation and dephosphorylation level of target proteins. Once identified target substrates of StkP *in vivo* are DivIVA, GlmM, PpaC, MurC, MapZ, and StkP itself (Hammond et al. 2019; Fleurie et al. 2014b; Falk and Weisblum 2013; Nováková et al. 2010; Osaki et al. 2009). Still, most of the targets and target sites of StkP remain to be detected and characterized. However, the function of PhpP is poorly described. To gather further information on the activity, targets and target sites of PhpP and StkP and to be capable to correlate the phenotypic observations to protein phosphorylation patterns, a gel-free phosphopeptide enrichment with TiO_2 was performed followed by LC-MS/MS measurement and a spectral library based data evaluation. In order to raise the efficiency of the general applied approach for phosphoproteomic investigations for the analysis of pneumococcal samples, the classical sample preparation method was adapted and a new, extended and strict filtered spectral library including diverse in-house generated and available data was constructed.

6.5.1. MODIFICATION OF THE CLASSICAL WORKFLOW FOR PHOSPHOPROTEOME ANALYSIS

The classical workflow for the phosphoproteome analysis includes a sample fractionation with strong cation exchange (SCX) chromatography, which requires an amount of 50 mg protein per sample (Olsen and Macek 2009). To decrease the amount of necessary cell material, it was evaluated whether the SCX can be omitted. Therefore, protein samples were generated exemplarily from the WT strain cultivated simultaneously under the same conditions in RPMI *modi* medium. For the data analysis of these samples, an already in the working group available spectral library for *S. pneumoniae D39* was used. Applying the workflow with SCX fractionation 48 phosphopeptides were identified whereas 53 phosphopeptides could be detected after sample preparation without SCX prefractionation (Figure 6-15). The consideration of the identified phosphoproteins revealed four additional identifications using the SCX-free protocol.

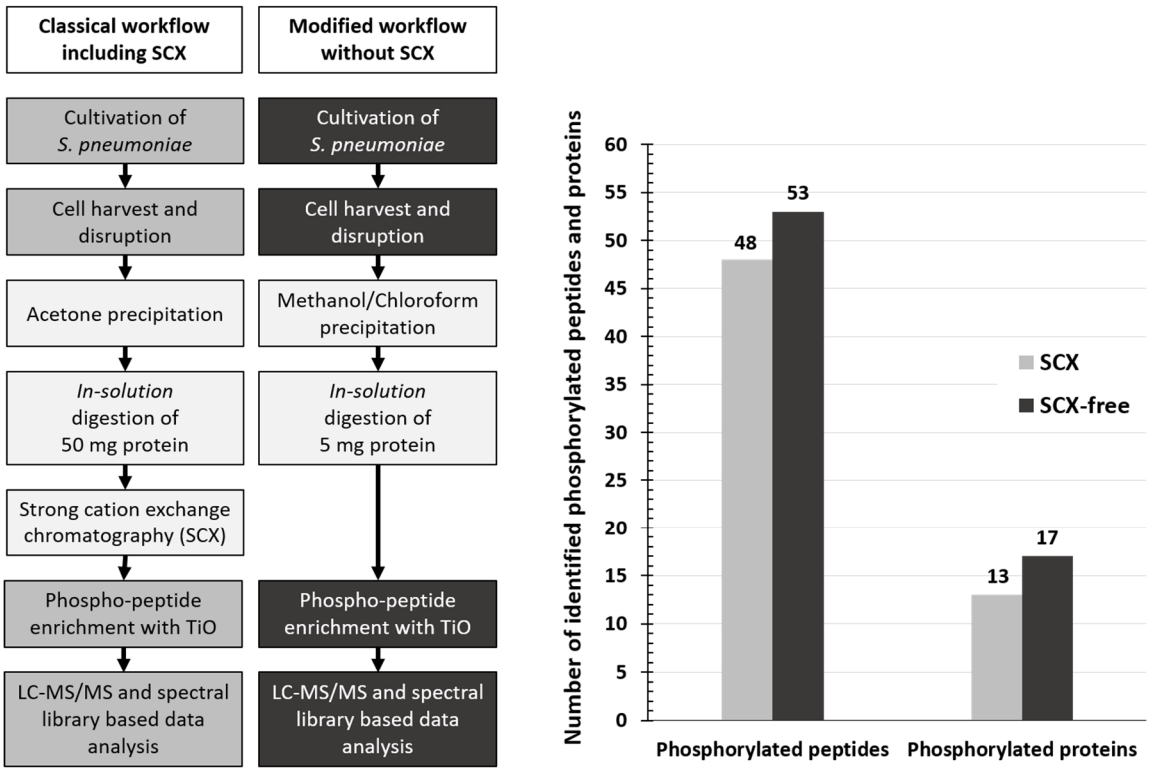

Figure 6-15: Comparison of classical workflow for phosphoproteome analysis and the modified workflow. The graphical account sums up the amount of identified phosphorylated peptides and proteins in the WT after classical sample preparation including SCX and after sample preparation according to the modified workflow.

Another slight modification of the workflow was the performance of the methanol/chloroform precipitation for protein samples instead of the acetone precipitation. This resulted in cleaner samples since the chemicals used were declared as LC-MS-grade. In the end, the modified protocol was tested successfully as suitable for further phosphoproteome analysis of the pneumococcal strains of interest.

6.5.2. SPECTRAL LIBRARY FOR PHOSPHOPROTEOMIC INVESTIGATIONS IN *S. PNEUMONIAE* D39

Studies of bacterial phosphoproteomes based on classical database search analysis usually uncovered less than 150 phosphorylated proteins. In previous investigations it has been reported, that the implementation of spectral libraries resulted in an improved sensitivity. With this in mind, a combined spectral library based on phosphopeptide-enriched samples and classical proteome samples was planned to be applied for the data evaluation for the investigation of the pneumococcal phosphoproteome in this work. However, the already existing in-house generated spectral library did not meet the requirements and recent needs for high-confidence protein and peptide, especially phosphopeptide identifications. Therefore, an advanced spectral library of *S. pneumoniae* D39 was created in this work.

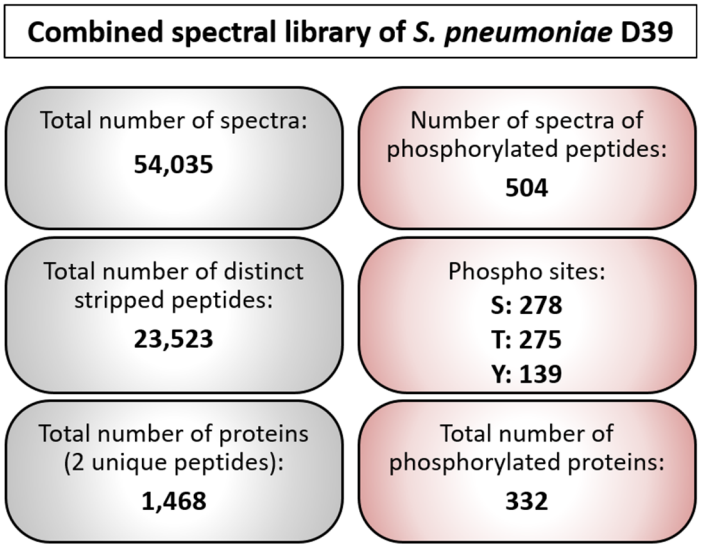

Figure 6-16: Key data of the spectral library of *S. pneumoniae* D39 suitable for phosphoproteome studies.

A high number of different in-house produced datasets (908 .raw files) from various proteomic experiments with *S. pneumoniae* D39 was the basis for the creation of this library. Among others samples used for the library building were obtained from pneumococci of the WT strain or the mutant strains Δ*stkP* and Δ*phpP,* from pneumococci cultivated in THY medium, RPMI 1640

medium and another self-prepared CDM, further from pneumococci under glucose limitation or iron limitation, moreover, samples from pneumococcal whole cell extracts and the supernatant from cell cultures, affinity bead-based protein enriched samples, *in-solution* digested samples, *in-gel* digested samples and SCX fractionated and phosphopeptide enriched samples. The built spectral library for *S. pneumoniae* D39 contains 23,140 spectra of non-phosphorylated peptides from 1,480 proteins and 504 spectra of phosphorylated peptides belonging to 332 proteins. Furthermore, the presented spectral library also includes datasets of SILAC (Stable Isotope Labeling by Amino Acids in Cell Culture) samples. So, it is also applicable for quantitative approaches using metabolic labeling techniques in future investigations.

6.5.3. Overview of identified phosphorylated peptides and proteins in *S. pneumoniae* applying the constructed spectral library

Finally, in this work it was of major interest to uncover possible new targets/target sites of the pneumococcal kinase StkP and especially of the phosphatase PhpP. For high-confidence identifications of phosphorylated peptides the recently built spectral library was applied. Only phosphorylated peptides that were detected in three out of three biological replicates in each strain were considered for the analysis.

Thus, 24 unique phosphopeptides were identified in the WT derived from 16 different proteins (Figure 6-17). In the kinase mutant Δ*stkP* 18 unique phosphopeptides (14 proteins) were detected while in the phosphatase mutant Δ*phpP* 28 unique peptides belonging to 21 proteins were found to be phosphorylated. Among the identified phosphorylated peptides, 26 phosphorylation sites were identified in the WT strain: 11 on serine, 14 on threonine and one on tyrosine. In Δ*stkP* 20 phosphorylation sites were determined: 11 on serine, seven on threonine and two on tyrosine and in Δ*phpP* 29 phosphorylation sites were noticed: 14 on serine, 14 on threonine and one on tyrosine. Overall, 10 phosphopeptides were identified commonly in each strain. These phosphorylated peptides were derived from six proteins, which are involved in the carbohydrate metabolism (phosphoglucomutase Pgm, phosphoglucosamine mutase GlmM, pyruvate kinase Pyk), signal transduction (competence factor transport protein ComB), transport and binding (phosphocarrier protein PtsH) and a single protein with yet unknown function (SPD_0361).

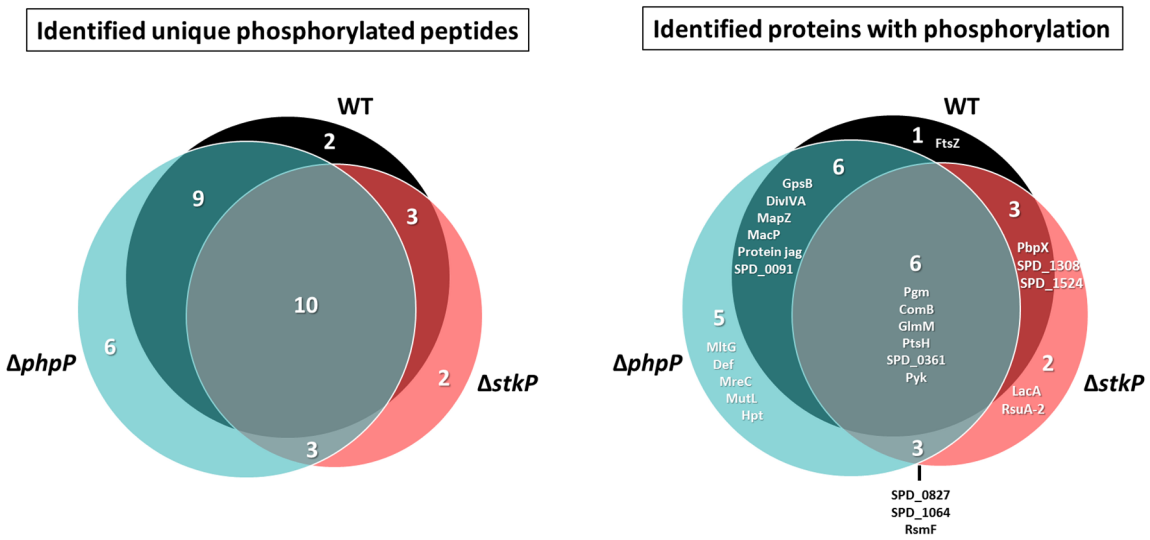

Figure 6-17: Phosphopeptide and phosphoprotein identifications in the WT and mutant strains (Hirschfeld et al. 2019). The first Venn diagram presents the numbers of phosphopeptides identified in the WT, Δ*phpP* and Δ*stkP* mutant and the overlap of identifications between the investigated strains. In the second Venn diagram, the overlap of phosphorylated proteins between the mutants and the WT is depicted. Only phosphorylations at serine, threonine, and tyrosine were considered.

6.5.4. Identification of putative StkP targets and target sites

In previous investigations it was shown that StkP localizes to the division sites in pneumococcal cells and that it is involved in the regulation of cell division in pneumococci. Pneumococcal mutants with lost or impaired *stkP* activity displayed affected cell wall synthesis and presented elongated morphologies with multiple, often delocalized cell division septa. Thus it was suggested that StkP modulates cell wall synthesis and cell division and contributes to the characteristic ovoid shape of the pneumococcus (Zucchini et al. 2018; Fleurie et al. 2014b; Beilharz et al. 2012). The morphological characterization of the kinase mutant Δ*stkP* by electron microscopy presented in 6.2. in this work already pointed out that the mutant had a different phenotype compared to the WT. This might be caused by an imbalance of phosphorylation and dephosphorylation events in the cell.

Since the pneumococcal kinase StkP was disrupted in the mutant, it was assumed that StkP targets were not phosphorylated as in the WT strain. Therefore, to pinpoint direct targets of the StkP, the data generated from the phosphopeptide-enriched samples were filtered for phosphorylated peptides which were detected in the WT in each of the three replicates but in none of the replicates of the kinase mutant Δ*stkP*. Consequently seven phosphoylation sites within eight unique peptides belonging to seven distinct proteins were identified. These identifications were considered with utmost probability to be targets of StkP (marked with *** in Table 6-1).

Table 6-1: Putative targets and target sites of pneumococcal kinase StkP identified in this study (Hirschfeld et al. 2019).

Significance	Locus ID	Peptides inclusive phosphosites	Protein description	Biological process
***	SPD_1040	DFHVVAE**T**$_{12}$GIHAR	Phosphocarrier protein HPr	Carbohydrates, organic alcohols and acids
***	SPD_1474	EVVSEVLGEPIPAPIEEEPIDM**T**$_{201}$R	Cell division protein DivIVA	Cell division
***	SPD_1479	HFDMAE**T**$_{356}$VELPK	Cell division protein FtsZ	Cell division
***	SPD_0342	EEFVE**T**$_{78}$QSLDDLIQEMR	Mid-cell-anchored protein MapZ	Cell division
***	SPD_0342	KEEFVE**T**$_{78}$QSLDDLIQEMR	Mid-cell-anchored protein MapZ	Cell division
***	SPD_0876	DHGFSQE**T**$_{56}$LK	Membrane protein MacP	Peptidoglycan biosynthesis
***	SPD_1849	TVSEE**T**$_{89}$VDLGHVVDAIK	Protein jag (SpoIIIJ-associated protein), putative	Unknown function
***	SPD_0091	EIVHLGLEDNDFDNDINPLE**T**$_{116}$GAYLSPK	UPF0176 protein SPD	Unknown function
**	SPD_1346	KAEQAGPETPTPA**T**$_{155}$ETVDIIR	Endolytic murein transglycosylase MltG	Peptidoglycan biosynthesis

Phosphorylated peptides that were identified in the WT in every replicate but in none of the replicates of the kinase mutant were considered as highly significant (***) putative target substrates of StkP. If the phosphorylation site was identified in two out of the bioreplicates of the WT but not in the kinase mutant, the protein was also considered to be a significant putative target of StkP (**). The phosphorylated amino acid is indicated as bold letter.

In this way a phosphorylation site on Thr201 of the cell division protein DivIVA was identified. Additionally, the early cell division mid-cell-anchored protein Z (MapZ), which tags the prospective cell division sites, was identified as a substrate of StkP as well. A phosphorylation site on Thr78 was reliably identified in all biological replicates of the WT strain, but not at all in the kinase mutant. Furthermore, the data show that the prokaryotic tubulin homologue FtsZ, an interaction partner of MapZ, is also phosphorylated in the presence of the kinase StkP. A phosphorylation site on Thr356 was detected in each replicate of the WT and on the other hand in none of the replicates of the Δ*stkP* mutant strain. Another phosphorylated protein identified in this study is MacP (SPD_0876). MacP is a membrane-anchored cofactor of the penicillin-binding protein PBP2a with involvement in peptidoglycan synthesis in *S. pneumoniae* (Fenton et al. 2018). Here, a phosphorylation on Thr56 was detected. Moreover, a phosphorylation on Thr12 was observed within the phosphocarrier protein PtsH in the WT strain but not in the mutant deficient for StkP. Nevertheless, serine phosphorylation in PtsH was identified in the Δ*stkP* mutant strain as well as in the WT strain on the positions Ser52 and Ser46. However, the lost threonine phosphorylation site in the Δ*stkP* mutant suggests a possible interaction of StkP and PtsH by phosphorylation. Additionally, proteins of unknown function, SPD_1849 (protein jag (SpoIIIJ-associated)) and SPD_0091 with detected phosphorylation sites in the WT but not in the kinase mutant were considered as putative StkP targets. A phosphoylation site within the endolytic murein transglycosylase MltG (Thr155) was detected in two out of three biological replicates of the WT strain and not found in the kinase mutant. In this case, MltG was considered as well as notable

putative target of StkP (labelled with ** in Table 6-1). All in all, the obtained MS data revealed obviously that phosphorylation of proteins on threonine is StkP dependent.

6.5.5. IDENTIFICATION OF PUTATIVE PHPP TARGETS AND TARGET SITES

Unlike StkP, the physiological role of the co-expressed PhpP is not well understood. One of the aims of this work was it to uncover previously unknown putative targets and target sites of PhpP. It is known that PhpP negatively controls the level of protein phosphorylation in the pneumococcus by direct dephosphorylation of target proteins and the cognate kinase StkP (Ulrych et al. 2016). For the identification of putative PhpP targets, phosphorylation sites that were found in at least two out of three bioreplicates in the phosphatase mutant Δ*phpP* were in the focus. Phosphorylation sites that were not found in any biological replicates of the WT, but in all replicates of the phosphatase mutant Δ*phpP*, were considered as highly significant putative target substrates of PhpP (labelled with *** in Table 6-2). Proteins fulfilling these criteria were the DNA mismatch repair protein MutL, phosphorylated on Ser119 and the hypoxanthine phosphoribosyltransferase Hpt with a phosphorylation site at Thr107. In principle, it is possible that target substrates of PhpP can also be identified phosphorylated in the WT strain. Therefore, those proteins were analyzed, too. In order to provide more confidence for that data, the counts of peptide spectrum matches (PSMs) per phosphorylated peptide and the PSMs of the corresponding not phosphorylated peptide were also taken into account in the analysis. Peptides, that were identified with a higher number of PSMs/phosphopeptide in the phosphatase mutant Δ*phpP* compared to the WT and additionally less or comparable PSM counts of the corresponding unphosphorylated peptide in Δ*phpP* were listed as notable putative targets as well as peptides with a higher phosphorylation incidence in the phosphatase mutant than in the WT (labelled with ** in Table 6-2). Among others, under these putative targets of PhpP were two proteins with a direct involvement in the process of cell division, the mid-cell-anchored protein Z (MapZ; phosphorylated peptide: 17 PSM counts in WT, 40 PSM counts in Δ*phpP*, unphosphorylated peptide: 0 PSMs for both strains) and the cell division protein DivIVA (phosphorylated peptide: 23 PSM counts in WT, 18 PSM counts in Δ*phpP*, unphosphorylated peptide: 79 PSM counts in WT, 20 PSM counts in Δ*phpP*). Both proteins, MapZ and DivIVA, were also identified as high confident target substrate of the kinase StkP. In addition to that, another notable putative target of PhpP is the DivIVA paralogue and cell cycle protein GpsB. (labelled with * in Table 6-2). Phosphorylation sites in GpsB were detected on Thr79 and Ser107. The phosphorylation site on Thr79 was exclusively identified in the phosphatase mutant but with only two PSMs in two of the three biological replicates (1 PSM for the unphosphorylated peptide). While in the WT the phosphorylation site on Ser107 was identified with at least 15 PSMs/phosphopeptide and 10 PSMs/unphosphorylated peptide, in the phosphatase mutant Δ*phpP* six PSMs/phosphopeptide and one PSM/unphosphorylated peptide were found. Moreover, under

the possible putative targets of PhpP were the endolytic murein transglycosylase MltG and the cell shape-determining protein MreC, both are participating in the peptidoglycan biosynthesis. Within MltG a phosphorylation site on Thr155 was detected with five PSM counts in the WT (unphosphorylated peptide: 4 PSM counts) and 15 PSM counts in the phosphatase mutant Δ*phpP* (unphosphorylated peptide: 6 PSM counts). Even three phosphorylation sites were identified in MreC in the WT and in the phosphatase mutant: Ser141, Ser155 and Ser157. Two PSM counts of the phosphorylated peptide were found in the WT strain and nine in the phosphatase mutant Δ*phpP*. The corresponding unphosphorylated form of the peptide was not detected in both strains. A third protein, that is supposed to participate in the peptidoglycan synthesis is MacP (SPD_0876). MacP was considered as a slightly significant putative target of PhpP in this work (labelled with * in Table 6-2), because in gerneral, the phosphorylated peptide of MacP was found with clearly more PSM counts in the WT compared to the phosphatase mutant on the other hand, the phosphorylation incidence was higher in the mutant Δ*phpP*. So, a phosphorylation site on Thr56 was identified in MacP with 55 PSM counts in the WT (unphosphorylated peptide: 43 PSM counts) and 24 PSM counts in the phosphatase mutant Δ*phpP* (unphosphorylated peptide: 7 PSM counts). Furthermore, the data indicate that SPD_1849, the putative protein Jag (SpoIIIJ-associated protein), is a target substrate of PhpP as well, because two phosphorylation sites, at Thr126 and Thr89, were detected in Δ*phpP* (labelled with ** in Table 6-2). While the peptide with the phosphorylation on Thr126 was identified with only one PSM in only one of the replicates of the WT, it was detected with 28 PSMs in the phosphatase mutant in two out of three bioreplicates. The corresponding unphosphorylated peptide was not identified in both strains. In addition to that, the peptide with the phosphorylation site on Thr89 counted 13 PSMs in the WT and 15 PSMs in the mutant, but zero PSMs for the unphosphorylated form in both cases. Other proteins that were included in the table of significant target substrates of PhpP (labelled with ** in Table 6-2) were: the phosphoglucomutase Pgm, the competence factor transport protein ComB and the NOL1/NOP2/sun family protein RsmF. Other phosphorylation sites or further proteins with detected phosphorylation sites in the phosphatase mutant and in the WT like LacA or AtpA could not be completely rejected from the putative PhpP target list, but were considered as not significantly prominent in this data set (labelled with [-] in Table 6-2).

Table 6-2: Putative targets and target sites of PhpP identified in this study (Hirschfeld et al. 2019).

Significance	Locus ID	Peptides inclusive phosphosites	Protein description	Biological process
***	SPD_0165	GEALPSIASVSVLTLLTAVDGA**S$_{119}$**HGTK	DNA mismatch repair protein MutL	DNA replication, recombination and repair
***	SPD_0012	HVLFVEDIIDTGQ**T$_{107}$**LK	Hypoxanthine phosphoribosyltransferase Hpt	Purine metabolism
**	SPD_1390	LGVLATPAVAYLVETEGASAGVMISA**S$_{101}$**HNPALDNGIK	Phosphoglucosamine mutase GlmM	Amino sugar and nucleotide sugar metabolism
*	SPD_1390	LGVLATPAVAYLVETEGA**S$_{93}$**AGV**M**ISASHNPALDNGIK	Phosphoglucosamine mutase GlmM	Amino sugar and nucleotide sugar metabolism
-	SPD_1390	LGVLATPAVAYLVETEGASAGVMI**S$_{99}$**ASHNPALDNGIK	Phosphoglucosamine mutase GlmM	Amino sugar and nucleotide sugar metabolism
**	SPD_1474	EVVSEVLGEPIPAPIEEEPID**MT$_{201}$**R	Cell division protein DivIVA	Cell division
*	SPD_1474	EVVSEVLGEPIPAPIEEEPIDM**T$_{201}$**R	Cell division protein DivIVA	Cell division
**	SPD_0342	KEEFVE**T$_{78}$**QSLDDLIQEMR	Mid-cell-anchored protein MapZ	Cell division
*	SPD_0342	EEFVE**T$_{78}$**QSLDDLIQEMR	Mid-cell-anchored protein MapZ	Cell division
*	SPD_0339	KPKPSPVQAEPLEAAI**T$_{79}$**SS**M**TNFDILK	Cell cycle protein GpsB	Cell division
*	SPD_0339	QILDN**S$_{107}$**DF	Cell cycle protein GpsB	Cell division
**	SPD_2045	GA**S$_{141}$**EN**M**LAIANGGLIG**S$_{155}$**V**S$_{157}$**K	Cell shape-determining protein MreC	Peptidoglycan biosynthesis
**	SPD_1346	KAEQAGPETPTPA**T$_{155}$**ETVDIIR	Endolytic murein transglycosylase MltG	Peptidoglycan biosynthesis
*	SPD_0876	DHGFSQE**T$_{56}$**LK	Membrane protein MacP	Peptidoglycan biosynthesis
**	SPD_0050	ASTSQQNETIASQNAAASQTQAEIGNLI**S$_{182}$**Q**T$_{184}$**EAK	Competence factor transport protein ComB	Two-component system
**	SPD_1326	HLN**C**FAGIMVTA**S$_{144}$**HNPAPFNGYK	Phosphogluco/mannomutase fam. protein Pgm	Glycolysis / Gluconeogenesis
*	SPD_1326	HLN**C**FAGIMV**T$_{142}$**ASHNPAPFNGYK	Phosphogluco/mannomutase fam. protein Pgm	Glycolysis / Gluconeogenesis
*	SPD_0790	AICEE**T$_{238}$**GNGHVQLFAK	Pyruvate kinase Pyk	Glycolysis / Gluconeogenesis
	SPD_0790	FNF**S$_{58}$**HGDHQEQGER	Pyruvate kinase Pyk	Glycolysis / Gluconeogenesis
*	SPD_1040	**S$_{46}$**IMGV**M**SLGVGQGADVTISAEGADADDAIAAISETMEK	Phosphocarrier protein PtsH	Carbohydrates, organic alcohols and acids
*	SPD_1040	SI**M**GV**MS$_{52}$**LGVGQGADVTISAEGADADDAIAAISET**M**EK	Phosphocarrier protein PtsH	Carbohydrates, organic alcohols and acids
*	SPD_1285	IVSHSVQDAALGEGEGCL**S$_{132}$**VDR	Peptide deformylase Def	Protein modification and repair
-	SPD_1053	EVVKDFLEKENFHLVDV**T$_{33}$**AEGQDFVDVTLAVAAEVNK	Galactose-6-phosphate isomerase subunit LacA	Galactose metabolism
-	SPD_1337	ELEAF**T$_{396}$**K	ATP synthase subunit alpha	Oxidative phosphorylation
-	SPD_1064	LVFAVDVG**T$_{115}$**NQLAWK	Hemolysin-like protein, putative	Pathogenesis
-	SPD_1524	LQIVSHTLEPNQQLP**T$_{36}$**VR	Transcriptional regulator, GntR fam. protein	Transcription factor
-	SPD_0592	ELPTV**M**DLLPSDIQ**S$_{92}$**DK	Pseudouridine synthase	tRNA and rRNA base modification
**	SPD_1233	FEPSFALGLALKP**S$_{371}$**QVEQ**S$_{376}$**VEIGQEAFVK	NOL1/NOP2/sun fam. protein	Unknown function
**	SPD_1849	HAS**T$_{126}$**ILEETGHIEILNELQIEEAMR	Protein jag (SpoIIJ-associated protein), putative	Unknown function
**	SPD_1849	TVSEE**T$_{89}$**VDLGHVVDAIK	Protein jag (SpoIIJ-associated protein), putative	Unknown function
*	SPD_0361	LLTESGFVTNEALQEC**T$_{109}$**K	Transcriptional regulator, putative	Unknown function
-	SPD_1308	**S$_{218}$**VAQIALAWSLAEGFLPLPK	Oxidoreductase, aldo/keto reductase fam. protein	Unknown function
-	SPD_0091	EIVHLGLEDNDFDNDINPLET**T$_{116}$**GAYLSPK	UPF0176 protein SPD	Unknown function

Phosphorylation sites that were not detected in the WT, but in each replicate of the ΔphpP mutant were considered as highly significant (***) putative target substrates of PhpP. Phosphopeptides with a higher number of PSMs/phosphopeptide in ΔphpP/WT and less or comparable PSM counts of the unphosphorylated peptide in ΔphpP as well as peptides with a higher phosphorylation incidence in the phosphatase mutant than in the WT are listed as notable (**) putative targets, too. Less significantly, but still mentionable putative target substrates of PhpP have more PSM counts for the identified unphosphorylated peptides and not remarkable more counts of PSMs for the phosphorylated peptides in ΔphpP in comparison to the WT (*). Proteins detected with phosphorylated peptides in ΔphpP are still in the putative PhpP target list, but were not significantly prominent in our data set (–). The phosphorylated amino acid is indicated as bold letter.

7. DISCUSSION

The presented work provides a complex comprehensive protein repository of high proteome coverage of the major human pathogen *S. pneumoniae* D39 inclusive identifications of serine, threonine and tyrosine phosphorylation. Due to the fact, that protein phosphorylation and dephosphorylation play a key role in the protein regulation of pathogenic organisms, it was of major interest to capture precise qualitative and quantitative information about the phosphoproteome of the pneumococcus. The pneumococcal eukaryotic-type Ser/Thr protein kinase StkP and the Ser/Thr phosphatases PhpP were in the focus of the investigations. Both proteins appear to constitute a functional signaling couple *in vivo* and likely belong to the same complex (Osaki et al. 2009). In order to figure out the global impact and physiological relevance of StkP and PhpP in the pneumococcus, a mass spectrometry based proteomic analysis with an emphasis on protein phosphorylation events which are linked to the regulation of cell morphology, growth and cell division (Massidda et al. 2013). Therefore, in this work the unencapsulated D39 serotype 2 strain D39Δ*cps* (WT) and two mutants, one deficient for StkP and the other one deficient for PhpP, were investigated.

7.1. EXPERIMENTAL DESIGN OF PROTEOMIC STUDY

7.1.1. EXPERIMENTAL STRAINS

In this work the unencapsulated mutant of D39 serotype 2 strain (D39Δ*cps* ≙ WT) and the kinase mutant D39Δ*cps*Δ*stkP* (Δ*stkP*) and the phosphatase mutant D39Δ*cps*Δ*phpP* (Δ*phpP*) were used as experimental strains. It is likely to raise the question that in the absence of the capsule the cell wall synthesis in pneumococci is probably compromised and some important targets of StkP and/or PhpP may directly or indirectly be unnoticed. However, the literature focussed on StkP/PhpP research comprises both, unencapsulated experimental strains (Rued et al. 2017; Ulrych et al. 2016) and encapsulated strains (Agarwal et al. 2012; Beilharz et al. 2012; Fleurie et al. 2012; Echenique et al. 2004). The experiments presented in this work were also performed using the unencapsulated D39 strain. The capsule gene cluster contains all gene encoding enzymes for the capsular polysaccharide (CPS) synthesis. Depending on the serotype, the number and complexity of the genes within the cluster differ. Besides in serotype 3 (Choi et al. 2016; Bender et al. 2003; Deng et al. 2000; Sørensen et al. 1990)), all pneumococcal CPS are anchored covalently to the peptidoglycan (Larson and Yother 2017; Bender et al. 2003; Deng et al. 2000; Sørensen et al. 1990). While some studies suggested that enzymes such as the phosphoglucomutase (PGM) are needed for pneumococcal fitness (Cieslewicz et al. 2001; Mollerach et al. 1998) others could not confirm these findings because of redundancies in the genome (Kadioglu et al. 2008; Hardy et al.

2001). In general, the absence or presence of the CPS does not influence significantly the defects of enzymes involved in cell elongation, cell division, teichoic acid biosynthesis or peptidoglycan turnover/biosynthesis. This has been shown, e.g. in studies analyzing the impact of the L,D- or D,D-carboxypeptidases, which are essential for the peptidoglycan turnover or of the TacL enzyme, that is important for anchoring the lipoteichoic acids (LTA) on the cell morphology of pneumococci (Heß et al. 2017; Abdullah et al. 2014). With this in mind, the unencapsulated WT and the derived mutants were considered as suitable experimental strains for this work.

7.1.2. Influence of cultivation medium and time-point of cell harvest

In order to get insights into the global proteome pattern of *S. pneumoniae* WT, the kinase mutant Δ*stkP* and the phosphatase mutant Δ*phpP*, pneumococci cultivated in two fundamentally different growth media and harvested in exponential and stationary phase were investigated. In general, a nutritionally rich broth such as THY medium supports a higher density growth and laboratory maintenance of the bacteria to investigate, here, pneumococci. Still, the exact composition of the components within the rich medium is unknown and can vary from batch to batch. However, in previously published studies investigations on pneumococcal StkP and PhpP were performed with pneumococcal strains grown in rich medium like THY, in casein-based semisynthetic C+Y medium or casein tryptone (CAT) medium or Trypticase soy broth (TSB) (Ulrych et al. 2016; Holečková et al. 2014; Agarwal et al. 2012; Beilharz et al. 2012; Sasková et al. 2007). So, in the first part of the work pneumococci for the global proteomic analysis were grown in THY medium. Nevertheless, for proteomic experiments it could be beneficial to use a reproducible medium of a clear defined chemical composition. Therefore, pneumococci were prepared for further investigations in the chemically defined RPMI 1640 medium supplemented with an extra of defined nutritive substances as well. As expected, pneumococci grown in THY medium reached higher optical densities (OD_{600} = 2.28 – 2.51) compared to those grown in RPMI *modi* medium (OD_{600} = 0.77 – 1.02). The reproducibility of growth of the biological replicates of each strain was indeed slightly better in pneumococci grown in RPMI *modi* medium, but this is can be considered as a marginal note, because the standard deviation was in all cases below three percent. Comparing the growth behavior of the WT and the mutant strains in THY medium, no remarkable differences were observed, which was not the case for the growth analysis in RPMI *modi* medium. Here, the phosphatase mutant revealed diminished growth in comparison to the WT and the kinase mutant, leading to the assumption that the loss of PhpP activity has a higher impact on pneumococci than the loss of the kinase activity. It is a commonly known fact, that influences of mutations or stress signatures become visible rather in minimal media than in rich media. Due to the limited nutrient supply in minimal media, pneumococci have to activate different metabolic pathways for the

production of required substrates for growth and survival. The morphological characterization of the WT and the mutant strains derived from cultures grown in both media also resulted in strong morphological effects in cultures grown in RPMI *modi* medium, especially in the phosphatase mutant. In THY medium grown pneumococci of both mutant strains revealed less severe abnormalities compared to those grown in RPMI *modi* medium and increased chain formation in comparison to the WT. The phenotypes observed in pneumococci cultivated in THY medium go along with phenotypes of *phpP* and *stkP* mutants described in earlier published studies (Ulrych et al. 2016; Agarwal et al. 2012). The phosphatase mutant grown in RPMI *modi* appeared very unusual compared to the phosphatase mutant derived from the non-encapsulated pneumococcal strain by Ulrych et al. (2016). But, in the studies published by Ulrych et al. 2016 and Agarwal et al. 2012 strains were cultivated in rich medium THY or in C+Y medium. Hence, it can be speculated that different phenotypic effects are not only strain-dependent but also cultivation media dependent. It has already been described that the medium used for cultivation can greatly influence the outcome of a physiological study in pneumococci (Hoyer et al. 2018). The global proteome analysis of the WT and the kinase and phosphatase mutant using a label free-quantification approach revealed an important observation which needed to be considered for further approaches. Conspicuous was the huge number of significantly differentially abundant proteins in the phosphatase mutant in comparison to the WT (659 proteins) in pneumococci cultivated in RPMI *modi* medium and harvested in the stationary growth phase. Additionally, it was surprising that changes within the cluster of ribosomal proteins occurred as well especially in the phosphatase mutant Δ*phpP* compared to the WT in RPMI *modi* and harvested in the stationary growth phase. It is already known that the regulation of the ribosome number is growth rate dependent (Tao et al. 1999). Here, it is important to recognize that the differences in the pattern of ribosomal proteins might occurred because the strains were not in the same state at the harvesting time-point. Both strains, Δ*phpP* and the WT were harvested two hours after entering the stationary growth phase. Nevertheless, the phosphatase mutant showed a remarkably slower growth compared to the WT or the kinase mutant strain in RPMI *modi* medium **(see 7.1.)**. Although the harvesting time-points of all strains were matched, variances in the proteome of the continuously slower growing phosphatase mutant due to growth effects cannot be excluded. Moreover, there is increased evidence that the nutritional status and metabolism affects the size and shape of bacteria (Vega and Margolin 2018).

Considering the summarized observations during the first part of this work, it was decided that the detailed analysis of changes in the proteome pattern of the mutants in comparison to the WT as well as the phosphoproteome analysis were performed with samples generated from pneumococci grown in RPMI *modi* medium and harvested in the exponential growth phase. A medium with known quantities of all ingredients, which is further closer to cell culture media for bacterial infection approaches was found to be a suitable for the fundamental proteomic investigations

performed in this work providing the basis for further research. In addition to that, in the exponential growth phase the growth conditions should be optimal for bacteria, because of the sufficient availability of nutrients and less competition of bacterial cells. Furthermore, it was ensured, that the reproducibility as a key element of proteomic investigations (Röst et al. 2015) was quite high regarding the bacterial growth within each strain in RPMI *modi* medium, the sample preparation and the quantification, seen during the analysis of the clustering of the biological replicates and the correlation.

7.1.3. LABEL-FREE QUANTIFICATION STRATEGY FOR GLOBAL PROTEOME ANALYSIS

The discovery of changes in protein abundances when comparing two or more physiological states of a biological system is a substantial but also challenging task in proteomics. For comprehensive, comparative investigations of proteome signatures a broad range of quantitative proteomics methods is available, including label-free, metabolic labeling, and isobaric chemical labeling using iTRAQ or TMT (Bantscheff et al. 2012; Li et al. 2012; Bantscheff et al. 2007). Each of the reported methods has its particular strength and weaknesses in terms of proteome coverage, quantification accuracy, precision, and reproducibility. The stable-isotope coding of proteins for example the metabolic labeling technique Stable Isotope Labeling by Amino Acids in Cell Culture (SILAC) (Ong et al. 2002) is still described as the most accurate relative quantification method in mass spectrometry (Chen et al. 2015). Due to the insertion of the stable isotope labels at the earliest time point of the experiment, during cell growth, this method provides lowest variations during the sample preparation workflow and the MS measurements and therefore high quantification accuracy (Lindemann et al. 2017). Within SILAC two biological populations are labelled respectively with light and heavy isotope amino acids, then cell lysates were combined and analyzed by LC-MS/MS. In the MS spectra, each isotope labelling peptide occurs as a doublet with specific mass differences. Afterwards, differential protein abundances between the two samples are calculated by comparing the intensity differences of the couple of isotope labelling peaks in MS. Still, SILAC depends on the metabolic incorporation of stable isotopes into the proteins during cultivation. A complete substitution of the natural amino acid with stable isotopic nuclei is required for high quantification efficiency. To reach almost complete incorporation (five to six generation times) of heavy labeled amino acids in SILAC standards, two subsequent pre-cultures of pneumococci are necessary (Hoyer et al. 2018). This is connected to a high cultivation effort, especially because pneumococci lagged growth with each inoculation step of fresh medium. Furthermore, the incorporation of the labelled standard raises the complexity of a sample and therefore sample fractionation and increased measurement time become indispensable. However,

the application of label-free quantification strategies combined with improved sensitive LC-MS systems is more and more successful in proteomics (Bantscheff et al. 2012).

To get an insight into the proteomes of the pneumococcal strains that have obviously different growth characteristics and phenotypes, in this work bacteria were cultivated in three independent biological replicates, each with one pre-culture to obtain reproducible growth and samples of the soluble proteins were analyzed in a relative label-free quantification (LFQ) experiment using GeLC-MS/MS. For data processing and statistical evaluation, the MaxQuant and Perseus software were used. The straightforward cultivation of pneumococci, the established sample preparation workflow and the ease of use of Maxquant LFQ, implemented in the freely available MaxQuant software, were the main reasons for choosing this quantification strategy. Moreover, the novel MaxQuant LFQ algorithm overcomes the problem of comparing sample fractions that have been slightly varying in handling during the sample preparation and analyzed with different MS performance with an included so called “Delayed normalization”. Protein abundance profiles were merged utilizing the maximum information from MS signals, considering the variation of the presence of quantifiable peptides from sample to sample. Another implemented algorithm extracts the maximum ratio information from peptide signals in random numbers of samples to obtain the highest possible quantification accuracy (Cox et al. 2014). Indeed, the results within this work showed that using the LFQ method a good quantification efficiency in the range of 83-96% for each strain comparison was achieved. In addition to that, the LFQ values of the biological replicates correlate as well under the different conditions ($R^2 \geq 0.94$).

7.1.4. Enrichment of phosphorylated peptides and spectral library based data evaluation for phosphoproteome analysis

In order to gather further information on the activity, targets and target sites of PhpP and StkP an in-depth analysis of the phosphoproteome was performed. The characterization of phosphorylated proteins in bacteria is a challenging analytical task since many of the phosphorylated proteins are low in abundance. Highly efficient enrichment procedures and sensitive mass spectrometry are required to decipher bacterial phosphoproteomes. An established method to analyze the phosphoproteome is the enrichment of phosphorylated peptides with TiO_2. The classical workflow includes a sample fractionation using strong cation exchange chromatography (SCX), which requires an amount of 50 mg protein per sample (Olsen and Macek 2009). In this work it could be shown that it is possible to decrease the necessary cell material down to five milligrams when omitting the SCX without losing phosphopeptide identifications. However, studies of bacterial phosphoproteomes applying classical database search approaches to enriched proteomic samples usually reported less than 150 phosphorylated proteins (Ge and Shan 2011). The identification of phosphorylated proteins in shotgun proteomics is not only impeded by the low abundance of target

substrates but also by the potential loss of phosphorylation signals during fragmentation resulting in a limited predictability of fragment patterns required for peptide-to-spectrum-matches within classical database searches (Kim et al. 2016). Although the field of phosphoproteomics has progressed at an amazing rate in data analysis developing novel algorithms for database search or software for phosphosite annotation (Suni et al. 2018; Lee et al. 2015; Jünger and Aebersold 2014), the advances contributed mostly to more accurate phosphoproteome analysis of eukaryotic systems (Riley and Coon 2016). Previous investigations on bacterial phosphoproteomes showed that the application of spectral libraries results in an improved sensitivity and reproducibility (Junker et al. 2018b). A benefit of spectral library searching is the consideration of major qualitative and quantitative information of fragment spectra, that have already been detected, reliably annotated and collected as applicable spectral libraries. Nevertheless, searching against a spectral library requires an a priori built high quality spectral library (Wiese et al. 2014). But afterwards, spectral library based data search has the major advantage of increased speed of analysis through less calculation power. Furthermore, the depth of spectrum-spectrum matching also supports the mapping of query spectra, which are not perfectly appropriate for classical database searching e.g. due to higher background noise. Especially for PTM analysis, spectral library searching is profitable as spectral features may be exploited for pattern matching besides the main ion series including neutral losses, unpredicted or unknown fragmentation and peak intensities observed in a particular analytical platform (Lam 2011; Lam et al. 2007).

In this work, a comprehensive and validated spectral library of the *S. pneumoniae* D39 with an emphasis on protein phosphorylations was constructed. This library includes a high number of samples (908 raw-files) generated from pneumococci of different growth stages, conditions and different growth media and different applied methods for sample preparation. So, the recently built spectral library contains 54,024 spectra of 23,512 peptides from 1,468 pneumococcal proteins. This results in a proteome coverage of 76.5 %. Moreover, 504 spectra of manually validated phosphorylated peptides belonging to 332 proteins are included in the library.

7.2. PROTEIN IDENTIFICATION AND LFQ ANALYSIS OF KINASE AND PHOSPHATASE MUTANT GROWN IN CHEMICAL DEFINED MEDIUM

In order to characterize the impact of StkP and PhpP on cellular pneumococcal physiology, a mass-spectrometry based label-free quantitative (LFQ) approach followed by an in-depth analysis of changes in protein abundances in pneumococci deficient for StkP or PhpP was performed. Among others, intresting notable changes in the protein abundances in the mutants Δ*stkP* and Δ*phpP* in comparison to the WT strain were observed in the functional categories of anions, cations and iron carrying compounds, two-component systems as well as in pyrimidine and purine metabolism.

7.2.1. Loss of function of PhpP increased abundance of proteins in phosphate uptake system Pst

Different from other bacterial species, for example *E. coli*, *B. subtilis*, or *C. crescentus*, that contain a single Pst transporter, the pneumococcus encodes two evolutionarily distinct phosphate ABC pump transporters, Pst1 and Pst2, that constitute a subtle biochemical adaptation of this microorganism for its growth and survival under different phosphate-limiting conditions in specific niches in the human host (Zheng et al. 2016; Botella et al. 2014; Moreno-Letelier et al. 2011; Hsieh and Wanner 2010; Lanie et al. 2007). The operons *pst*1-*pho*U1 and *pst*2-*pho*U2 are completely separated in the pneumococcal chromosome. A previous study demonstrated, that the Pst2 transporter is constitutively expressed under high and low Pi conditions. *Pst*1 level increases under low Pi concentrations (Zheng et al. 2016). The analysis of proteins belonging to the *pst*2 operon revealed a contrary regulation in Δ*phpP*/WT compared to Δ*stkP*/WT. Most striking was the observation that the ABC transporter complex PstSCAB, which is involved in the phosphate import in the pneumococcal cell, showed a higher abundance in key proteins attached to this mechanism in the phosphatase mutant Δ*phpP* whereas these proteins were less abundant in the kinase mutant Δ*stkP* compared to the WT. All proteins included in the pst2 operon, (PhoU2, PstA2, PstB2_1, PstB2_2, PstBC2 and PstS2) were identified and quantified in the phosphatase mutant Δ*phpP*. This was not the case within the kinase mutant. The putative phosphate ABC transporter protein PstC2 did not meet the criteria for quantification and the membrane channel protein PstA2 was not identified at all in the kinase mutant. Moreover, the phosphate-binding ABC transporter protein PstS1 of the pneumococcal inorganic phosphate uptake system 1 was identified only in the phosphatase mutant and not in the WT or in the kinase mutant. Further components of the pneumococcal *pst*1 operon were not detected in any of the investigated strains. From the obtained results it can be hypothesized, that especially the phosphatase PhpP affects the phosphate uptake system Pst2 and additionally probably also the second system Pst1. Pst1 and Pst2 transporters have to mediate Pi acquisition within different niches with vastly varying Pi concentrations in human hosts (Orihuela et al. 2001). Since PhpP is responsible for the dephosphorylation of phosphorylated StkP and its target proteins, it could be speculated that the lacking dephosphorylation of the kinase StkP could effect the homoestatic phospohorylation/dephosphorylation level in the pneumococcus. Consequently pneumococcal cells may react by increasing abundances of proteins involved in the Pst system. However, this would need further experimental investigation. Still, there is another hint, that indicates an influence of PhpP on the overall phosphate uptake in pneumococcal cells, because the Na/Pi-cotransporter II-related protein SPD_0443 have been exclusively identified in the Δ*phpP* mutant.

7.2.2. SIGNIFICANT CHANGES IN PROTEIN ABUNDANCE IN PURINE AND PYRIMIDINE METABOLISM IN Δ*PHPP* AND Δ*STKP* MUTANTS

The proteome analysis demonstrated that also proteins involved in the nucleotide metabolism of pneumococci were affected by the loss of function of StkP and escpecially PhpP. This focussed functional cluster comprises proteins assigned to the purine and pyrimidine metabolism. Purine and pyrimidine nucleotides are major energy carriers for cellular processes, subunits of nucleic acids, precursors for the synthesis of nucleotide cofactors and moreover they are used for the activation of precursors in the polysaccharide and lipid synthesis (Janczarek et al. 2018; Turnbough and Switzer 2008; Kilstrup et al. 2005). Furthermore it has been shown, that ESTKs and ESTKPs, like pneumococcal StkP and PhpP, are indispensible for the accurate balance of purine nucleotide pools and the regulation of purine biosynthesis (Rajagopal et al. 2005a). Amongst others, the data conducted in this study showed that proteins involved in the *de novo* purine biosynthesis (PurC, PurF, PurM) were "off" in the phosphatase mutant and less abundant in Δ*stkP*/WT. Consistently proteins belonging to the inosine monophosphate (IMP) *de novo* biosynthesis and adenosine monophosphate (AMP) biosynthesis were significantly less abundant and down regulated in both mutants in comparison to WT pneumococci. An earlier study focussed on investigations on the regulation of purine biosynthesis by a eukaryotic-type kinase in *Streptococcus agalactiae* the authors provided evidence that Stk1 deficient strains of group B streptococci are unable to maintain *de novo* purine biosynthesis and are growth arrested (Rajagopal et al. 2005a). Growth defects of the kinase mutant have not been observed in this work, but the phosphatase mutant showed diminished growth. Therefore, it could arise the hypothesis, that both, StkP and PhpP as a functional signalling couple affect the purine synthesis, whereas the influence of the loss of PhpP activity probably seems to cause stronger effects. Moreover, in this study, a contrary regulation was observed regarding the ribose-phosphate pyrophosphokinase (PrsA, SPD_0033). PrsA plays a crucial role in the biosynthesis of the central metabolite phospho-*alpha*-D-ribosyl-1-pyrophosphate and was significantly more abundant in the phosphatase mutant, but not significantly altered in abundance in the kinase mutant compared to the WT. This was also the case for the diadenylate cyclase DacA, part of the cyclic-AMP biosynthetic process. Unlike its eukaryotic counterpart StkP, there are only poor information about the physiological role of PhpP available. In contrast to StkP, PhpP lacks obvious regulatory domains (Dworkin 2015). One issue interpreting data generated from phosphatase mutant strains in terms of physiological involvements are complications in untangling direct effects of dephosphorylation events of single targets from indirect, supposedly pleiotropic global effects, resulting from dephosphorylation of the cognate kinase.

Figuring out the influence of PhpP and StkP on pneumococcal physiology changes within the protein pattern of the related process of pyrimidine biosynthesis were also in the focus. An earlier

published transcriptomic study indicated that a deletion mutant of an ESTK in *Staphylococcus aureus* affected the expression of genes included in regulons that are involved in purine and also in pyrimidine biosynthesis (Donat et al. 2009). As a result of the proteome analysis of the deletion mutants Δ*phpP* and Δ*stkP* performed in this work, significant changes in protein abundances in the functional cluster of pyrimidine metabolism were shown, especially in the phosphatase mutant. Intrestingly svereal key proteins of this pathway were found to be higher in their abuncance in the phosphatase mutant in comparison to the WT and not notably changed in the kinase mutant. So, the orotate phosphoribosyltransferase PurE and the orotidine 5'-phosphate decarboxylase PyrF, both with participance in the uridine monophosphate (UMP) *de novo* biosynthetic pathway, were found with a significant more abundance in Δ*phpP*/WT. This was also the case for the uracil phosphoribosyl transferase Upp, the pyrimidine-nucleoside phosphorylase Pdp, the uridine kinase Udk, the carbamoyl-phosphate synthase CarB, the bifunctional protein PyrR and the cytidylate kinase Cmk. In addition to that, the thymidine kinase Tdk was identified in all replicates of Δ*phpP* but not at all in the WT. In the kinase mutant all these proteins were not remarkable changed in their abundance. Up to date there are no detailed information about the influence of ESTPs on pyrimidine metabolism in bacteria explained.

Therefore, it can only be speculated, that less purine nucleotide synthesis and less ATP synthesis, ATP synthase epsilon chain (AtpC) and ATP subunit b (AtpF) were also significantly lower abundant in the phosphatase mutant, results in less CTP (cytidine-triphosphate), that act as an inhibitor of pyrimidine synthesis, which lead to a relative higher amount of key proteins involved in pyrimidine synthesis in pneumococci.

7.2.3. Interaction of StkP and PhpP with two-component systems

It is reported for a broad range of prokaryotes that ESTKs and ESTPs crosstalk with two-component systems (Burnside and Rajagopal 2012; Didier et al. 2010; Lin et al. 2009; Ulijasz et al. 2009). The obtained results of the comparative proteome analysis of the deletion mutants Δ*phpP* and Δ*stkP* revealed variations of protein abundances in the pneumococcal ComCDE and ComAB systems, both with critical functions for pneumococcal competence and involvement in sensing, activating and regulating the pneumococcal transformation machinery under specific environmental situations (Gómez-Mejia et al. 2017). Beside the response regulator ComE, which was significantly lower abundant in both mutants compared to the WT, the putative sensor histidine kinase ComD, the competence factor transporting ATP-binding/permease protein ComA and the competence factor transport protein ComB, that were confidentially identified in each bioreplicate of the WT, were not identified at all in the kinase mutant and in the phosphatase mutant. In exponentially growing pneumococcal cells the transient competence development is a stress response to alkaline pH conditions controlled by the two-component system ComDE (Claverys et

al. 2006). In this quorum sensing system, ComD, which is processed and secreted by the ABC transporter system ComAB, senses the extracellular accumulation of a competence stimulating peptide and if this reaches a critical concentration, the response regulator ComE will be phosphorylated by ComD and the transcription of *comCDE*, *comAB* and *comX* is initiated (Martin et al. 2010; Claverys and Havarstein 2002; Håvarstein et al. 1995). Subsequently ComX initiates the transcription of genes, which products participate in DNA binding, uptake and recombination (Lee and Morrison 1999). According to that, the proteome data also revealed that amongst others the competence proteins CelA, CglA and CglC were "off" in the kinase mutant as well as in the phosphatase mutant in comparison to the WT. It is reported, that the kinase StkP is additionally involved in the activation of the *comCDE* operon and thus regulates pneumococcal competence. Furthermore, it was shown that pneumococci deficient for StkP do not develop natural competence (Echenique et al. 2004). Moreover, it is suggested, that the positive regulation of *comCDE* expression by StkP is balanced by the repression through the two-component system CiaRH (Mascher et al. 2003). In case of the CiaRH (competence induction and altered cefotaxime susceptibility) system, a contrarily regulation in Δ*phpP*/WT and Δ*stkP*/WT was noticed in the present study. While the DNA-binding response regulator CiaR was significantly more abundant in the phosphatase mutant it was significantly less abundant in the kinase mutant in comparison to the WT. CiaH, the corresponding sensor histidine kinase, was not identified in all strains. Since sensor histidine kinases are only low in abundance and located in the membrane, it is not surprising, that most of them were under the detection limit in this approach. Still, it might be the case that the lower abundance of proteins belonging to the ComCDE and ComAB systems is a direct effect of the absence of StkP in the kinase mutant, whereas in the phosphatase mutant it could be an indirect effect due to the lack of PhpP and the hindered dephosphorylation of autophosphorylated StkP. In addition to that the lack of dephosphorylation of StkP in the phosphatase mutant could be the reason for the higher abundance of the response regulator CiaR in reaction of the imbalance of phosphorylated/active and dephosphorylated/inactive StkP. In an other study it was reported, that CiaR causes an upregulation of the virulence factor HtrA (DegP) (Stevens et al. 2011). This could not be confirmed within this study. Here, the serine protease DegP was significantly lower abundant in Δ*phpP*/WT and slightly higher abundant in Δ*stkP*/WT.

An influence of the abcense of PhpP and StkP was observed in the LiaRS two-component system, too. As already mentioned, LiaRS also participates in regulating the competence process by responding to peptidoglycan cleavage by LytA, CbpD and LytC murein hydrolases (Gómez-Mejia et al. 2017; Eldholm et al. 2010). The choline binding protein CbpD was reliable identified in the WT but it was "off" in the mutants Δ*phpP* and Δ*stkP*. The abundance of the autolysin/N-acetylmuramoyl-L-alanine amidase LytA was significantly lower in both mutants in comparison to the WT as well. Moreover, the DNA-binding response regulator LiaR was significantly less abundant in Δ*phpP*/WT and Δ*stkP*/WT. The cognate sensor histidine kinase LiaS was only

quantified in Δ*phpP* and WT, but no appriciable changes in abundance were noticed. Nevertheless, until now, the activation signal of the LiaRS system remains unknown and only poor information about it can be found in literature.

However, changes in protein abundances were indeed observed for a further pneumococcal two-component system, that is involved in the regulation of competence, namely VicRK (TCS02, WalRK). The VicX ancillary protein encoded in the *vicRK* operon was significantly lower abundant in the kinase mutant and less abundant in Δ*phpP*/WT as well. While there were no differences in the abundance of the sensory box sensor histidine kinase VicK in the kinase mutant, this protein was significantly more abundant in the phosphatase mutant compared to the WT strain The DNA-binding response regulator VicR was only slightly higher in abundance in Δ*phpP*/WT and less abundant in Δ*stkP*/WT. Importantly, the essentiality of VicR in *S. pneumoniae* is due to its positive regulation of a gene encoding a putative peptidoglycan hydrolase (PcsB, SPD_2043) that plays a critical role in cell wall biosynthesis and cell division and therewith influences pneumococcal morphology. It is reported that the protein PcsB interacts with the cell division complex FtsE/FtsX (Sham et al. 2011). PcsB was detected in all three strains. In the phosphatase mutant, PcsB was higher in abundance, while no changes were observed in the kinase mutant strain. The cell division proteins FtsE (ATP-binding) and FtsX were significantly less abundant in the kinase mutant Δ*stkP* compared to the WT. Surprisingly, no significant changes were detected in the abundance of FtsE or FtsX in the phosphatase mutant Δ*phpP*/WT, although this mutant was characterized by stronger morphological effects and impaired cell division and separation. Referring to literature it is the deletion of the *pcsB* gene, that causes abnormal mutation and not an overexpression (Bartual et al. 2014; Giefing-Kröll et al. 2011). Looking on this issue in more detail, there is a difference between the earlier published studies including morphological analysis of *pcsB* mutants and *phpP* and *stkP* mutants and the performed analysis presented in this work. In the studies published by Giefing-Kröll et al. 2011, Bartual et al. 2014 or Agarwal et *al.* 2012 and Ulrych et *al.* 2016 pneumococcal strains were cultivated in rich medium THY or in C+Y medium. In this work, all investigations were performed in cultures grown in chemically defined RPMI cell culture medium. It has already been described that the medium used for cultivation can greatly influence the outcome of a physiological study in pneumococci (Hoyer et al. 2018). Hence, it can be speculated that different phenotypic effects as well as proteomic responses, also regarding the slightly higher abundance of PcsB in the recent dataset are not only strain-dependent but also cultivation media dependent. Still, a phenotype similar to that observed in our study was described by Agarwal et *al.* 2011 for an ESTP deletion mutant instead of a *pcsB* mutant in *S. pyogenes,* also showing multiple asymmetric and parallel septa formation comparable to the observed morphological observations.

7.3. COMPARATIVE PHOSPHOPROTEOMIC ANALYSIS OF ΔSTKP, ΔPHPP AND WT

In consideration of the obtained LFQ results it an be suggested that PhpP and StkP are involved in the regulation of pneumococcal morphogenesis by modulating proteins participating in cell division and associated processes like peptidoglycan biosynthesis through balancing the phosphorylation and dephosphorylation level of specific target proteins. Already detected target substrates of StkP *in vivo* are DivIVA, GlmM, PpaC, MurC, MapZ, and StkP itself (Hammond et al. 2019; Fleurie et al. 2014b; Falk and Weisblum 2013; Nováková et al. 2010; Osaki et al. 2009). Nonetheless, most of the target sites of StkP remain to be identified. Still, the role and involvement of the cognate phosphatase PhpP is not well described. In order to be able to correlate the phenotypic observations from the electron microscopic analysis to protein phosphorylation patterns, a gel-free phosphopeptide enrichment with TiO_2 followed by MS/MS measurement and spectral library based data evaluation was performed. Above all, a major interest of this work was the discovery of more possible new targets/target sites of the pneumococcal kinase StkP and especially of the phosphatase PhpP.

For getting an overview of the phospho-identifications, phosphorylated peptides inclusive unique phosphosites that were found in three out of three biological replicates in each strain were in the focus. All in all, 38 phosphosites, 18 on serine, 18 on threonine and two on tyrosine within 35 peptides belonging to 26 proteins were highly confidential identified in the dataset. In general, multiple amino acid residues can be targets for phosphorylation and therewith affect protein function. Protein phosphorylation in eukaryotes commonly occurs on serine, threonine and tyrosine amino acids at an estimated ratio of 1000:100:1 (Raggiaschi et al. 2005). In contrast to the serine/threonine and tyrosine kinase cascade systems in eukaryotes, signal transduction in prokaryotic organisms is predominantly maintained by two-component systems. Nevertheless, earlier published studies have shown that eukaryotic- ESTKs as well as ESTPs function in a wide range of bacterial species and in parallel or overlapping signaling networks thereby constituting another important signaling mechanism for the regulation of different cellular functions (Janczarek et al. 2018; Zhang et al. 2017; Shi et al. 2014; Wright and Ulijasz 2014). Still, they are only less in abundance and therefore identification numbers of Ser/Thr/Tyr phosphorylations in bacteria are much lower. Furthermore, the lack of reproducibility due to the immense sample preparation effort decreases high-confident identification numbers. Moreover, it was already observed in other proteomic studies of bacterial phosphoproteomes, that tyrosine phosphorylations were under-represented, perhaps resulting from the method of phosphopeptide enrichment (Soares et al. 2013; Macek et al. 2008). However, to pinpoint targets of StkP and PhpP, phosphorylation events on serine and threonine were in the spotlight of the performed analysis.

7.3.1. IDENTIFICATION OF PREVIOUSLY OBSERVED STKP TARGETS AND DETECTION OF PUTATIVE NEW TARGET SUBSTRATES

The pneumococcal kinase StkP has been extensively investigated. It is known that StkP localizes to the division sites and participates in the regulation of cell division in pneumococci. In previous studies it was demonstrated that pneumococci with *stkP* mutations revealed disrupted cell wall synthesis and displayed elongated morphologies with multiple, often delocalized, cell division septa. So, it arises the assumption that StkP modulates cell wall synthesis and cell division and thus contributes to the characteristic ovoid shape of the pneumococcus (Zucchini et al. 2018; Fleurie et al. 2014b; Beilharz et al. 2012). This assumption is supported by several studies mentioned before, applying *in vitro* and *in vivo* phospho-assays and identified target proteins of StkP like DivIVA, MapZ and others, all involved in cell division or peptidoglycan synthesis. To uncover targets of StkP with the presented mass-spectrometry based proteomic approach the obtained phospho-data were filtered for phosphorylated peptides detected in the WT in every replicate but in none of the replicates of the kinase mutant. This way of data treatment was executed inconsideration of the fact that the kinase StkP is disrupted in the mutant and therfore it should be unable to phosphorylate its targets anymore, which is not the case for the WT. Finally, the presented data support the assumption of privious studies that the cell division proteins DivIVA and MapZ are targets of the StkP. Within the analysis of the phosphopeptide-enriched samples, a phosphorylation site on Thr201 of DivIVA was detected. This phosphorylation site of DivIVA was already described in an earlier study of the phosphoproteome of *S. pneumoniae* (Sun et al. 2010). In addition to that, other studies of the pneumococcus revealed that phosphorylation of proteins on threonine is StkP dependent (Fleurie et al. 2012; Nováková et al. 2010). The results of this work indicate that the prokaryotic tubulin homologue FtsZ, which is involved in the formation of the cell division septum and interacts with MapZ, is directly phosphorylated by StkP. A phosphorylation site on Thr356 of FtsZ was identified in all replicates of the WT but in none of the replicates of the Δ*stkP* mutant strain. Since identifications in two out of three biological replicates can also be considered as confidential, the data evaluation was extended. So, a phosphoylation site within the endolytic murein transglycosylase MltG on Thr155 was identified in two out of three WT bioreplicates but not at all in the Δ*stkP* mutant. Thus, MltG could be a new and notable putative target of StkP. MltG also participates in the peptidoglycan synthesis in pneumococci, therefore it could strengthens the assumption that StkP plays a major role in modulating proteins involved in pneumococcal morphogenisis. Another phosphorylated protein that was identified in this study is MacP (SPD_0876). MacP is a membrane-anchored cofactor of the penicillin-binding protein PBP2a involved in peptidoglycan synthesis in pneumococci, too (Fenton et al. 2018). A phosphoproteome study by Sun *et al. in* 2010 (Sun et al. 2010) led to the detection of a phosphorylation site on Thr32 in the until that date unknown protein SPD_0876. In

2018, Fenton *et al.* (Fenton et al. 2018) reported the identification of MacP as a substrate of the kinase StkP. Moreover, the phosphorylation at residue Thr32 was confirmed by performing *in vitro* approaches including antiphospho-threonine immunoblots. Here, in this work, phosphorylation in MacP was detected *in vivo*. Interestingly, the identified phosphorylation site is located on a different position than described in the previous publication. Fity-five peptide spectrum matches (PSMs) of the peptide with the phosphorylation on Thr56 were found in the WT and 43 PSM counts were assigned to the corresponding unphosphorylated peptide. Regarding these numbers, it can be considered as a highly significant putative target site of StkP. Going back to the LFQ data, the MacP protein was found to be significantly higher in abundance in the kinase mutant in comparison to the WT. Accordingly, it can be speculated that the inability of protein activation by the inactive StkP leads to the accumulation of the protein in the kinase mutant.

Finally, there are other proteins that have already been described as StkP targets like MurC and GlmM were not found within the phosphoproteome analysis in this study. Surprisingly GlmM, which was identified *in vitro* and *in vivo* as StkP target in earlier published studies (Nováková et al. 2010; Nováková et al. 2005), was excluded from the StkP target list generated in this work. Within the MS-based in-depth phosphoproteome analysis, phosphorylated peptides of GlmM were identified in all biological replicates of the Δ*stkP* mutant including phosphorylation sites on Ser93, Ser99 and Ser101 with three to 200 PSM counts for the specific phosphorylated peptides. Therefore, it can be speculated that maybe another, yet unknown and not annotated kinase in D39 might be responsible for the phosphorylation of further proteins.

All in all, the obtained results from the performed phosphoproteome analysis led to the extension of the list of putative target and target sites of StkP and offers the opportunity for more specific investigations of the involvement of the mode of action of StkP and the potential target proteins.

7.3.2. PHOSPHOPROTEOME ANALYSIS UNCOVERED PREVIOUSLY UNKNOWN PUTATIVE TARGETS OF PHPP

In contrast to StkP there are only few things described about the cognate phosphatase PhpP. StkP and PhpP appear to constitute a functional signaling couple *in vivo* and likely belong to the same complex (Osaki et al. 2009). It is known that PhpP negatively controls the level of protein phosphorylation in *S. pneumoniae* by direct dephosphorylation of target proteins and by dephosphorylation of the kinase StkP (Ulrych et al. 2016). In case of the StkP, it is assumed, that the kinase stays in the phosphorylated form in the phosphatase mutant. Here, it has to be mentioned that the phosphorylated form of StkP was not identified within the phosphoproteome dataset. Nevertheless, this result can be explained by the low abundance of the StkP protein (Figure 7-1). The protein quantification here was done with whole protein extracts of pneumococci. Since the StkP is a membrane protein, it is likely to assume, that it is underrepresented in the extract in

comparison to the real appearance. This should not be relevant for the investigation of the targeted proteins, because the active center of the kinase is located in the intracellular space, therefore the precondition to identify the target proteins is fulfilled. In case of PhpP, which is located in the cytoplasm this is not worth mentioning (Beilharz et al. 2012).

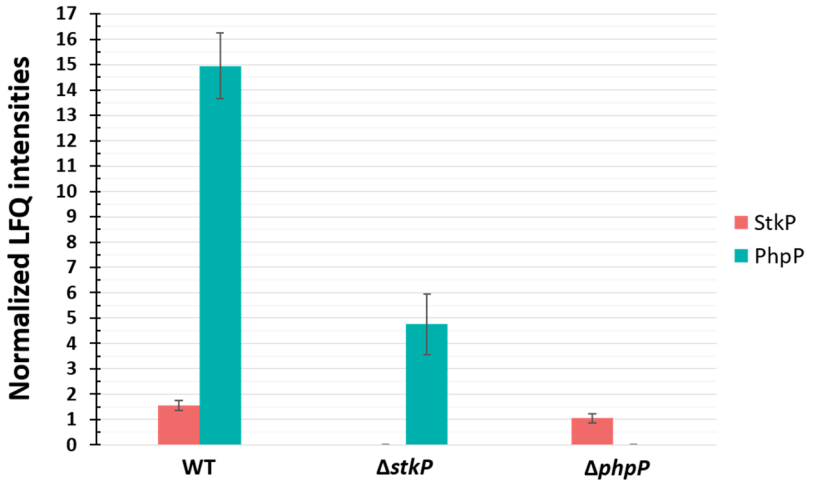

Figure 7-1: MaxQuant-LFQ intensities of the proteins StkP and PhpP in the investigated strains.

However, in a previous study it was described that PhpP dephosphorylates MapZ, which is a target of StkP (Fleurie et al. 2014a). In another approach towards the characterization of the pneumococcal phosphatase PhpP it was also suggested that PhpP and StkP cooperatively regulate cell division of *S. pneumoniae*, moreover, the authors revealed a novel PhpP substrate, SPD_1849, a putative RNA binding protein Jag (SpoIIIJ-associated protein) (Ulrych et al. 2016). Yet, there are no mass spectrometry based phosphoproteomic investigations focusing on the identification of multiple possible new target substrates presented in the earlier and recently published literature. A reason for that could be the already mentioned difficulty to note direct effects of dephosphorylation events of individual targets, because it is not clearly distinguishable from indirect effects caused by the dephosphorylation of the co-transcribed kinase StkP. However, the performed mass spectrometry based comparative phosphoproteome analysis aimed at providing a collection of proteins, which are worth to be considered as possible target substrates of PhpP. To set up a suitable strategy for the data analysis, it was considered that the absence of PhpP activity in the pneumococcal cell results in the loss of dephosphorylation of its direct targets in the mutant. With this in mind, it was expected, that the targets of PhpP have a higher phosphorylation level compared to the WT or, proteins, that were not phosphorylated in the WT are found with a phosphorylation in the phosphatase mutant. So, first of all, the phospho-data generated in this work were checked for phosphorylation sites, which were not identified in the WT, but in all replicates of the phosphatase mutant. Proteins, that meet these criteria, were threatened as highly significant potential target substrates of PhpP. This category of putative target proteins include the DNA

mismatch repair protein MutL (Ser119) and the hypoxanthine phosphoribosyltransferase Hpt (Thr107). Due to the fact that the target substrates of PhpP can also be found phosphorylated in the WT, those proteins were analyzed as well. In addition to that, the identification of putative PhpP targets was extended regarding phosphorylation sites that were found in at least two out of three biological replicates in Δ*phpP*. To provide more confidence, a quantitative dimension was necessary to inspect, whether the phosphorylation incidence is higher in the phosphatase mutant compared to the WT. For this reason, the counts of peptide spectrum matches (PSMs) per phosphorylated peptide and PSMs of the corresponding unphosphorylated peptide were included in the analysis. Phosphopeptides with a higher number of PSMs/phosphopeptide in the phosphatase mutant compared to the WT and less or comparable PSM counts of the unphosphorylated peptide in Δ*phpP* were categorized as notable putative targets of PhpP. Within this group of putative phosphatase targets are four proteins with a direct involvement in cell division (MapZ, DivIVA) and peptidoglycan biosynthesis (MltG, MreC). An important implication of these findings is that it may link the abnormal cell morphology of the Δ*phpP* pneumococci to the phosphorylation status of critical cell division proteins. Additionally, MapZ and DivIVA are targets of StkP, too. These observations again support the assumption that PhpP and StkP are acting as a functional signaling couple as previously suggested (Osaki et al. 2009) and participate in the process of cell division and morphogenesis in *S. pneumoniae*. Another, but only slightly significant putative target of PhpP is, beside others, the cell cycle protein GpsB. For the DivIVA paralog GpsB it was reported that it is necessary for correct StkP localization and activity and hence, for StkP-dependent phosphorylation of DivIVA. Up to date, a phosphorylation site in GpsB was not determined (Fleurie et al. 2014a). Surprisingly, in the evaluated proteome data set, phosphorylation sites in GpsB were detected on Thr79 and Ser107. This finding provides a strong hint that phosphorylation might occur in GpsB itself as well. According to these observations, GpsB seems to be dephosphorylated by the phosphatase PhpP, but it is not directly phosphorylated by StkP. In the StkP deficient mutant the phosphorylation site in GpsB on Ser107 was detected confidentially in two out of three biological replicates. In *Bacillus subtilis* for example, it is known that the Ser/Thr kinase PrkC, also localized at the division septum, phosphorylates GpsB on Thr75 (Pompeo et al. 2015). Nevertheless, more experimental assays are necessary to confirm the putative phosphorylation site or sites in GpsB in the pneumococcus. In a recent study it is reported that GpsB functions as an adapter for multiple cell wall enzymes in *B. subtilis, Listeria monocytogenes* and importantly in *S. pneumoniae*, too. In this manner, an interaction with the cell shape-determining protein MreC was confirmed in the pneumococcus (Cleverley et al. 2019). The data of the mass spectrometry based phosphoproteome analysis conducted in this work provide evidence, that MreC is phosphorylated in the pneumococcus and its dephosphorylation is executed by the phosphatase PhpP. In the WT and in the phosphatase mutant, even three phosphorylation sites were confidentially identified in MreC: Ser141, Ser155 and Ser157, meanwhile, the

unphosphorylated counterpart of the peptide was not detected at all in both strains. Unfortunately, the membrane spanning cell wall synthetic factor MreC is until now only poorly characterized. Surprisingly, each of the detected phosphorylation sites is located in the periplasmic like region according to the structure model of MreC (Lovering and Strynadka 2007). This arises the question, whether a phosphorylation of MreC in this part is possible and whether the result is reliable, this has to be clarified. Furthermore, an intersting point is, that MreC was not found to be a direct target substrate of the kinase StkP. This lead to the question whether PhpP, which mainly dephosphorylates the StkP and its targets, is truly the only present Ser/Thr kinase in the pneumococcus. There are indeed information about another predicted, but yet uncharacterized serine/threonine protein phosphatase (SPD_1061) in *S. pneumoniae* D39 with yet unknown function, but there were no sequence similarities of PhpP to SPD_1061 or any other unknown and putative protein (Agarwal et al. 2012). The missing sequence homologies were confirmed within this work as well. Moreover, it was also examined, that conserved catalytic motifs (I-XI), that are characteristic for the eukaryotic-like PP2C family of phosphatases, are missing in SPD_1061, too. Clearly, further research will be required to uncover which enzyme or what kind of interaction could be responsible for the phosphorylation in the protein MreC.

In addition to that and according to the study of Ulrych et al. (2016), the observed results indicated that SPD_1849, the putative protein Jag (SpoIIIJ-associated protein), is a direct target of PhpP. Within the protein Jag, two phosphorylation sites, at Thr126 and Thr89, were identified in the phosphatase mutant strain. This observation is circumstantiated by the number of PSMs for the peptide including the phosphorylation on Thr126, because it was identified with a single PSM in only one replicate of the WT whereas it was reliable detected with 28 PSMs in the phosphatase mutant in two out of three bioreplicates. Furthermore, the unphosphorylated form of this peptide was not identified in both strains. This result provides strong evidence, that the detected phosphorylation site on Thr126 is targeted by PhpP. On the other hand, there is a second peptide with an identified phosphorylation site on Thr89 counted 13 PSMs in the WT and 15 PSMs in the mutant. Interestingly, exactly this phosphorylation site, which is considered as less significant in this work, was just described in the non-proteomic study of Ulrych et *al.* (2016). From the perspective of the presented data it is possible that both phosphorylation sites are target site for pneumococcal PhpP. Further research of this issue would surely be of interest. Nevertheless, it is possible to conclude, that the presented highly confident phosphorylation site identifications can hint to yet unknown dephosphorylation targets of the pneumococcal PhpP and thus provide the basis for a deeper insight into the regulatory mechanisms of this phosphatase.

However, phosphorylation and dephosphorylation events are dynamic processes and can change rapidly under varying environmental conditions (Calder et al. 2016; Macek et al. 2009). Certainly, not all of the targets and target sites for phosphorylation dephosphorylation could have been detected within this MS based approach aiming at an extension of only to a minor agree available

phosphoproteomic data for *S. pneumoniae* with an emphasis on the StkP/PhpP couple. On a wider level, a more detailed and complete description of proteins targeted for phosphorylation and dephosphorylation events can be observed when combining different techniques, for example structural analyses of possible target proteins, phenotypic characterizations of different gene mutants for possible targets or well established phosphoactivity assays.

7.4. CONCLUSION

In summary, the results conducted in this work provide a complex and comprehensive protein repository of high proteome coverage of *S. pneumoniae* D39 containing confidential identifications of serine/threonine/tyrosine phosphorylations, that will facilitate future investigations of this important human pathogen. The comparative global proteome analysis of the generated pneumococcal kinase and phosphatase mutants demonstrated once more the essential role of ESTKs and ESTPs in the functional protein regulation of the pneumococcus. Within the LFQ approach, changes in protein patterns were observed in diverse biological processes in both mutants lacking PhpP or StkP activity. Moreover, the acquired data revealed that the loss of function of especially the phosphatase PhpP resulted in an increased abundance of proteins attached to the pneumococcal phosphate uptake system Pst. Furthermore, the observed data showed that the activity loss of either PhpP or StkP influenced proteins belonging to the pneumococcal two component-signaling systems ComDE, CiaRH, LiaRS and VicRK. Significantly altered protein abundances in the purine and pyrimidine metabolism in Δ*phpP* and Δ*stkP* mutants also refer to the more promiscuous mode of action of serine/threonine kinases compared to histidine kinases in common bacterial two-component systems. Still, the rsults indicate that there are several bottle necks during the data analysis regarding direct involvements of especially the phosphatase PhpP due to numberous pleiotropic effects or indirect effects caused by the activity or inactivity of the co-transcribed kinase StkP. However, recent studies of the StkP/PhpP couple demonstrated that both play an essential role in cell growth, cell division and cell separation. Concordantly, growth analyses and the phenotypic characterization of the mutants by electron-microscopy figured out that Δ*phpP* and Δ*stkP* possess obviously different growth characteristics and abnormal cell division and cell separation. These observations could not be explained by differences in protein abundances on a global scale. Thus, in order to extend the available knowledge about PhpP and StkP regarding their influence in pneumococcal morphogenesis (Figure 7-2), perhaps by modulating proteins participating in this mechanism, an in depth analysis of the phosphoproteome was indispensable.

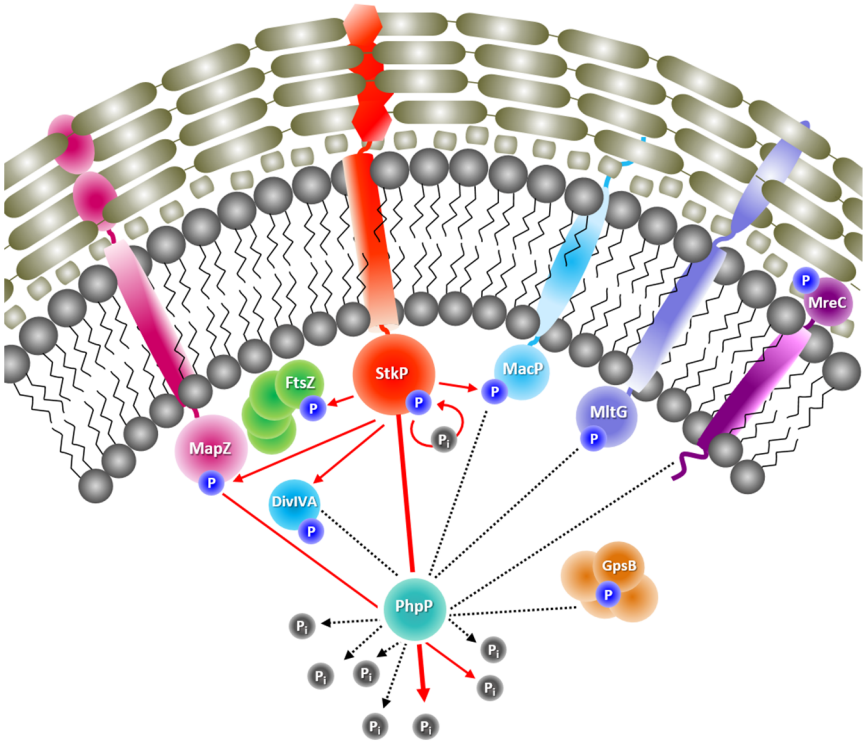

Figure 7-2: Identified putative target proteins of StkP and PhpP involved in pneumococcal cell division and peptidoglycan synthesis (Hirschfeld et al. 2019). Phosphorylated proteins participating in pneumococcal morphogenesis are presented. It is known, that StkP autophosphorylates and PhpP dephosphorylates StkP. StkP also phosphorylates the cell division proteins FtsZ and DivIVA as well as MapZ and MacP, both involved in peptidoglycan synthesis. For MapZ it was shown, that it is dephosphorylated by PhpP (red arrows = known interactions from literature, partially validated in this study). Data from this study also provide hints for an interaction of PhpP with the cell division proteins DivIVA and GpsB and moreover with MacP, MltG, and MreC, which are also participating in peptidoglycan synthesis (black dashed lines = putative interactions derived from this study).

Up to date, studies of bacterial phosphoproteomes applying classical database search approaches usually reported less than 150 phosphorylated proteins. Here, slight modifications of the workflow for phospho-sample preparation and the application of the recently build combined spectral library, including phospho-enriched samples and classical proteome samples of numerous different datasets highly enhanced reliable and reproducible identification of phosphorylated proteins in this work. Finally, already described targets and target sites of the pneumococcal StkP and PhpP, detected and characterized in previous studies applying different methodologies, have been identified as a proof of principle applying the presented MS based phosphoproteome approach. Particularly, the obtained results remarkably extended the list of potential targets and target sites of PhpP. All in all, the presented data provide an extensive source of information for future investigations of new possible targets and target sites of the pneumococcal StkP/PhpP couple.

7.5. PUBLICATION OF MAIN RESULTS

The main results of this PhD thesis addressing the impact of StkP/PhpP on pneumococcal physiology applying proteomics with an emphasis on phosphorylation and dephosphorylation events were summarized and published in the comprehensive research article "Proteomic Investigation Uncovers Potential Targets and Target Sites of Pneumococcal Serine-Threonine Kinase StkP and Phosphatase PhpP" (Hirschfeld, C.; Gómez-Mejia, A.; Bartel, J.; Hentschker, C.; Rohde, M.; Maaß, S.; Hammerschmidt, S.; Becher, D. 2020. Front. Microbiol., doi: 10.3389/fmicb.2019.03101). In particular, the publication is based on the results from the chapters 6.4. (6.4.1., 6.4.2. (6.4.2.1. – 6.4.2.3.)) and 6.5. (6.5.2. – 6.5.5.). Within the framework of this manuscript, the MS proteomic data, the spectral library and the MaxQuant outputs have been deposited to the ProteomeXchange Consortium via the PRIDE partner repository (Vizcaíno et al. 2016) with the dataset identifier PXD015268. Annotated MS/MS spectra of the spectral library search results can be viewed with the help of the identified peptide sequence and the freely available MS-Viewer tool, accessible through the Protein Prospector suite of software at the following URL: http://prospector2.ucsf.edu/prospector/cgi-bin/msform.cgi?form=msviewer, with the search key: t3hpidqwm8.

8. PUBLICATIONS

8.1. PEER-REVIEWED SCIENTIFIC ARTICLES

Hirschfeld, C., Gómez-Mejia, A., Bartel, J., Hentschker, C., Rohde, M., Maaß, S., Hammerschmidt, S., & Becher, D. (2020). Proteomic Investigation Uncovers Potential Targets and Target Sites of Pneumococcal Serine-Threonine Kinase StkP and Phosphatase PhpP. *Frontiers in microbiology*, *10*, 3101. https://doi.org/10.3389/fmicb.2019.03101.

Schultz, D., Zühlke, D., Bernhardt, J., Francis, T. B., Albrecht, D., **Hirschfeld, C.**, Markert, S., & Riedel, K. (2020). An optimized metaproteomics protocol for a holistic taxonomic and functional characterization of microbial communities from marine particles. *Environmental microbiology reports*, 10.1111/1758-2229.12842. Advance online publication. https://doi.org/10.1111/1758-2229.12842.

Quintieri, L., Zühlke, D., Fanelli, F., Caputo, L., Liuzzi, V. C., Logrieco, A. F., **Hirschfeld, C.**, Becher, D., & Riedel, K. (2019). Proteomic analysis of the food spoiler *Pseudomonas fluorescens* ITEM 17298 reveals the antibiofilm activity of the pepsin-digested bovine lactoferrin. *Food microbiology*, *82*, 177-193. https://doi.org/10.1016/j.fm.2019.02.003.

Sokolov, E. P., Markert, S., Hinzke, T., **Hirschfeld, C.**, Becher, D., Ponsuksili, S., & Sokolova, I. M. (2019). Effects of hypoxia-reoxygenation stress on mitochondrial proteome and bioenergetics of the hypoxia-tolerant marine bivalve *Crassostrea gigas*. *Journal of proteomics*, *194*, 99-111. https://doi.org/10.1016/j.jprot.2018.12.009.

Chinchilla, D., Bruisson, S., Meyer, S., Zühlke, D., **Hirschfeld, C.**, Joller, C., L'Haridon, F., Mène-Saffrané, L., Riedel, K., & Weisskopf, L. (2019). A sulfur-containing volatile emitted by potato-associated bacteria confers protection against late blight through direct anti-oomycete activity. *Scientific reports*, *9*(1), 18778. https://doi.org/10.1038/s41598-019-55218-3.

Sievers, S., Metzendorf, N. G., Dittmann, S., Troitzsch, D., Gast, V., Tröger, S. M., Wolff, C., Zühlke, D., **Hirschfeld, C.**, Schlüter, R., & Riedel, K. (2019). Differential View on the Bile Acid Stress Response of *Clostridioides difficile*. *Frontiers in microbiology*, *10*, 258. https://doi.org/10.3389/fmicb.2019.00258.

Hoyer, J., Bartel, J., Gómez-Mejia, A., Rohde, M., **Hirschfeld, C.**, Heß, N., Sura, T., Maaß, S., Hammerschmidt, S., & Becher, D. (2018). Proteomic response of *Streptococcus pneumoniae* to

iron limitation. *International journal of medical microbiology: IJMM*, *308*(6), 713-721. https://doi.org/10.1016/j.ijmm.2018.02.001.

8.2. ORAL PRESENTATIONS AT INTERNATIONAL AND NATIONAL CONFERENCES

Hirschfeld, C., Gómez-Mejia, A., Bartel, J., Rohde, M., Maaß, S., Hammerschmidt, S., & Becher, D. Proteomic investigation of the pneumococcal kinase and phosphatase couple StkP/PhpP. 14th European Meeting on the Molecular Biology of the Pneumococcus (Europneumo), June 11-14, 2019, Greifswald, Germany

Hirschfeld, C., Gómez-Mejia, A., Bartel, J., Rohde, M., Maaß, S., Hammerschmidt, S., & Becher, D. Proteomic investigation of the pneumococcal kinase and phosphatase couple StkP/PhpP. 4th German Pneumococcal and Streptococcal Symposium, October 22-24, 2018, Berlin, Germany

8.3. POSTER PRESENTATIONS AT INTERNATIONAL AND NATIONAL CONFERENCES

Hirschfeld, C., Hentschker, C., Gómez-Mejia, A., Rohde, M., Maaß, S., Hammerschmidt, S., & Becher, D. Proteomic investigation of the pneumococcal kinase and phosphatase couple StkP/PhpP. 12th European Summer School "Advanced Proteomics" July 29-August 4, 2018, Brixen/Bressanone, South Tirol, Italy

Hirschfeld, C., Hentschker, C., Gómez-Mejia, A., Rohde, M., Maaß, S., Hammerschmidt, S., & Becher, D. Proteomic investigation of the pneumococcal kinase and phosphatase couple StkP/PhpP. Annual Conference of the Association for General and Applied Microbiology (VAAM) 2018 April 15-18, 2018, Wolfsburg, Germany

Hirschfeld, C., Hentschker, C., Junker, S., Gómez-Mejia, A., Rohde, M., Maaß, S., Hammerschmidt, S., & Becher, D. Investigation of the phosphoproteome of *Streptococcus pneumoniae*. 1st International Conference on Respiratory Pathogens November 1-3, 2017, Rostock, Germany

Hirschfeld, C., Hentschker, C., Hoyer, J., Junker, S., Gómez-Mejia, A., Hammerschmidt, S., Maaß, S., & Becher, D. Investigation of the phosphoproteome of *Streptococcus pneumoniae.* 1st Summer School "Infection Biology" September 28-30, 2016, Greifswald/Riems, Germany

Hirschfeld, C., Hentschker, C., Hoyer, J., Junker, S., Gómez-Mejia, A., Hammerschmidt, S., Maaß, S., & Becher, D. Investigation of the phosphoproteome of *Streptococcus pneumoniae.* 3rd German Pneumococcal and Streptococcal Symposium September 9-10, 2016, Braunschweig, Germany

9. REFERENCES

Abdullah, Mohammed R.; Gutiérrez-Fernández, Javier; Pribyl, Thomas; Gisch, Nicolas; Saleh, Malek; Rohde, Manfred et al. (2014): Structure of the pneumococcal l,d-carboxypeptidase DacB and pathophysiological effects of disabled cell wall hydrolases DacA and DacB. In: *Molecular microbiology* 93 (6), p. 1183–1206. DOI: 10.1111/mmi.12729.

Abeyta, Melanie; Hardy, Gail G.; Yother, Janet (2003): Genetic alteration of capsule type but not PspA type affects accessibility of surface-bound complement and surface antigens of *Streptococcus pneumoniae*. In: *Infection and immunity* 71 (1), p. 218–225. DOI: 10.1128/iai.71.1.218-225.2003.

Agarwal, Shivangi; Agarwal, Shivani; Pancholi, Preeti; Pancholi, Vijay (2012): Strain-specific regulatory role of eukaryote-like serine/threonine phosphatase in pneumococcal adherence. In: *Infection and immunity* 80 (4), p. 1361–1372. DOI: 10.1128/IAI.06311-11.

Agarwal, Shivani; Agarwal, Shivangi; Pancholi, Preeti; Pancholi, Vijay (2011): Role of serine/threonine phosphatase (SP-STP) in *Streptococcus pyogenes* physiology and virulence. In: *The Journal of biological chemistry* 286 (48), p. 41368–41380. DOI: 10.1074/jbc.M111.286690.

Aivaliotis, Michalis; Macek, Boris; Gnad, Florian; Reichelt, Peter; Mann, Matthias; Oesterhelt, Dieter (2009): Ser/Thr/Tyr protein phosphorylation in the archaeon *Halobacterium salinarum*--a representative of the third domain of life. In: *PloS one* 4 (3), e4777. DOI: 10.1371/journal.pone.0004777.

Alber, Tom (2009): Signaling mechanisms of the *Mycobacterium tuberculosis* receptor Ser/Thr protein kinases. In: *Current opinion in structural biology* 19 (6), p. 650–657. DOI: 10.1016/j.sbi.2009.10.017.

Anderson, Johnathon D.; Johansson, Henrik J.; Graham, Calvin S.; Vesterlund, Mattias; Pham, Missy T.; Bramlett, Charles S. et al. (2016): Comprehensive Proteomic Analysis of Mesenchymal Stem Cell Exosomes Reveals Modulation of Angiogenesis via Nuclear Factor-KappaB Signaling. In: *Stem cells (Dayton, Ohio)* 34 (3), p. 601–613. DOI: 10.1002/stem.2298.

Anderson, N. L.; Anderson, N. G. (1998): Proteome and proteomics: new technologies, new concepts, and new words. In: *Electrophoresis* 19 (11), p. 1853–1861. DOI: 10.1002/elps.1150191103.

Aoki, Kiyoko F.; Kanehisa, Minoru (2005): Using the KEGG database resource. In: *Current protocols in bioinformatics* Chapter 1, Unit 1.12. DOI: 10.1002/0471250953.bi0112s11.

Arora, Gunjan; Sajid, Andaleeb; Arulanandh, Mary Diana; Singhal, Anshika; Mattoo, Abid R.; Pomerantsev, Andrei P. et al. (2012): Unveiling the novel dual specificity protein kinases in *Bacillus anthracis*: identification of the first prokaryotic dual specificity tyrosine phosphorylation-regulated kinase (DYRK)-like kinase. In: *The Journal of biological chemistry* 287 (32), p. 26749–26763. DOI: 10.1074/jbc.M112.351304.

Atsushi, Matsumoto; Soon-Kwang, Hong; Hiroshi, Ishizuka; Sueharu, Horinouchi; Teruhiko, Beppu (1994): Phosphorylation of the AfsR protein involved in secondary metabolism in *Streptomyces* species by a eukary otic-type protein kinase. In: *Gene* 146 (1), p. 47–56. DOI: 10.1016/0378-1119(94)90832-X.

Austrian, R. (1999): The pneumococcus at the millennium: not down, not out. In: *The Journal of infectious diseases* 179 Suppl. 2, S338-41. DOI: 10.1086/513841.

Austrian, R.; Douglas, R. M.; Schiffman, G.; Coetzee, A. M.; Koornhof, H. J.; Hayden-Smith, S.; Reid, R. D. (1976): Prevention of pneumococcal pneumonia by vaccination. In: *Transactions of the Association of American Physicians* 89, p. 184–194.

Avery, Oswald T.; MacLeod, Colin M.; McCarty, Maclyn (1944): Studies on the Chemical Nature of the Substance Inducing Transformation of Pneumococcal Types. Induction of Transformation by a Desoxyribonucleic Acid Fraction Isolated from Pneumococcus Type III. In: *Journal of Experimental Medicine* 79 (2), p. 137–158. DOI: 10.1084/jem.79.2.137.

Av-Gay, Yossef; Everett, Martin (2000): The eukaryotic-like Ser/Thr protein kinases of *Mycobacterium tuberculosis*. In: *Trends in microbiology* 8 (5), p. 238–244. DOI: 10.1016/S0966-842X(00)01734-0.

Bantscheff, Marcus; Lemeer, Simone; Savitski, Mikhail M.; Kuster, Bernhard (2012): Quantitative mass spectrometry in proteomics: critical review update from 2007 to the present. In: *Analytical and bioanalytical chemistry* 404 (4), p. 939–965. DOI: 10.1007/s00216-012-6203-4.

Bantscheff, Marcus; Schirle, Markus; Sweetman, Gavain; Rick, Jens; Kuster, Bernhard (2007): Quantitative mass spectrometry in proteomics. A critical review. In: *Analytical and bioanalytical chemistry* 389 (4), p. 1017–1031. DOI: 10.1007/s00216-007-1486-6.

Banu, Liliana Danusia; Conrads, Georg; Rehrauer, Hubert; Hussain, Haitham; Allan, Elaine; van der Ploeg, Jan R. (2010): The *Streptococcus mutans* serine/threonine kinase, PknB, regulates competence development, bacteriocin production, and cell wall metabolism. In: *Infection and immunity* 78 (5), p. 2209–2220. DOI: 10.1128/IAI.01167-09.

Barák, Imrich (2014): Complexity of bacterial phosphorylation interaction network. In: *Frontiers in microbiology* 5, p. 725. DOI: 10.3389/fmicb.2014.00725.

Barford, David (1995): Protein phosphatases. In: *Current opinion in structural biology* 5 (6), p. 728–734. DOI: 10.1016/0959-440X(95)80004-2.

Bartual, Sergio G.; Straume, Daniel; Stamsås, Gro Anita; Muñoz, Inés G.; Alfonso, Carlos; Martínez-Ripoll, Martín et al. (2014): Structural basis of PcsB-mediated cell separation in *Streptococcus pneumoniae*. In: *Nature communications* 5, p. 3842. DOI: 10.1038/ncomms4842.

Beilharz, Katrin; Nováková, Linda; Fadda, Daniela; Branny, Pavel; Massidda, Orietta; Veening, Jan-Willem (2012): Control of cell division in *Streptococcus pneumoniae* by the conserved Ser/Thr protein kinase StkP. In: *Proceedings of the National Academy of Sciences of the United States of America* 109 (15), E905-13. DOI: 10.1073/pnas.1119172109.

Beltramini, Amanda M.; Mukhopadhyay, Chitrangada D.; Pancholi, Vijay (2009): Modulation of cell wall structure and antimicrobial susceptibility by a *Staphylococcus aureus* eukaryote-like serine/threonine kinase and phosphatase. In: *Infection and immunity* 77 (4), p. 1406–1416. DOI: 10.1128/IAI.01499-08.

Bender, Matthew H.; Cartee, Robert T.; Yother, Janet (2003): Positive correlation between tyrosine phosphorylation of CpsD and capsular polysaccharide production in *Streptococcus pneumoniae*. In: *Journal of bacteriology* 185 (20), p. 6057–6066. DOI: 10.1128/jb.185.20.6057-6066.2003.

Bernhardt, Jörg; Michalik, Stephan; Wollscheid, Bernd; Völker, Uwe; Schmidt, Frank (2013): Proteomics approaches for the analysis of enriched microbial subpopulations and visualization of complex functional information. In: *Current opinion in biotechnology* 24 (1), p. 112–119. DOI: 10.1016/j.copbio.2012.10.009.

Bogaert, D.; Groot, R. de; Hermans, P. W.M. (2004): *Streptococcus pneumoniae* colonisation. The key to pneumococcal disease. In: *The Lancet Infectious Diseases* 4 (3), p. 144–154. DOI: 10.1016/S1473-3099(04)00938-7.

Bonn, Florian; Bartel, Jürgen; Büttner, Knut; Hecker, Michael; Otto, Andreas; Becher, Dörte (2014): Picking vanished proteins from the void: how to collect and ship/share extremely dilute proteins in a reproducible and highly efficient manner. In: *Analytical chemistry* 86 (15), p. 7421–7427. DOI: 10.1021/ac501189j.

Bork, P.; Brown, N. P.; Hegyi, H.; Schultz, J. (1996): The protein phosphatase 2C (PP2C) superfamily: detection of bacterial homologues. In: *Protein science: a publication of the Protein Society* 5 (7), p. 1421–1425. DOI: 10.1002/pro.5560050720.

Botella, Eric; Devine, Susanne Krogh; Hubner, Sebastian; Salzberg, Letal I.; Gale, Robert T.; Brown, Eric D. et al. (2014): PhoR autokinase activity is controlled by an intermediate in wall teichoic acid metabolism that is sensed by the intracellular PAS domain during the PhoPR-

mediated phosphate limitation response of *Bacillus subtilis*. In: *Molecular microbiology* 94 (6), p. 1242–1259. DOI: 10.1111/mmi.12833.

Bradford, Marion M. (1976): A rapid and sensitive method for the quantitation of microgram quantities of protein utilizing the principle of protein-dye binding. In: *Analytical Biochemistry* 72, p. 248–254.

Bridy-Pappas, Angela E.; Margolis, Marya B.; Center, Kimberly J.; Isaacman, Daniel J. (2005): *Streptococcus pneumoniae*: description of the pathogen, disease epidemiology, treatment, and prevention. In: *Pharmacotherapy* 25 (9), p. 1193–1212. DOI: 10.1592/phco.2005.25.9.1193.

Brown, James Howard (1919): The use of blood agar for the study of streptococci. The Rockefeller Institute for Medical Research, New York.

Burnside, Kellie; Lembo, Annalisa; Los Reyes, Melissa de; Iliuk, Anton; Binhtran, Nguyen-Thao; Connelly, James E. et al. (2010): Regulation of hemolysin expression and virulence of *Staphylococcus aureus* by a serine/threonine kinase and phosphatase. In: *PloS one* 5 (6), e11071. DOI: 10.1371/journal.pone.0011071.

Burnside, Kellie; Rajagopal, Lakshmi (2012): Regulation of prokaryotic gene expression by eukaryotic-like enzymes. In: *Current opinion in microbiology* 15 (2), p. 125–131. DOI: 10.1016/j.mib.2011.12.006.

Calder, Bridget; Albeldas, Claudia; Blackburn, Jonathan M.; Soares, Nelson C. (2016): Mass Spectrometry Offers Insight into the Role of Ser/Thr/Tyr Phosphorylation in the Mycobacteria. In: *Frontiers in microbiology* 7, p. 141. DOI: 10.3389/fmicb.2016.00141.

Centers for Disease Control and Prevention (CDC) (2019): Pneumococcal Vaccination: What Everyone Should Know. National Center for Immunization and Respiratory Diseases. Online verfügbar unter https://www.cdc.gov/vaccines/vpd/pneumo/public/index.html, zuletzt aktualisiert am 11/21/2019.

Chen, Songbiao; Songkumarn, Pattavipha; Liu, Jianli; Wang, Guo-Liang (2009): A versatile zero background T-vector system for gene cloning and functional genomics. In: *Plant physiology* 150 (3), p. 1111–1121. DOI: 10.1104/pp.109.137125.

Chen, Xiulan; Wei, Shasha; Ji, Yanlong; Guo, Xiaojing; Yang, Fuquan (2015): Quantitative proteomics using SILAC. Principles, applications, and developments. In: *Proteomics* 15 (18), p. 3175–3192. DOI: 10.1002/pmic.201500108.

Choi, Eun Hwa; Zhang, Fan; Lu, Ying-Jie; Malley, Richard (2016): Capsular Polysaccharide (CPS) Release by Serotype 3 Pneumococcal Strains Reduces the Protective Effect of Anti-Type 3

CPS Antibodies. In: *Clinical and vaccine immunology: CVI* 23 (2), p. 162–167. DOI: 10.1128/CVI.00591-15.

Cieslewicz, M. J.; Kasper, D. L.; Wang, Y.; Wessels, M. R. (2001): Functional analysis in type Ia group B Streptococcus of a cluster of genes involved in extracellular polysaccharide production by diverse species of streptococci. In: *The Journal of biological chemistry* 276 (1), p. 139–146. DOI: 10.1074/jbc.M005702200.

Claudia Rennemeier (2007): Charakterisierung der Thrombospondin-1 vermittelten Anheftung von *Streptococcus pneumoniae* an humane Wirtszellen. Dissertation. Julius-Maximilians-Universität Würzburg, Würzburg. Institut für Molekulare Infektionsbiologie.

Claverys, Jean-Pierre; Havarstein, Leiv Sigve (2002): Extracellular-peptide control of competence for genetic transformation in *Streptococcus pneumoniae*. In: *Frontiers in bioscience: a journal and virtual library* 7, d1798-814. DOI: 10.2741/claverys.

Claverys, Jean-Pierre; Prudhomme, Marc; Martin, Bernard (2006): Induction of competence regulons as a general response to stress in gram-positive bacteria. In: *Annual review of microbiology* 60, p. 451–475. DOI: 10.1146/annurev.micro.60.080805.142139.

Cleverley, Robert M.; Rutter, Zoe J.; Rismondo, Jeanine; Corona, Federico; Tsui, Ho-Ching Tiffany; Alatawi, Fuad A. et al. (2019): The cell cycle regulator GpsB functions as cytosolic adaptor for multiple cell wall enzymes. In: *Nature communications* 10 (1), p. 261. DOI: 10.1038/s41467-018-08056-2.

Cox, Jürgen; Hein, Marco Y.; Luber, Christian A.; Paron, Igor; Nagaraj, Nagarjuna; Mann, Matthias (2014): Accurate proteome-wide label-free quantification by delayed normalization and maximal peptide ratio extraction, termed MaxLFQ. In: *Molecular & cellular proteomics: MCP* 13 (9), p. 2513–2526. DOI: 10.1074/mcp.M113.031591.

Cox, Jürgen; Mann, Matthias (2008): MaxQuant enables high peptide identification rates, individualized p.p.b.-range mass accuracies and proteome-wide protein quantification. In: *Nature biotechnology* 26 (12), p. 1367–1372. DOI: 10.1038/nbt.1511.

Cox, Jürgen; Neuhauser, Nadin; Michalski, Annette; Scheltema, Richard A.; Olsen, Jesper V.; Mann, Matthias (2011): Andromeda. A peptide search engine integrated into the MaxQuant environment. In: *Journal of proteome research* 10 (4), p. 1794–1805. DOI: 10.1021/pr101065j.

Daniels, Calvin C.; Rogers, P. David; Shelton, Chasity M. (2016): A Review of Pneumococcal Vaccines: Current Polysaccharide Vaccine Recommendations and Future Protein Antigens. In: *The Journal of Pediatric Pharmacology and Therapeutics: JPPT* 21 (1), p. 27–35. DOI: 10.5863/1551-6776-21.1.27.

Deng, L.; Kasper, D. L.; Krick, T. P.; Wessels, M. R. (2000): Characterization of the linkage between the type III capsular polysaccharide and the bacterial cell wall of group B Streptococcus. In: *The Journal of biological chemistry* 275 (11), p. 7497–7504. DOI: 10.1074/jbc.275.11.7497.

Didier, Jean-Philippe; Cozzone, Alain J.; Duclos, Bertrand (2010): Phosphorylation of the virulence regulator SarA modulates its ability to bind DNA in *Staphylococcus aureus*. In: *FEMS microbiology letters* 306 (1), p. 30–36. DOI: 10.1111/j.1574-6968.2010.01930.x.

Donat, Stefanie; Streker, Karin; Schirmeister, Tanja; Rakette, Sonja; Stehle, Thilo; Liebeke, Manuel et al. (2009): Transcriptome and functional analysis of the eukaryotic-type serine/threonine kinase PknB in *Staphylococcus aureus*. In: *Journal of bacteriology* 191 (13), p. 4056–4069. DOI: 10.1128/JB.00117-09.

Doran, Kelly S.; Fulde, Marcus; Gratz, Nina; Kim, Brandon J.; Nau, Roland; Prasadarao, Nemani et al. (2016): Host-pathogen interactions in bacterial meningitis. In: *Acta neuropathologica* 131 (2), p. 185–209. DOI: 10.1007/s00401-015-1531-z.

Durek, Pawel; Schmidt, Robert; Heazlewood, Joshua L.; Jones, Alexandra; MacLean, Daniel; Nagel, Axel et al. (2010): PhosPhAt: The *Arabidopsis thaliana* phosphorylation site database. An update. In: *Nucleic acids research* 38 (Database issue), D828-34. DOI: 10.1093/nar/gkp810.

Dworkin, Jonathan (2015): Ser/Thr phosphorylation as a regulatory mechanism in bacteria. In: *Current opinion in microbiology* 24, p. 47–52. DOI: 10.1016/j.mib.2015.01.005.

Echenique, J.; Kadioglu, A.; Romao, S.; Andrew, P. W.; Trombe, M.-C. (2004): Protein Serine/Threonine Kinase StkP Positively Controls Virulence and Competence in *Streptococcus pneumoniae*. In: *Infection and immunity* 72 (4), p. 2434–2437. DOI: 10.1128/IAI.72.4.2434-2437.2004.

Eldholm, Vegard; Johnsborg, Ola; Straume, Daniel; Ohnstad, Hilde Solheim; Berg, Kari Helene; Hermoso, Juan A.; Håvarstein, Leiv Sigve (2010): Pneumococcal CbpD is a murein hydrolase that requires a dual cell envelope binding specificity to kill target cells during fratricide. In: *Molecular microbiology* 76 (4), p. 905–917. DOI: 10.1111/j.1365-2958.2010.07143.x.

Facklam, Richard (2002): What Happened to the Streptococci. Overview of Taxonomic and Nomenclature Changes. In: *Clinical Microbiology Reviews* 15 (4), p. 613–630. DOI: 10.1128/CMR.15.4.613-630.2002.

Falk, Shaun P.; Weisblum, Bernard (2013): Phosphorylation of the *Streptococcus pneumoniae* cell wall biosynthesis enzyme MurC by a eukaryotic-like Ser/Thr kinase. In: *FEMS microbiology letters* 340 (1), p. 19–23. DOI: 10.1111/1574-6968.12067.

Fedson, David S.; Nicolas-Spony, Laurence; Klemets, Peter; van der Linden, Mark; Marques, Agostinho; Salleras, Luis; Samson, Sandrine I. (2011): Pneumococcal polysaccharide vaccination for adults: new perspectives for Europe. In: *Expert review of vaccines* 10 (8), p. 1143–1167. DOI: 10.1586/erv.11.99.

Fenn, J. B.; Mann, M.; Meng, C. K.; Wong, S. F.; Whitehouse, C. M. (1989): Electrospray ionization for mass spectrometry of large biomolecules. In: *Science* 246 (4926), p. 64. DOI: 10.1126/science.2675315.

Fenton, Andrew K.; Manuse, Sylvie; Flores-Kim, Josué; Garcia, Pierre Simon; Mercy, Chryslène; Grangeasse, Christophe et al. (2018): Phosphorylation-dependent activation of the cell wall synthase PBP2a in *Streptococcus pneumoniae* by MacP. In: *Proceedings of the National Academy of Sciences of the United States of America* 115 (11), p. 2812–2817. DOI: 10.1073/pnas.1715218115.

Ferrándiz, M. J.; Pérez-Trallero, E.; Marimón, J. M.; La Campa, A. G. de (2005): Clinical Isolates of the Spain14-5 clone of *Streptococcus pneumoniae* carry a recombinant rpoB gene. In: *Antimicrobial agents and chemotherapy* 49 (11), p. 4811–4813. DOI: 10.1128/AAC.49.11.4811-4813.2005.

Fleurie, Aurore; Cluzel, Caroline; Guiral, Sébastien; Freton, Céline; Galisson, Frédéric; Zanella-Cleon, Isabelle et al. (2012): Mutational dissection of the S/T-kinase StkP reveals crucial roles in cell division of *Streptococcus pneumoniae*. In: *Molecular microbiology* 83 (4), p. 746–758. DOI: 10.1111/j.1365-2958.2011.07962.x.

Fleurie, Aurore; Lesterlin, Christian; Manuse, Sylvie; Zhao, Chao; Cluzel, Caroline; Lavergne, Jean-Pierre et al. (2014a): MapZ marks the division sites and positions FtsZ rings in *Streptococcus pneumoniae*. In: *Nature* 516 (7530), p. 259–262. DOI: 10.1038/nature13966.

Fleurie, Aurore; Manuse, Sylvie; Zhao, Chao; Campo, Nathalie; Cluzel, Caroline; Lavergne, Jean-Pierre et al. (2014b): Interplay of the serine/threonine-kinase StkP and the paralogs DivIVA and GpsB in pneumococcal cell elongation and division. In: *PLoS genetics* 10 (4), e1004275. DOI: 10.1371/journal.pgen.1004275.

Fortuin, Suereta; Tomazella, Gisele G.; Nagaraj, Nagarjuna; Sampson, Samantha L.; van Gey Pittius, Nicolaas C.; Soares, Nelson C. et al. (2015): Phosphoproteomics analysis of a clinical *Mycobacterium tuberculosis* Beijing isolate. Expanding the mycobacterial phosphoproteome catalog. In: *Frontiers in microbiology* 6, p. 6. DOI: 10.3389/fmicb.2015.00006.

Fraenkel, A. (1884): Über die genuine Pneumonie. Berlin (Verhandlungen des III. Congresses für Innere Medizin) (3), p. 17–31.

Friedländer, C. (1883): Die Mikrokokken der Pneumonie. In: *Fortschr Med* (1), p. 715–733.

Gamez, G.; Hammerschmidt, S. (2012): Combat Pneumococcal Infections: Adhesins as Candidates for Protein- Based Vaccine Development. In: *Current Drug Targets* 13 (3), p. 323–337.

Ge, Ruiguang; Shan, Weiran (2011): Bacterial Phosphoproteomic Analysis Reveals the Correlation Between Protein Phosphorylation and Bacterial Pathogenicity. In: *Genomics, Proteomics & Bioinformatics* 9 (4-5), p. 119–127. DOI: 10.1016/S1672-0229(11)60015-6.

Geno, K. Aaron; Gilbert, Gwendolyn L.; Song, Joon Young; Skovsted, Ian C.; Klugman, Keith P.; Jones, Christopher et al. (2015): Pneumococcal Capsules and Their Types. Past, Present, and Future. In: *Clinical Microbiology Reviews* 28 (3), p. 871–899. DOI: 10.1128/CMR.00024-15.

Geno, K. Aaron; Saad, Jamil S.; Nahm, Moon H. (2017): Discovery of Novel Pneumococcal Serotype 35D, a Natural WciG-Deficient Variant of Serotype 35B. In: *Journal of clinical microbiology* 55 (5), p. 1416–1425. DOI: 10.1128/JCM.00054-17.

Giefing, Carmen; Jelencsics, Kira E.; Gelbmann, Dieter; Senn, Beatrice M.; Nagy, Eszter (2010): The pneumococcal eukaryotic-type serine/threonine protein kinase StkP co-localizes with the cell division apparatus and interacts with FtsZ in vitro. In: *Microbiology (Reading, England)* 156 (Pt 6), p. 1697–1707. DOI: 10.1099/mic.0.036335-0.

Giefing-Kröll, Carmen; Jelencsics, Kira E.; Reipert, Siegfried; Nagy, Eszter (2011): Absence of pneumococcal PcsB is associated with overexpression of LysM domain-containing proteins. In: *Microbiology (Reading, England)* 157 (Pt 7), p. 1897–1909. DOI: 10.1099/mic.0.045211-0.

Gladstone, Rebecca A.; Lo, Stephanie W.; Lees, John A.; Croucher, Nicholas J.; van Tonder, Andries J.; Corander, Jukka et al. (2019): International genomic definition of pneumococcal lineages, to contextualise disease, antibiotic resistance and vaccine impact. In: *EBioMedicine* 43, p. 338–346. DOI: 10.1016/j.ebiom.2019.04.021.

Gómez-Mejia, Alejandro; Gámez, Gustavo; Hammerschmidt, Sven (2017): *Streptococcus pneumoniae* two-component regulatory systems. The interplay of the pneumococcus with its environment. In: *International journal of medical microbiology: IJMM*. DOI: 10.1016/j.ijmm.2017.11.012.

Gotzmann, Nadine (2013): Untersuchungen zum Proteom von bakteriellen Meningitiserregern. Diploma thesis. University Greifswald, Greifswald. Interfaculty Institute for Genetics and Functional Genomics.

Grabenstein, John D.; Manoff, Susan B. (2012): Pneumococcal polysaccharide 23-valent vaccine: long-term persistence of circulating antibody and immunogenicity and safety after revaccination in adults. In: *Vaccine* 30 (30), p. 4435–4444. DOI: 10.1016/j.vaccine.2012.04.052.

Grangeasse, Christophe (2016): Rewiring the Pneumococcal Cell Cycle with Serine/Threonine- and Tyrosine-kinases. In: *Trends in microbiology* 24 (9), p. 713–724. DOI: 10.1016/j.tim.2016.04.004.

Gray, B. M.; Musher, D. M. (2008): The History of pneumococcal disease. In: George R. Siber, Keith P. Klugman und P. Helena Mäkelä (Hg.): Pneumococcal vaccines. The impact of conjugate vaccine. Washington, DC: ASM Press (Monograph, ASM Press), p. 3–17.

Griffith, Fred (1928): The Significance of Pneumococcal Types. In: *Journal of Hygiene* 27 (2), p. 113–159.

Gygi, Steven P.; Corthals, Garry L.; Zhang, Yanni; Rochon, Yvan; Aebersold, Ruedi (2000): Evaluation of two-dimensional gel electrophoresis-based proteome analysis technology. In: *Proceedings of the National Academy of Sciences* 97 (17), p. 9390. DOI: 10.1073/pnas.160270797.

Haft, D. H.; Loftus, B. J.; Richardson, D. L.; Yang, F.; Eisen, J. (2001): TIGRFAMs: a protein family resource for the functionalidentification of proteins. In: *Nucleic acids research* 29 (1), p. 41–43.

Hammond, Lauren R.; White, Maria L.; Eswara, Prahathees J. (2019): ¡vIVA la DivIVA! In: *Journal of bacteriology*. DOI: 10.1128/JB.00245-19.

Hanks, S. K.; Quinn, A. M.; Hunter, T. (1988): The protein kinase family: conserved features and deduced phylogeny of the catalytic domains. In: *Science (New York, N.Y.)* 241 (4861), p. 42–52. DOI: 10.1126/science.3291115.

Hanks, Steven K.; Hunter, Tony (1995): The eukaryotic protein kinase superfamily: kinase (catalytic) domain structure and classification 1. In: *FASEB j.* 9 (8), p. 576–596. DOI: 10.1096/fasebj.9.8.7768349.

Hardy, G. G.; Magee, A. D.; Ventura, C. L.; Caimano, M. J.; Yother, J. (2001): Essential role for cellular phosphoglucomutase in virulence of type 3 *Streptococcus pneumoniae*. In: *Infection and immunity* 69 (4), p. 2309–2317. DOI: 10.1128/IAI.69.4.2309-2317.2001.

Håvarstein, L. S.; Coomaraswamy, G.; Morrison, D. A. (1995): An unmodified heptadecapeptide pheromone induces competence for genetic transformation in *Streptococcus pneumoniae*. In: *Proceedings of the National Academy of Sciences of the United States of America* 92 (24), p. 11140–11144. DOI: 10.1073/pnas.92.24.11140.

Herbert, Jenny A.; Mitchell, Andrea M.; Mitchell, Timothy J. (2015): A Serine-Threonine Kinase (StkP) Regulates Expression of the Pneumococcal Pilus and Modulates Bacterial Adherence to Human Epithelial and Endothelial Cells *In Vitro*. In: *PloS one* 10 (6), e0127212. DOI: 10.1371/journal.pone.0127212.

Heß, Nathalie; Waldow, Franziska; Kohler, Thomas P.; Rohde, Manfred; Kreikemeyer, Bernd; Gómez-Mejia, Alejandro et al. (2017): Lipoteichoic acid deficiency permits normal growth but impairs virulence of *Streptococcus pneumoniae*. In: *Nature communications* 8 (1), p. 2093. DOI: 10.1038/s41467-017-01720-z.

Hinc, Krzysztof; Nagórska, Krzysztofa; Iwanicki, Adam; Wegrzyn, Grzegorz; Séror, Simone J.; Obuchowski, Michal (2006): Expression of genes coding for GerA and GerK spore germination receptors is dependent on the protein phosphatase PrpE. In: *Journal of bacteriology* 188 (12), p. 4373–4383. DOI: 10.1128/JB.01877-05.

Hirschfeld, Claudia; Gómez-Mejia, Alejandro; Bartel, Jürgen; Hentschker, Christian; Rohde, Manfred; Maaß, Sandra et al. (2019): Proteomic Investigation Uncovers Potential Targets and Target Sites of Pneumococcal Serine-Threonine Kinase StkP and Phosphatase PhpP. In: *Frontiers in microbiology* 10, p. 3101. DOI: 10.3389/fmicb.2019.03101.

Hoch, James A. (2000): Two-component and phosphorelay signal transduction. In: *Current opinion in microbiology* 3 (2), p. 165–170. DOI: 10.1016/S1369-5274(00)00070-9.

Hohmann, Angelika (2012): Etablierung von Methoden für die quantitative Proteomanalyse von bakteriellen Meningitis-Erregern. Diploma thesis. University Greifswald, Greifswald. Interfaculty Institute for Genetics and Functional Genomics.

Holečková, Nela; Doubravová, Linda; Massidda, Orietta; Molle, Virginie; Buriánková, Karolína; Benada, Oldřich et al. (2014): LocZ is a new cell division protein involved in proper septum placement in *Streptococcus pneumoniae*. In: *mBio* 6 (1), e01700-14. DOI: 10.1128/mBio.01700-14.

Holmes, Ann R.; McNab, Roderick; Millsap, Kevin W.; Rohde, Manfred; Hammerschmidt, Sven; Mawdsley, Jane L.; Jenkinson, Howard F. (2001): The pavA gene of *Streptococcus pneumoniae* encodes a fibronectin-binding protein that is essential for virulence. In: *Molecular microbiology* 41 (6), p. 1395–1408. DOI: 10.1046/j.1365-2958.2001.02610.x.

Hoyer, Juliane; Bartel, Jürgen; Gómez-Mejia, Alejandro; Rohde, Manfred; Hirschfeld, Claudia; Heß, Nathalie et al. (2018): Proteomic response of *Streptococcus pneumoniae* to iron limitation. In: *International journal of medical microbiology: IJMM* 308 (6), p. 713–721. DOI: 10.1016/j.ijmm.2018.02.001.

Hsieh, Yi-Ju; Wanner, Barry L. (2010): Global regulation by the seven-component Pi signaling system. In: *Current opinion in microbiology* 13 (2), p. 198–203. DOI: 10.1016/j.mib.2010.01.014.

Hunt, D. F.; Henderson, R. A.; Shabanowitz, J.; Sakaguchi, K.; Michel, H.; Sevilir, N. et al. (1992): Characterization of peptides bound to the class I MHC molecule HLA-A2.1 by mass spectrometry. In: *Science* 255 (5049), p. 1261. DOI: 10.1126/science.1546328.

Huse, Morgan; Kuriyan, John (2002): The Conformational Plasticity of Protein Kinases. In: *Cell* 109 (3), p. 275–282. DOI: 10.1016/S0092-8674(02)00741-9.

Hyams, Catherine; Camberlein, Emilie; Cohen, Jonathan M.; Bax, Katie; Brown, Jeremy S. (2010): The *Streptococcus pneumoniae* capsule inhibits complement activity and neutrophil phagocytosis by multiple mechanisms. In: *Infection and immunity* 78 (2), p. 704–715. DOI: 10.1128/IAI.00881-09.

Iwanicki, Adam; Herman-Antosiewicz, Anna; Pierechod, Marcin; Séror, Simone J.; Obuchowski, Michał (2002): PrpE, a PPP protein phosphatase from *Bacillus subtilis* with unusual substrate specificity. In: *The Biochemical journal* 366 (Pt 3), p. 929–936. DOI: 10.1042/BJ20011591.

Janczarek, Monika; Vinardell, José-María; Lipa, Paulina; Karaś, Magdalena (2018): Hanks-Type Serine/Threonine Protein Kinases and Phosphatases in Bacteria. Roles in Signaling and Adaptation to Various Environments. In: *International journal of molecular sciences* 19 (10). DOI: 10.3390/ijms19102872.

Jin, Hong; Pancholi, Vijay (2006): Identification and biochemical characterization of a eukaryotic-type serine/threonine kinase and its cognate phosphatase in *Streptococcus pyogenes*. Their biological functions and substrate identification. In: *Journal of molecular biology* 357 (5), p. 1351–1372. DOI: 10.1016/j.jmb.2006.01.020.

Jones, Greg; Dyson, Paul (2006): Evolution of transmembrane protein kinases implicated in coordinating remodeling of gram-positive peptidoglycan: inside versus outside. In: *Journal of bacteriology* 188 (21), p. 7470–7476. DOI: 10.1128/JB.00800-06.

Jung, Kirsten; Fried, Luitpold; Behr, Stefan; Heermann, Ralf (2012): Histidine kinases and response regulators in networks. In: *Current opinion in microbiology* 15 (2), p. 118–124. DOI: 10.1016/j.mib.2011.11.009.

Jünger, Martin A.; Aebersold, Ruedi (2014): Mass spectrometry-driven phosphoproteomics: patterning the systems biology mosaic. In: *Wiley interdisciplinary reviews. Developmental biology* 3 (1), p. 83–112. DOI: 10.1002/wdev.121.

Junker, Sabryna; Maaß, Sandra; Otto, Andreas; Hecker, Michael; Becher, Dörte (2018a): Toward the Quantitative Characterization of Arginine Phosphorylations in *Staphylococcus aureus*. In: *Journal of proteome research*. DOI: 10.1021/acs.jproteome.8b00579.

Junker, Sabryna; Maaβ, Sandra; Otto, Andreas; Michalik, Stephan; Morgenroth, Friedrich; Gerth, Ulf et al. (2018b): Spectral Library Based Analysis of Arginine Phosphorylations in *Staphylococcus aureus*. In: *Molecular & cellular proteomics: MCP* 17 (2), p. 335–348. DOI: 10.1074/mcp.RA117.000378.

Kadioglu, Aras; Weiser, Jeffrey N.; Paton, James C.; Andrew, Peter W. (2008): The role of *Streptococcus pneumoniae* virulence factors in host respiratory colonization and disease. In: *Nature reviews. Microbiology* 6 (4), p. 288–301. DOI: 10.1038/nrmicro1871.

Kanehisa, Minoru; Goto, Susumu (2000): KEGG: Kyoto Encyclopedia of Genes and Genomes. In: *Nucleic acids research* 28 (1), p. 27–30.

Karas, Michael.; Bachmann, Doris.; Hillenkamp, Franz. (1985): Influence of the wavelength in high-irradiance ultraviolet laser desorption mass spectrometry of organic molecules. In: *Analytical chemistry* 57 (14), p. 2935–2939. DOI: 10.1021/ac00291a042.

Kennelly, Peter J. (2002): Protein kinases and protein phosphatases in prokaryotes: a genomic perspective. In: *FEMS microbiology letters* 206 (1), p. 1–8. DOI: 10.1111/j.1574-6968.2002.tb10978.x.

Kennelly, Peter J. (2014): Protein Ser/Thr/Tyr phosphorylation in the Archaea. In: *The Journal of biological chemistry* 289 (14), p. 9480–9487. DOI: 10.1074/jbc.R113.529412.

Kilstrup, Mogens; Hammer, Karin; Ruhdal Jensen, Peter; Martinussen, Jan (2005): Nucleotide metabolism and its control in lactic acid bacteria. In: *FEMS microbiology reviews* 29 (3), p. 555–590. DOI: 10.1016/j.femsre.2005.04.006.

Kim, Min-Sik; Zhong, Jun; Pandey, Akhilesh (2016): Common errors in mass spectrometry-based analysis of post-translational modifications. In: *Proteomics* 16 (5), p. 700–714. DOI: 10.1002/pmic.201500355.

Klose, J. (1975): Protein mapping by combined isoelectric focusing and electrophoresis of mouse tissues. In: *Humangenetik* 26 (3), p. 231–243. DOI: 10.1007/BF00281458.

Kobir, Ahasanul; Shi, Lei; Boskovic, Ana; Grangeasse, Christophe; Franjevic, Damjan; Mijakovic, Ivan (2011): Protein phosphorylation in bacterial signal transduction. In: *Biochimica et biophysica acta* 1810 (10), p. 989–994. DOI: 10.1016/j.bbagen.2011.01.006.

Kohler, Sylvia; Voß, Franziska; Gómez Mejia, Alejandro; Brown, Jeremy S.; Hammerschmidt, Sven (2016): Pneumococcal lipoproteins involved in bacterial fitness, virulence, and immune evasion. In: *FEBS letters* 590 (21), p. 3820–3839. DOI: 10.1002/1873-3468.12352.

Koppe, Uwe; Suttorp, Norbert; Opitz, Bastian (2012): Recognition of Streptococcus pneumoniae by the innate immune system. In: *Cellular microbiology* 14 (4), p. 460–466. DOI: 10.1111/j.1462-5822.2011.01746.x.

Kornev, Alexandr P.; Taylor, Susan S. (2010): Defining the conserved internal architecture of a protein kinase. In: *Biochimica et biophysica acta* 1804 (3), p. 440–444. DOI: 10.1016/j.bbapap.2009.10.017.

Kupronis, Benjamin A.; Richards, Chesley L.; Whitney, Cynthia G. (2003): Invasive pneumococcal disease in older adults residing in long-term care facilities and in the community. In: *Journal of the American Geriatrics Society* 51 (11), p. 1520–1525. DOI: 10.1046/j.1532-5415.2003.51501.x.

Laemmli, U. K. (1970): Cleavage of Structural Proteins during the Assembly of the Head of Bacteriophage T4. In: *Nature* (227), p. 680–685. DOI: 10.1038/227680a0.

Lai, Sio Mei; Le Moual, Hervé (2005): PrpZ, a *Salmonella enterica* serovar Typhi serine/threonine protein phosphatase 2C with dual substrate specificity. In: *Microbiology (Reading, England)* 151 (Pt 4), p. 1159–1167. DOI: 10.1099/mic.0.27585-0.

Lam, Henry (2011): Building and searching tandem mass spectral libraries for peptide identification. In: *Molecular & cellular proteomics: MCP* 10 (12), R111.008565. DOI: 10.1074/mcp.R111.008565.

Lam, Henry; Deutsch, Eric W.; Eddes, James S.; Eng, Jimmy K.; King, Nichole; Stein, Stephen E.; Aebersold, Ruedi (2007): Development and validation of a spectral library searching method for peptide identification from MS/MS. In: *Proteomics* 7 (5), p. 655–667. DOI: 10.1002/pmic.200600625.

Lanie, Joel A.; Ng, Wai-Leung; Kazmierczak, Krystyna M.; Andrzejewski, Tiffany M.; Davidsen, Tanja M.; Wayne, Kyle J. et al. (2007): Genome sequence of Avery's virulent serotype 2 strain D39 of *Streptococcus pneumoniae* and comparison with that of unencapsulated laboratory strain R6. In: *Journal of bacteriology* 189 (1), p. 38–51. DOI: 10.1128/JB.01148-06.

Larsen, Martin R.; Thingholm, Tine E.; Jensen, Ole N.; Roepstorff, Peter; Jørgensen, Thomas J. D. (2005): Highly selective enrichment of phosphorylated peptides from peptide mixtures using titanium dioxide microcolumns. In: *Mol Cell Proteomics* 4 (7), p. 873–886. DOI: 10.1074/mcp.T500007-MCP200.

Larson, Thomas R.; Yother, Janet (2017): *Streptococcus pneumoniae* capsular polysaccharide is linked to peptidoglycan via a direct glycosidic bond to β-D-N-acetylglucosamine. In: *Proceedings of the National Academy of Sciences of the United States of America* 114 (22), p. 5695–5700. DOI: 10.1073/pnas.1620431114.

Lee, Dave C. H.; Jones, Andrew R.; Hubbard, Simon J. (2015): Computational phosphoproteomics: from identification to localization. In: *Proteomics* 15 (5-6), p. 950–963. DOI: 10.1002/pmic.201400372.

Lee, Myeong S.; Morrison, Donald A. (1999): Identification of a New Regulator in *Streptococcus pneumoniae* Linking Quorum Sensing to Competence for Genetic Transformation. In: *Journal of bacteriology* 181 (16), p. 5004–5016.

Li, Zhou; Adams, Rachel M.; Chourey, Karuna; Hurst, Gregory B.; Hettich, Robert L.; Pan, Chongle (2012): Systematic comparison of label-free, metabolic labeling, and isobaric chemical labeling for quantitative proteomics on LTQ Orbitrap Velos. In: *Journal of proteome research* 11 (3), p. 1582–1590. DOI: 10.1021/pr200748h.

Lin, Wan-Jung; Walthers, Don; Connelly, James E.; Burnside, Kellie; Jewell, Kelsea A.; Kenney, Linda J.; Rajagopal, Lakshmi (2009): Threonine phosphorylation prevents promoter DNA binding of the Group B Streptococcus response regulator CovR. In: *Molecular microbiology* 71 (6), p. 1477–1495. DOI: 10.1111/j.1365-2958.2009.06616.x.

Lindemann, Claudia; Thomanek, Nikolas; Hundt, Franziska; Lerari, Thilo; Meyer, Helmut E.; Wolters, Dirk; Marcus, Katrin (2017): Strategies in relative and absolute quantitative mass spectrometry based proteomics. In: *Biological chemistry* 398 (5-6), p. 687–699. DOI: 10.1515/hsz-2017-0104.

Lithgow, Gordon J.; Driscoll, Monica; Phillips, Patrick (2017): A long journey to reproducible results. In: *Nature* 548 (7668), p. 387–388. DOI: 10.1038/548387a.

Lomas-Lopez, Rodrigo; Paracuellos, Patricia; Riberty, Mylène; Cozzone, Alain J.; Duclos, Bertrand (2007): Several enzymes of the central metabolism are phosphorylated in *Staphylococcus aureus*. In: *FEMS microbiology letters* 272 (1), p. 35–42. DOI: 10.1111/j.1574-6968.2007.00742.x.

Loughran, Allister J.; Orihuela, Carlos J.; Tuomanen, Elaine I. (2019): *Streptococcus pneumoniae*: Invasion and Inflammation. In: *Microbiology spectrum* 7 (2). DOI: 10.1128/microbiolspec.GPP3-0004-2018.

Lovering, Andrew L.; Strynadka, Natalie C. J. (2007): High-resolution structure of the major periplasmic domain from the cell shape-determining filament MreC. In: *Journal of molecular biology* 372 (4), p. 1034–1044. DOI: 10.1016/j.jmb.2007.07.022.

Macek, Boris; Gnad, Florian; Soufi, Boumediene; Kumar, Chanchal; Olsen, Jesper V.; Mijakovic, Ivan; Mann, Matthias (2008): Phosphoproteome analysis of *E. coli* reveals evolutionary conservation of bacterial Ser/Thr/Tyr phosphorylation. In: *Molecular & cellular proteomics: MCP* 7 (2), p. 299–307. DOI: 10.1074/mcp.M700311-MCP200.

Macek, Boris; Mann, Matthias; Olsen, Jesper V. (2009): Global and site-specific quantitative phosphoproteomics: principles and applications. In: *Annual review of pharmacology and toxicology* 49, p. 199–221. DOI: 10.1146/annurev.pharmtox.011008.145606.

Macek, Boris; Mijakovic, Ivan; Olsen, Jesper V.; Gnad, Florian; Kumar, Chanchal; Jensen, Peter R.; Mann, Matthias (2007): The serine/threonine/tyrosine phosphoproteome of the model bacterium *Bacillus subtilis*. In: *Mol Cell Proteomics* 6 (4), p. 697–707. DOI: 10.1074/mcp.M600464-MCP200.

MacLeod, Colin M.; Hodges, Richard G.; Heidelberger, Michael; Bernhard, William G. (1945): PREVENTION OF PNEUMOCOCCAL PNEUMONIA BY IMMUNIZATION WITH SPECIFIC CAPSULAR POLYSACCHARIDES. In: *Journal of Experimental Medicine* 82 (6), p. 445–465.

Mann, Matthias; Ong, Shao-En; Grønborg, Mads; Steen, Hanno; Jensen, Ole N.; Pandey, Akhilesh (2002): Analysis of protein phosphorylation using mass spectrometry: deciphering the phosphoproteome. In: *Trends in Biotechnology* 20 (6), p. 261–268. DOI: 10.1016/S0167-7799(02)01944-3.

Manuse, Sylvie; Fleurie, Aurore; Zucchini, Laure; Lesterlin, Christian; Grangeasse, Christophe (2016): Role of eukaryotic-like serine/threonine kinases in bacterial cell division and morphogenesis. In: *FEMS microbiology reviews* 40 (1), p. 41–56. DOI: 10.1093/femsre/fuv041.

Martin, Bernard; Granadel, Chantal; Campo, Nathalie; Hénard, Vincent; Prudhomme, Marc; Claverys, Jean-Pierre (2010): Expression and maintenance of ComD-ComE, the two-component signal-transduction system that controls competence of *Streptococcus pneumoniae*. In: *Molecular microbiology* 75 (6), p. 1513–1528. DOI: 10.1111/j.1365-2958.2010.07071.x.

Mascher, Thorsten; Zähner, Dorothea; Merai, Michelle; Balmelle, Nadège; Saizieu, Antoine B. de; Hakenbeck, Regine (2003): The *Streptococcus pneumoniae cia* regulon: CiaR target sites and transcription profile analysis. In: *Journal of bacteriology* 185 (1), p. 60–70. DOI: 10.1128/jb.185.1.60-70.2003.

Massidda, Orietta; Nováková, Linda; Vollmer, Waldemar (2013): From models to pathogens: how much have we learned about *Streptococcus pneumoniae* cell division? In: *Environmental microbiology* 15 (12), p. 3133–3157. DOI: 10.1111/1462-2920.12189.

Mehr, Sam; Wood, Nicholas (2012): *Streptococcus pneumoniae* – a review of carriage, infection, serotype replacement and vaccination. In: *Paediatric Respiratory Reviews* 13 (4), p. 258–264. DOI: 10.1016/j.prrv.2011.12.001.

Metsalu, Tauno; Vilo, Jaak (2015): ClustVis: a web tool for visualizing clustering of multivariate data using Principal Component Analysis and heatmap. In: *Nucleic acids research* 43 (W1), W566-70. DOI: 10.1093/nar/gkv468.

Mijakovic, Ivan; Grangeasse, Christophe; Turgay, Kürşad (2016): Exploring the diversity of protein modifications: special bacterial phosphorylation systems. In: *FEMS microbiology reviews* 40 (3), p. 398–417. DOI: 10.1093/femsre/fuw003.

Missiakas, D.; Raina, S. (1997): Signal transduction pathways in response to protein misfolding in the extracytoplasmic compartments of E. coli: role of two new phosphoprotein phosphatases PrpA and PrpB. In: *The EMBO journal* 16 (7), p. 1670–1685. DOI: 10.1093/emboj/16.7.1670.

Mitchell, T. J. (2000): Virulence factors and the pathogenesis of disease caused by *Streptococcus pneumoniae*. In: *Res. Microbiol.* 151, p. 413–419.

Mollerach, M.; López, R.; García, E. (1998): Characterization of the galU gene of *Streptococcus pneumoniae* encoding a uridine diphosphoglucose pyrophosphorylase: a gene essential for capsular polysaccharide biosynthesis. In: *The Journal of experimental medicine* 188 (11), p. 2047–2056. DOI: 10.1084/jem.188.11.2047.

Moreno-Letelier, Alejandra; Olmedo, Gabriela; Eguiarte, Luis E.; Martinez-Castilla, Leon; Souza, Valeria (2011): Parallel Evolution and Horizontal Gene Transfer of the *pst* Operon in Firmicutes from Oligotrophic Environments. In: *International journal of evolutionary biology* 2011, p. 781642. DOI: 10.4061/2011/781642.

Morlot, C.; Bayle, L.; Jacq, M.; Fleurie, A.; Tourcier, G.; Galisson, F. et al. (2013): Interaction of Penicillin-Binding Protein 2x and Ser/Thr protein kinase StkP, two key players in *Streptococcus pneumoniae* R6 morphogenesis. In: *Molecular microbiology* 90 (1), p. 88–102. DOI: 10.1111/mmi.12348.

Mougous, Joseph D.; Gifford, Casey A.; Ramsdell, Talia L.; Mekalanos, John J. (2007): Threonine phosphorylation post-translationally regulates protein secretion in *Pseudomonas aeruginosa*. In: *Nature cell biology* 9 (7), p. 797–803. DOI: 10.1038/ncb1605.

Mukhopadhyay, Subhendu; Kapatral, Vinayak; Xu, Wenbin; Chakrabarty, A. M. (1999): Characterization of a Hank's Type Serine/Threonine Kinase andSerine/Threonine Phosphoprotein Phosphatase in *Pseudomonas aeruginosa*. In: *Journal of bacteriology* (Vol.181, No. 21), p. 6615–6622.

Muñoz-Dorado, José; Inouye, Sumiko; Inouye, Masayori (1991): A gene encoding a protein serine/threonine kinase is required for normal development of *M. xanthus*, a gram-negative bacterium. In: *Cell* 67 (5), p. 995–1006. DOI: 10.1016/0092-8674(91)90372-6.

Musher, D. M. (2004): A pathogenetic categorization of clinical syndromes caused by *Streptococcus pneumoniae*. In: Elaine I. Tuomanen, Timothy J. Mitchell, Donald Morrison und Brian G. Spratt (Hg.): The Pneumococcus. Washington, DC.: ASM Press, p. 211–220.

Needham, Elise J.; Parker, Benjamin L.; Burykin, Timur; James, David E.; Humphrey, Sean J. (2019): Illuminating the dark phosphoproteome. In: *Science signaling* 12 (565). DOI: 10.1126/scisignal.aau8645.

Nováková, Linda; Bezousková, Silvia; Pompach, Petr; Spidlová, Petra; Sasková, Lenka; Weiser, Jaroslav; Branny, Pavel (2010): Identification of multiple substrates of the StkP Ser/Thr protein kinase in *Streptococcus pneumoniae*. In: *Journal of bacteriology* 192 (14), p. 3629–3638. DOI: 10.1128/JB.01564-09.

Nováková, Linda; Sasková, Lenka; Pallová, Petra; Janecek, Jirí; Novotná, Jana; Ulrych, Ales et al. (2005): Characterization of a eukaryotic type serine/threonine protein kinase and protein phosphatase of *Streptococcus pneumoniae* and identification of kinase substrates. In: *The FEBS journal* 272 (5), p. 1243–1254. DOI: 10.1111/j.1742-4658.2005.04560.x.

Nühse, Thomas S.; Stensballe, Allan; Jensen, Ole N.; Peck, Scott C. (2004): Phosphoproteomics of the Arabidopsis plasma membrane and a new phosphorylation site database. In: *The Plant cell* 16 (9), p. 2394–2405. DOI: 10.1105/tpc.104.023150.

Ochoa, David; Jarnuczak, Andrew F.; Viéitez, Cristina; Gehre, Maja; Soucheray, Margaret; Mateus, André et al. (2020): The functional landscape of the human phosphoproteome. In: *Nature biotechnology* 38 (3), p. 365–373. DOI: 10.1038/s41587-019-0344-3.

O'Farrell, P. H. (1975): High resolution two-dimensional electrophoresis of proteins. In: *Journal of Biological Chemistry* 250 (10), p. 4007–4021.

Oggioni, Marco R.; Memmi, Guido; Maggi, Tiziana; Chiavolini, Damiana; Iannelli, Francesco; Pozzi, Gianni (2004): Pneumococcal zinc metalloproteinase ZmpC cleaves human matrix metalloproteinase 9 and is a virulence factor in experimental pneumonia. In: *Molecular microbiology* 49 (3), p. 795–805. DOI: 10.1046/j.1365-2958.2003.03596.x.

Olsen, Jesper V.; Macek, Boris (2009): High accuracy mass spectrometry in large-scale analysis of protein phosphorylation. In: *Methods in molecular biology (Clifton, N.J.)* 492, p. 131–142. DOI: 10.1007/978-1-59745-493-3_7.

Ong, Shao-En; Blagoev, Blagoy; Kratchmarova, Irina; Kristensen, Dan Bach; Steen, Hanno; Pandey, Akhilesh; Mann, Matthias (2002): Stable Isotope Labeling by Amino Acids in Cell Culture, SILAC, as a Simple and Accurate Approach to Expression Proteomics. In: *Mol Cell Proteomics* 1 (5), p. 376–386. DOI: 10.1074/mcp.M200025-MCP200.

Oosterhuis-Kafeja, Froukje; Beutels, Philippe; van Damme, Pierre (2007): Immunogenicity, efficacy, safety and effectiveness of pneumococcal conjugate vaccines (1998–2006). In: *Vaccine* 25 (12), p. 2194–2212. DOI: 10.1016/j.vaccine.2006.11.032.

Orihuela, C. J.; Mills, J.; Robb, C. W.; Wilson, C. J.; Watson, D. A.; Niesel, D. W. (2001): *Streptococcus pneumoniae* PstS production is phosphate responsive and enhanced during growth in the murine peritoneal cavity. In: *Infection and immunity* 69 (12), p. 7565–7571. DOI: 10.1128/IAI.69.12.7565-7571.2001.

Osaki, Makoto; Arcondéguy, Tania; Bastide, Amandine; Touriol, Christian; Prats, Hervé; Trombe, Marie-Claude (2009): The StkP/PhpP signaling couple in *Streptococcus pneumoniae*. Cellular organization and physiological characterization. In: *Journal of bacteriology* 191 (15), p. 4943–4950. DOI: 10.1128/JB.00196-09.

Ozlu, Nurhan; Akten, Bikem; Timm, Wiebke; Haseley, Nathan; Steen, Hanno; Steen, Judith A. J. (2010): Phosphoproteomics. In: *Wiley interdisciplinary reviews. Systems biology and medicine* 2 (3), p. 255–276. DOI: 10.1002/wsbm.41.

Pagano, Giovanni J.; Arsenault, Ryan J. (2019): Advances, challenges and tools in characterizing bacterial serine, threonine and tyrosine kinases and phosphorylation target sites. In: *Expert review of proteomics* 16 (5), p. 431–441. DOI: 10.1080/14789450.2019.1601015.

Paradiso, Peter R. (2012): Pneumococcal conjugate vaccine for adults: a new paradigm. In: *Clinical infectious diseases: an official publication of the Infectious Diseases Society of America* 55 (2), p. 259–264. DOI: 10.1093/cid/cis359.

Pasteur, L. (1881): Note sur la maladie nouvelle provoquée par la salive d'un enfant mort de la rage. In: *Bull Acad Med* (10), p. 94–103.

Pasteur, L.; Chamberland, C.; Roux, E. (1881): Sur une maladie nouvelle provoquée par la salive d'un enfant mort de la rage. In: *Compt Rend Acad Sci* (92), p. 159–165.

Pawson, Tony; Scott, John D. (2005): Protein phosphorylation in signaling--50 years and counting. In: *Trends in Biochemical Sciences* 30 (6), p. 286–290. DOI: 10.1016/j.tibs.2005.04.013.

Pereira, Sandro F. F.; Goss, Lindsie; Dworkin, Jonathan (2011): Eukaryote-like serine/threonine kinases and phosphatases in bacteria. In: *Microbiology and molecular biology reviews : MMBR* 75 (1), p. 192–212. DOI: 10.1128/MMBR.00042-10.

Pérez, J.; Castañeda-García, A.; Jenke-Kodama, H.; Müller, R.; Muñoz-Dorado, J. (2008): Eukaryotic-like protein kinases in the prokaryotes and the myxobacterial kinome. In: *Proceedings of the National Academy of Sciences of the United States of America* 105 (41), p. 15950–15955. DOI: 10.1073/pnas.0806851105.

Pérez-Dorado, I.; Galan-Bartual, S.; Hermoso, J. A. (2012): Pneumococcal surface proteins: when the whole is greater than the sum of its parts. In: *Molecular oral microbiology* 27 (4), p. 221–245. DOI: 10.1111/j.2041-1014.2012.00655.x.

Peyrani, Paula; Mandell, Lionel; Torres, Antoni; Tillotson, Glenn S. (2019): The burden of community-acquired bacterial pneumonia in the era of antibiotic resistance. In: *Expert review of respiratory medicine* 13 (2), p. 139–152. DOI: 10.1080/17476348.2019.1562339.

Piñas, Germán E.; Reinoso-Vizcaino, Nicolás M.; Yandar Barahona, Nubia Y.; Cortes, Paulo R.; Duran, Rosario; Badapanda, Chandan et al. (2018): Crosstalk between the serine/threonine kinase StkP and the response regulator ComE controls the stress response and intracellular survival of *Streptococcus pneumoniae*. In: *PLoS Pathog* 14 (6), e1007118. DOI: 10.1371/journal.ppat.1007118.

Pompeo, Frédérique; Foulquier, Elodie; Serrano, Bastien; Grangeasse, Christophe; Galinier, Anne (2015): Phosphorylation of the cell division protein GpsB regulates PrkC kinase activity through a negative feedback loop in *Bacillus subtilis*. In: *Molecular microbiology* 97 (1), p. 139–150. DOI: 10.1111/mmi.13015.

Potel, Clement M.; Lin, Miao-Hsia; Heck, Albert J. R.; Lemeer, Simone (2018): Widespread bacterial protein histidine phosphorylation revealed by mass spectrometry-based proteomics. In: *Nature methods* 15 (3), p. 187–190. DOI: 10.1038/nmeth.4580.

Prisic, Sladjana; Dankwa, Selasi; Schwartz, Daniel; Chou, Michael F.; Locasale, Jason W.; Kang, Choong-Min et al. (2010): Extensive phosphorylation with overlapping specificity by *Mycobacterium tuberculosis* serine/threonine protein kinases. In: *Proceedings of the National Academy of Sciences of the United States of America* 107 (16), p. 7521–7526. DOI: 10.1073/pnas.0913482107.

Rabes, Anne; Suttorp, Norbert; Opitz, Bastian (2016): Inflammasomes in Pneumococcal Infection: Innate Immune Sensing and Bacterial Evasion Strategies. In: *Current topics in microbiology and immunology* 397, p. 215–227. DOI: 10.1007/978-3-319-41171-2_11.

Raggiaschi, Roberto; Gotta, Stefano; Terstappen, Georg C. (2005): Phosphoproteome analysis. In: *Bioscience reports* 25 (1-2), p. 33–44. DOI: 10.1007/s10540-005-2846-0.

Rajagopal, Lakshmi; Clancy, Anne; Rubens, Craig E. (2003): A eukaryotic type serine/threonine kinase and phosphatase in *Streptococcus agalactiae* reversibly phosphorylate an inorganic pyrophosphatase and affect growth, cell segregation, and virulence. In: *The Journal of biological chemistry* 278 (16), p. 14429–14441. DOI: 10.1074/jbc.M212747200.

Rajagopal, Lakshmi; Vo, Anthony; Silvestroni, Aurelio and Rubens, C.E. (2005a): Regulation of purine biosynthesis by a eukaryotic-type kinase in *Streptococcus agalactiae*. In: *Molecular microbiology* 56(5), p. 1329–1346.

Rajagopal, Lakshmi; Vo, Anthony; Silvestroni, Aurelio and Rubens, C.E. (2005b): Regulation of purine biosynthesis by a eukaryotic-type kinase in *Streptococcus agalactiae*. In: *Molecular microbiology* 56(5), p. 1329–1346.

Ramirez, Mário; Carriço, Joáo A.; van der Linden, Mark; Melo-Cristino, José (2015): Molecular Epidemiology of *Streptococcus pneumoniae*. In: *Streptococcus Pneumoniae*: Elsevier, p. 3–19.

Rennemeier, Claudia; Hammerschmidt, Sven; Niemann, Silke; Inamura, Seiichi; Zähringer, Ulrich; Kehrel, Beate E. (2007): Thrombospondin-1 promotes cellular adherence of gram-positive pathogens via recognition of peptidoglycan. In: *FASEB journal: official publication of the Federation of American Societies for Experimental Biology* 21 (12), p. 3118–3132. DOI: 10.1096/fj.06-7992com.

Riley, Nicholas M.; Coon, Joshua J. (2016): Phosphoproteomics in the Age of Rapid and Deep Proteome Profiling. In: *Analytical chemistry* 88 (1), p. 74–94. DOI: 10.1021/acs.analchem.5b04123.

Röst, Hannes L.; Malmström, Lars; Aebersold, Ruedi (2015): Reproducible quantitative proteotype data matrices for systems biology. In: *Molecular biology of the cell* 26 (22), p. 3926–3931. DOI: 10.1091/mbc.E15-07-0507.

Rued, Britta E.; Zheng, Jiaqi J.; Mura, Andrea; Tsui, Ho-Ching T.; Boersma, Michael J.; Mazny, Jeffrey L. et al. (2017): Suppression and synthetic-lethal genetic relationships of Δ*gpsB* mutations indicate that GpsB mediates protein phosphorylation and penicillin-binding protein interactions in *Streptococcus pneumoniae* D39. In: *Molecular microbiology* 103 (6), p. 931–957. DOI: 10.1111/mmi.13613.

Saiki, Randall K.; Gelfand, David H.; Stoffel, Susanne; Scharf, Stephen J.; Higuchi, Russel; Horn, Glenn T. et al. (1988): Primer-directed enzymatic amplification of DNA with a thermostable DNA polymerase. In: *Science 239*, p. 487–491.

Sajid, Andaleeb; Arora, Gunjan; Singhal, Anshika; Kalia, Vipin C.; Singh, Yogendra (2015): Protein Phosphatases of Pathogenic Bacteria. Role in Physiology and Virulence. In: *Annual review of microbiology* 69, p. 527–547. DOI: 10.1146/annurev-micro-020415-111342.

Saleh, Malek; Bartual, Sergio G.; Abdullah, Mohammed R.; Jensch, Inga; Asmat, Tauseef M.; Petruschka, Lothar et al. (2013): Molecular architecture of *Streptococcus pneumoniae* surface thioredoxin-fold lipoproteins crucial for extracellular oxidative stress resistance and maintenance of virulence. In: *EMBO molecular medicine* 5 (12), p. 1852–1870. DOI: 10.1002/emmm.201202435.

Sasková, Lenka; Nováková, Linda; Basler, Marek; Branny, Pavel (2007): Eukaryotic-type serine/threonine protein kinase StkP is a global regulator of gene expression in *Streptococcus pneumoniae*. In: *Journal of bacteriology* 189 (11), p. 4168–4179. DOI: 10.1128/JB.01616-06.

Scheele, G. A. (1975): Two-dimensional gel analysis of soluble proteins. Charaterization of guinea pig exocrine pancreatic proteins. In: *Journal of Biological Chemistry* 250 (14), p. 5375–5385.

Schubert, Olga T.; Gillet, Ludovic C.; Collins, Ben C.; Navarro, Pedro; Rosenberger, George; Wolski, Witold E. et al. (2015): Building high-quality assay libraries for targeted analysis of SWATH MS data. In: *Nature protocols* 10 (3), p. 426–441. DOI: 10.1038/nprot.2015.015.

Schulz, Christian; Gierok, Philipp; Petruschka, Lothar; Lalk, Michael; Mäder, Ulrike; Hammerschmidt, Sven (2014): Regulation of the arginine deiminase system by ArgR2 interferes with arginine metabolism and fitness of *Streptococcus pneumoniae*. In: *mBio* 5 (6). DOI: 10.1128/mBio.01858-14.

Schulz, Christian; Hammerschmidt, Sven (2013): Exploitation of physiology and metabolomics to identify pneumococcal vaccine candidates. In: *Expert review of vaccines* 12 (9), p. 1061–1075. DOI: 10.1586/14760584.2013.824708.

Semanjski, Maja; Macek, Boris (2016): Shotgun proteomics of bacterial pathogens: advances, challenges and clinical implications. In: *Expert review of proteomics* 13 (2), p. 139–156. DOI: 10.1586/14789450.2016.1132168.

Sham, Lok-To; Barendt, Skye M.; Kopecky, Kimberly E.; Winkler, Malcolm E. (2011): Essential PcsB putative peptidoglycan hydrolase interacts with the essential $FtsX_{Spn}$ cell division protein in *Streptococcus pneumoniae* D39. In: *Proceedings of the National Academy of Sciences of the United States of America* 108 (45), E1061-9. DOI: 10.1073/pnas.1108323108.

Sham, Lok-To; Tsui, Ho-Ching T.; Land, Adrian D.; Barendt, Skye M.; Winkler, Malcolm E. (2012): Recent advances in pneumococcal peptidoglycan biosynthesis suggest new vaccine and antimicrobial targets. In: *Current opinion in microbiology* 15 (2), p. 194–203. DOI: 10.1016/j.mib.2011.12.013.

Shi, Lei; Pigeonneau, Nathalie; Ravikumar, Vaishnavi; Dobrinic, Paula; Macek, Boris; Franjevic, Damjan et al. (2014): Cross-phosphorylation of bacterial serine/threonine and tyrosine protein kinases on key regulatory residues. In: *Frontiers in microbiology* 5, p. 495. DOI: 10.3389/fmicb.2014.00495.

Shi, Yigong (2009): Serine/threonine phosphatases: mechanism through structure. In: *Cell* 139 (3), p. 468–484. DOI: 10.1016/j.cell.2009.10.006.

Sickmann, Albert; Meyer, Helmut E. (2001): Phosphoamino acid analysis. In: *Proteomics* 1 (2), p. 200–206. DOI: 10.1002/1615-9861(200102)1:2<200::AID-PROT200>3.0.CO;2-V.

Siemens, Nikolai; Oehmcke-Hecht, Sonja; Mettenleiter, Thomas C.; Kreikemeyer, Bernd; Valentin-Weigand, Peter; Hammerschmidt, Sven (2017): Port d'Entrée for Respiratory Infections - Does the Influenza A Virus Pave the Way for Bacteria? In: *Frontiers in microbiology* 8, p. 2602. DOI: 10.3389/fmicb.2017.02602.

Soares, Nelson C.; Spät, Philipp; Krug, Karsten; Macek, Boris (2013): Global dynamics of the *Escherichia coli* proteome and phosphoproteome during growth in minimal medium. In: *Journal of proteome research* 12 (6), p. 2611–2621. DOI: 10.1021/pr3011843.

Soares, Nelson C.; Spät, Philipp; Méndez, Jose Antonio; Nakedi, Kehilwe; Aranda, Jesús; Bou, German (2014): Ser/Thr/Tyr phosphoproteome characterization of *Acinetobacter baumannii*: comparison between a reference strain and a highly invasive multidrug-resistant clinical isolate. In: *Journal of proteomics* 102, p. 113–124. DOI: 10.1016/j.jprot.2014.03.009.

Song, Joon Young; Nahm, Moon H.; Moseley, M. Allen (2013): Clinical implications of pneumococcal serotypes. Invasive disease potential, clinical presentations, and antibiotic resistance. In: *Journal of Korean medical science* 28 (1), p. 4–15. DOI: 10.3346/jkms.2013.28.1.4.

Sørensen, Uffe B. Skov; Henrichsen, Jørgen; Chen, Hao-Chia; Szu, Shousun Chen (1990): Covalent linkage between the capsular polysaccharide and the cell wall peptidoglycan of *Streptococcus pneumoniae* revealed by immunochemical methods. In: *Microbial Pathogenesis* 8 (5), p. 325–334. DOI: 10.1016/0882-4010(90)90091-4.

Spratt, B. G.; Hanage W.P.; Brueggemann, A. B. (2004): Evolutionary and population biology of *Streptococcus pneumoniae*. In: E. I. Tuomanen, T. J. Mitchell, D. A. Morrison und Spratt, B. G., editors. (Hg.): The Pneumococcus. Washington, DC.: ASM Press, p. 119–135.

Stancik, Ivan Andreas; Šestak, Martin Sebastijan; Ji, Boyang; Axelson-Fisk, Marina; Franjevic, Damjan; Jers, Carsten et al. (2018): Serine/Threonine Protein Kinases from Bacteria, Archaea and Eukarya Share a Common Evolutionary Origin Deeply Rooted in the Tree of Life. In: *Journal of molecular biology* 430 (1), p. 27–32. DOI: 10.1016/j.jmb.2017.11.004.

Steen, Hanno; Jebanathirajah, Judith A.; Rush, John; Morrice, Nicolas; Kirschner, Marc W. (2006): Phosphorylation analysis by mass spectrometry: myths, facts, and the consequences for qualitative and quantitative measurements. In: *Mol Cell Proteomics* 5 (1), p. 172–181. DOI: 10.1074/mcp.M500135-MCP200.

Steen, Hanno; Jebanathirajah, Judith A.; Springer, Michael; Kirschner, Marc W. (2005): Stable isotope-free relative and absolute quantitation of protein phosphorylation stoichiometry by MS. In: *Proceedings of the National Academy of Sciences of the United States of America* 102 (11), p. 3948–3953. DOI: 10.1073/pnas.0409536102.

Sternberg, G. M.; Joseph Meredith Toner Collection (Library of Congress); National Board of Health (U.S.). (1881): A fatal form of septicaemia in the rabbit produced by the subcutaneous injection of human saliva: an experimental research. Baltimore: John Murphy & Co.

Stevens, Kathleen E.; Chang, Diana; Zwack, Erin E.; Sebert, Michael E. (2011): Competence in *Streptococcus pneumoniae* is regulated by the rate of ribosomal decoding errors. In: *mBio* 2 (5). DOI: 10.1128/mBio.00071-11.

Stock, J. B.; Stock, A. M.; Mottonen, J. M. (1990): Signal transduction in bacteria. In: *Nature* 344 (6265), p. 395–400. DOI: 10.1038/344395a0.

Subramanian, Karthik; Henriques-Normark, Birgitta; Normark, Staffan (2019): Emerging concepts in the pathogenesis of the Streptococcus pneumoniae: From nasopharyngeal colonizer to intracellular pathogen. In: *Cellular microbiology*, e13077. DOI: 10.1111/cmi.13077.

Sun, Xuesong; Ge, Feng; Xiao, Chuan-Le; Yin, Xing-Feng; Ge, Ruiguang; Zhang, Liu-Hui; He, Qing-Yu (2010): Phosphoproteomic analysis reveals the multiple roles of phosphorylation in pathogenic bacterium *Streptococcus pneumoniae*. In: *Journal of proteome research* 9 (1), p. 275–282. DOI: 10.1021/pr900612v.

Suni, Veronika; Suomi, Tomi; Tsubosaka, Tomoya; Imanishi, Susumu Y.; Elo, Laura L.; Corthals, Garry L. (2018): SimPhospho: a software tool enabling confident phosphosite assignment. In: *Bioinformatics (Oxford, England)* 34 (15), p. 2690–2692. DOI: 10.1093/bioinformatics/bty151.

Talamon, C. (1883): Coccus de la pneumonie. In: *Bull Soc Anat Paris* (58), p. 475–481.

Tao, Han; Bausch, Christoph; Richmond, Craig; Blattner, Frederick R.; Conway, Tyrrell (1999): Functional Genomics: Expression Analysis of *Escherichia coli* Growing on Minimal and Rich Media. In: *Journal of bacteriology* 181 (20), p. 6425–6440.

Tettelin, Hervé; Nelson, Karen E.; Paulsen, Ian T.; Eisen, Jonathan A.; Read, Timothy D.; Peterson, Scott et al. (2001): Complete Genome Sequence of a Virulent Isolate of *Streptococcus pneumoniae*. In: *Science (New York, N.Y.)* 293 (5529), p. 498–506. DOI: 10.1126/science.1059581.

Turnbough, Charles L.; Switzer, Robert L. (2008): Regulation of pyrimidine biosynthetic gene expression in bacteria. Repression without repressors. In: *Microbiology and molecular biology reviews: MMBR* 72 (2), 266-300, table of contents. DOI: 10.1128/MMBR.00001-08.

Tusher, V. G.; Tibshirani, R.; Chu, G. (2001): Significance analysis of microarrays applied to the ionizing radiation response. In: *Proceedings of the National Academy of Sciences of the United States of America* 98 (9), p. 5116–5121. DOI: 10.1073/pnas.091062498.

Tyanova, Stefka; Temu, Tikira; Sinitcyn, Pavel; Carlson, Arthur; Hein, Marco Y.; Geiger, Tamar et al. (2016): The Perseus computational platform for comprehensive analysis of (prote)omics data. In: *Nature methods* 13 (9), p. 731–740. DOI: 10.1038/nmeth.3901.

Uhrig, R. Glen; Kerk, David; Moorhead, Greg B. (2013): Evolution of bacterial-like phosphoprotein phosphatases in photosynthetic eukaryotes features ancestral mitochondrial or archaeal origin and possible lateral gene transfer. In: *Plant physiology* 163 (4), p. 1829–1843. DOI: 10.1104/pp.113.224378.

Ulijasz, Andrew T.; Falk, Shaun P.; Weisblum, Bernard (2009): Phosphorylation of the RitR DNA-binding domain by a Ser-Thr phosphokinase. Implications for global gene regulation in the streptococci. In: *Molecular microbiology* 71 (2), p. 382–390. DOI: 10.1111/j.1365-2958.2008.06532.x.

Ulrych, Aleš; Holečková, Nela; Goldová, Jana; Doubravová, Linda; Benada, Oldřich; Kofroňová, Olga et al. (2016): Characterization of pneumococcal Ser/Thr protein phosphatase *phpP* mutant and identification of a novel PhpP substrate, putative RNA binding protein Jag. In: *BMC microbiology* 16 (1), p. 247. DOI: 10.1186/s12866-016-0865-6.

van Oudenhove, Laurence; Devreese, Bart (2013): A review on recent developments in mass spectrometry instrumentation and quantitative tools advancing bacterial proteomics. In: *Applied Microbiology and Biotechnology* 97 (11), p. 4749–4762. DOI: 10.1007/s00253-013-4897-7.

Vega, Daniel E.; Margolin, William (2018): Suppression of a Thermosensitive *zipA* Cell Division Mutant by Altering Amino Acid Metabolism. In: *Journal of bacteriology* 200 (2). DOI: 10.1128/JB.00535-17.

Verma, Renu; Pinto, Sneha Maria; Patil, Arun Hanumana; Advani, Jayshree; Subba, Pratigya; Kumar, Manish et al. (2017): Quantitative Proteomic and Phosphoproteomic Analysis of H37Ra and H37Rv Strains of *Mycobacterium tuberculosis*. In: *Journal of proteome research* 16 (4), p. 1632–1645. DOI: 10.1021/acs.jproteome.6b00983.

Villén, Judit; Gygi, Steven P. (2008): The SCX/IMAC enrichment approach for global phosphorylation analysis by mass spectrometry. In: *Nature protocols* 3 (10), p. 1630–1638. DOI: 10.1038/nprot.2008.150.

Vizcaíno, Juan Antonio; Csordas, Attila; del-Toro, Noemi; Dianes, José A.; Griss, Johannes; Lavidas, Ilias et al. (2016): 2016 update of the PRIDE database and its related tools. In: *Nucleic acids research* 44 (D1), D447-56. DOI: 10.1093/nar/gkv1145.

Voß, Franziska; Kohler, Thomas P.; Meyer, Tanja; Abdullah, Mohammed R.; van Opzeeland, Fred J.; Saleh, Malek et al. (2018): Intranasal Vaccination With Lipoproteins Confers Protection Against Pneumococcal Colonisation. In: *Frontiers in immunology* 9, p. 2405. DOI: 10.3389/fimmu.2018.02405.

Voss, S.; Gámez, G.; Hammerschmidt, S. (2012): Impact of pneumococcal microbial surface components recognizing adhesive matrix molecules on colonization. In: *Molecular oral microbiology* 27 (4), p. 246–256. DOI: 10.1111/j.2041-1014.2012.00654.x.

Wasinger, V. C.; Cordwell, S. J.; Cerpa-Poljak, A.; Yan, J. X.; Gooley, A. A.; Wilkins, M. R. et al. (1995): Progress with gene-product mapping of the Mollicutes: *Mycoplasma genitalium*. In: *Electrophoresis* 16 (7), p. 1090–1094. DOI: 10.1002/elps.11501601185.

Weiser, Jeffrey N.; Ferreira, Daniela M.; Paton, James C. (2018): *Streptococcus pneumoniae*. Transmission, colonization and invasion. In: *Nature Reviews Microbiology* 16 (6), p. 355–367. DOI: 10.1038/s41579-018-0001-8.

Welte, T.; Torres, A.; Nathwani, D. (2012): Clinical and economic burden of community-acquired pneumonia among adults in Europe. In: *Thorax* 67 (1), p. 71–79. DOI: 10.1136/thx.2009.129502.

Wheeler, Richard; Mesnage, Stéphane; Boneca, Ivo G.; Hobbs, Jamie K.; Foster, Simon J. (2011): Super-resolution microscopy reveals cell wall dynamics and peptidoglycan architecture in ovococcal bacteria. In: *Molecular microbiology* 82 (5), p. 1096–1109. DOI: 10.1111/j.1365-2958.2011.07871.x.

Widdowson, C. A.; Adrian, P. V.; Klugman, K. P. (2000): Acquisition of chloramphenicol resistance by the linearization and integration of the entire staphylococcal plasmid pC194 into the chromosome of *Streptococcus pneumoniae*. In: *Antimicrobial agents and chemotherapy* 44 (2), p. 393–395. DOI: 10.1128/aac.44.2.393-395.2000.

Wiese, Heike; Kuhlmann, Katja; Wiese, Sebastian; Stoepel, Nadine S.; Pawlas, Magdalena; Meyer, Helmut E. et al. (2014): Comparison of alternative MS/MS and bioinformatics approaches for confident phosphorylation site localization. In: *Journal of proteome research* 13 (2), p. 1128–1137. DOI: 10.1021/pr400402s.

Wilkins, Marc R.; Sanchez, Jean-Charles; Gooley, Andrew A.; Appel, Ron D.; Humphery-Smith, Ian; Hochstrasser, Denis F.; Williams, Keith L. (1996): Progress with Proteome Projects. Why all Proteins Expressed by a Genome Should be Identified and How To Do It. In: *Biotechnology and Genetic Engineering Reviews* 13 (1), p. 19–50. DOI: 10.1080/02648725.1996.10647923.

Winter, A. J.; Comis, S. D.; Osborne, M. P.; Tarlow, M. J.; Stephen, J.; Andrew, P. W. et al. (1997): A role for pneumolysin but not neuraminidase in the hearing loss and cochlear damage induced by experimental pneumococcal meningitis in guinea pigs. In: *Infection and immunity* 65 (11), p. 4411–4418.

World Health Organization (WHO) (2016): Pneumonia. Fact sheet. Online verfügbar unter https://www.who.int/news-room/fact-sheets/detail/pneumonia, zuletzt aktualisiert am 11/7/2016.

Wright, David P.; Ulijasz, Andrew T. (2014): Regulation of transcription by eukaryotic-like serine-threonine kinases and phosphatases in Gram-positive bacterial pathogens. In: *Virulence* 5 (8), p. 863–885. DOI: 10.4161/21505594.2014.983404.

Wu, Wan-Ling; Lai, Shu-Jung; Yang, Jhih-Tian; Chern, Jeffy; Liang, Suh-Yuen; Chou, Chi-Chi et al. (2016): Phosphoproteomic analysis of *Methanohalophilus portucalensis* FDF1^{T} identified the role of protein phosphorylation in methanogenesis and osmoregulation. In: *Scientific reports* 6, p. 29013. DOI: 10.1038/srep29013.

Wyres, Kelly L.; Lambertsen, Lotte M.; Croucher, Nicholas J.; McGee, Lesley; Gottberg, Anne von; Liñares, Josefina et al. (2013): Pneumococcal capsular switching: a historical perspective. In: *The Journal of infectious diseases* 207 (3), p. 439–449. DOI: 10.1093/infdis/jis703.

Yagüe, Paula; Gonzalez-Quiñonez, Nathaly; Fernánez-García, Gemma; Alonso-Fernández, Sergio; Manteca, Angel (2019): Goals and Challenges in Bacterial Phosphoproteomics. In: *International journal of molecular sciences* 20 (22). DOI: 10.3390/ijms20225678.

Yeats, Corin; Finn, Robert D.; Bateman, Alex (2002): The PASTA domain: a β-lactam-binding domain. In: *Trends in Biochemical Sciences* 27 (9), p. 438–440. DOI: 10.1016/S0968-0004(02)02164-3.

Yen, C.-Y.; Houel, S.; Ahn, N. G.; Old, W. M. (2011): Spectrum-to-Spectrum Searching Using a Proteome-wide Spectral Library. In: *Mol Cell Proteomics* 10 (7).

Zhang, C. C. (1996): Bacterial signalling involving eukaryotic-type protein kinases. In: *Molecular microbiology* 20 (1), p. 9–15. DOI: 10.1111/j.1365-2958.1996.tb02483.x.

Zhang, Chunyan; Sun, Wen; Tan, Meifang; Dong, Mengmeng; Liu, Wanquan; Gao, Ting et al. (2017): The Eukaryote-Like Serine/Threonine Kinase STK Regulates the Growth and Metabolism of Zoonotic *Streptococcus suis*. In: *Frontiers in cellular and infection microbiology* 7, p. 66. DOI: 10.3389/fcimb.2017.00066.

Zheng, Jiaqi J.; Sinha, Dhriti; Wayne, Kyle J.; Winkler, Malcolm E. (2016): Physiological Roles of the Dual Phosphate Transporter Systems in Low and High Phosphate Conditions and in Capsule Maintenance of *Streptococcus pneumoniae* D39. In: *Frontiers in cellular and infection microbiology* 6, p. 63. DOI: 10.3389/fcimb.2016.00063.

Zucchini, Laure; Mercy, Chryslène; Garcia, Pierre Simon; Cluzel, Caroline; Gueguen-Chaignon, Virginie; Galisson, Frédéric et al. (2018): PASTA repeats of the protein kinase StkP interconnect cell constriction and separation of *Streptococcus pneumoniae*. In: *Nature microbiology* 3 (2), p. 197–209. DOI: 10.1038/s41564-017-0069-3.

10. APPENDIX

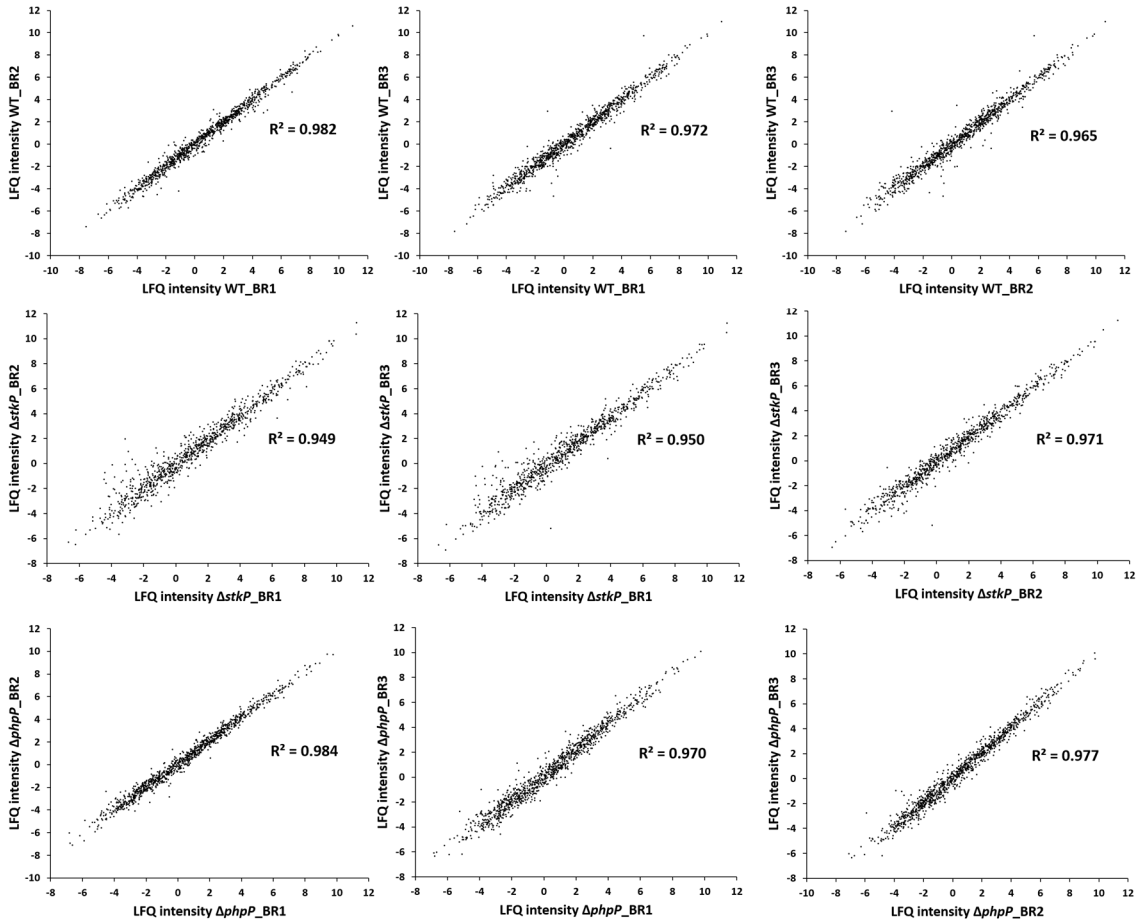

Figure 10-1: Scatter plots of biological replicates of pneumococci grown in RPMI *modi* medium, harvested in the exponential growth phase. The scatter plots were created from the quantitative data, i.e. the $\log_2$ transformed LFQ intensities of each biological replicate of the WT stain, the kinase mutant strain Δ*stkP* and the phosphatase mutant strain Δ*phpP*. The square of the correlation coefficient, R^2, is displayed within each plot.

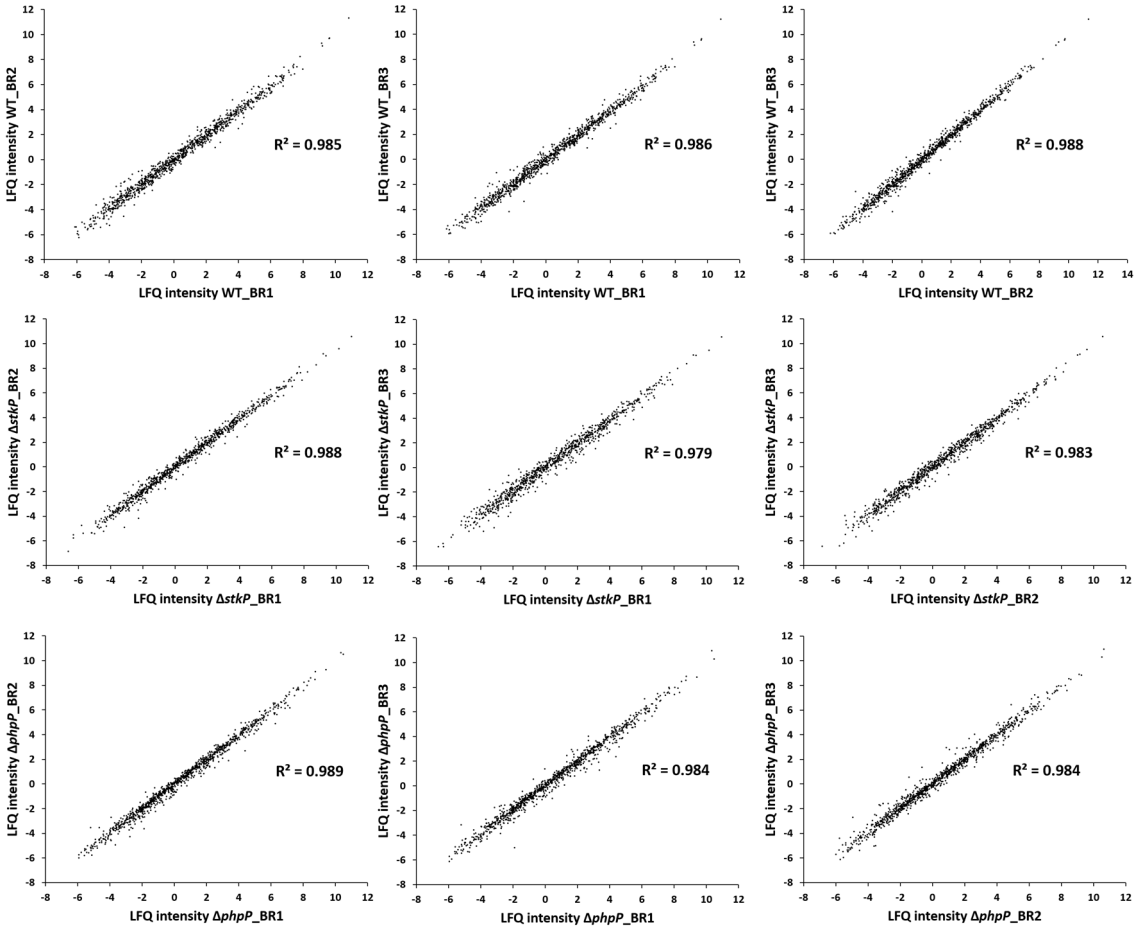

Figure 10-2: Scatter plots of biological replicates of pneumococci grown in RPMI *modi* medium, harvested in the stationary growth phase. The scatter plots were created from the quantitative data, i.e. the $\log_2$ transformed LFQ intensities of each biological replicate of the WT stain, the kinase mutant strain Δ*stkP* and the phosphatase mutant strain Δ*phpP*. The square of the correlation coefficient, R^2, is displayed within each plot.

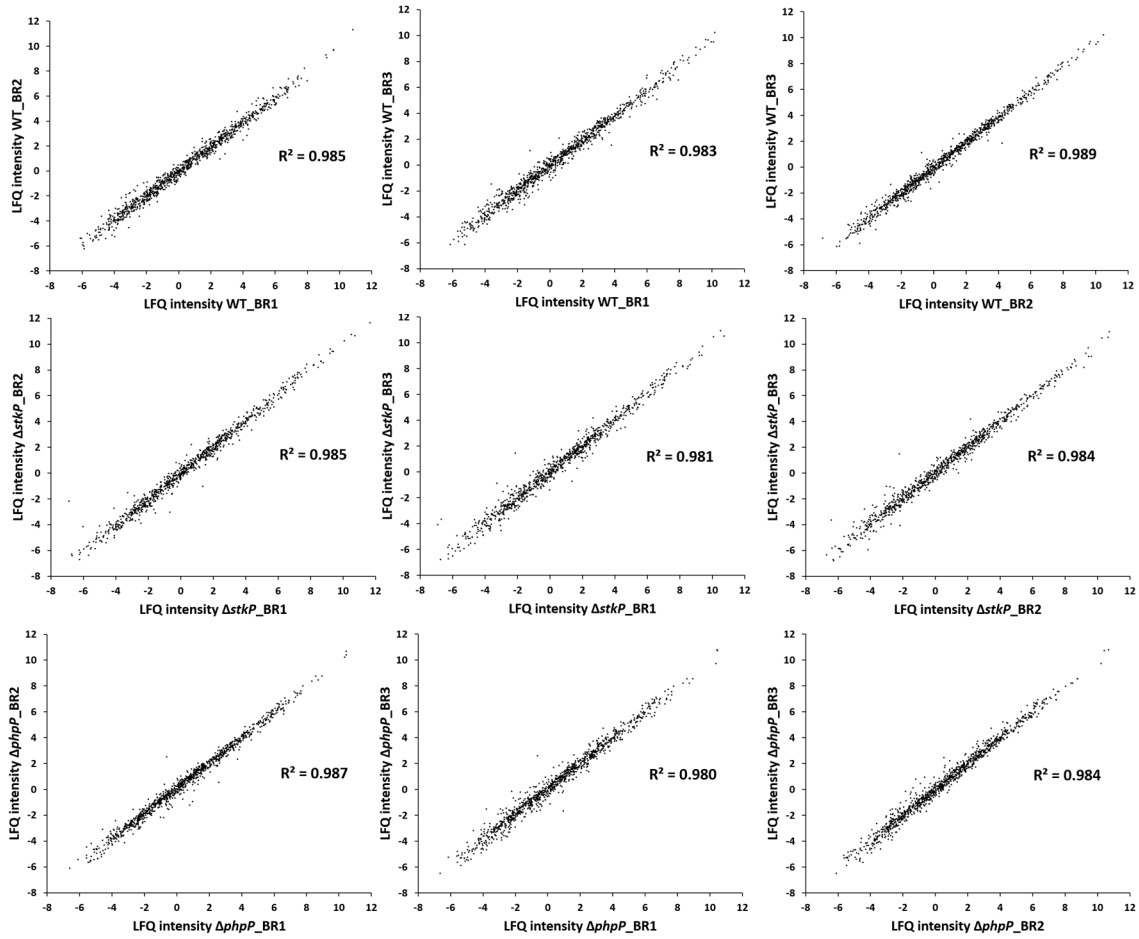

Figure 10-3: Scatter plots of biological replicates of pneumococci grown in THY medium, harvested in the exponential growth phase. The scatter plots were created from the quantitative data, i.e. the $\log_2$ transformed LFQ intensities of each biological replicate of the WT stain, the kinase mutant strain Δ*stkP* and the phosphatase mutant strain Δ*phpP.* The square of the correlation coefficient, R^2, is displayed within each plot.

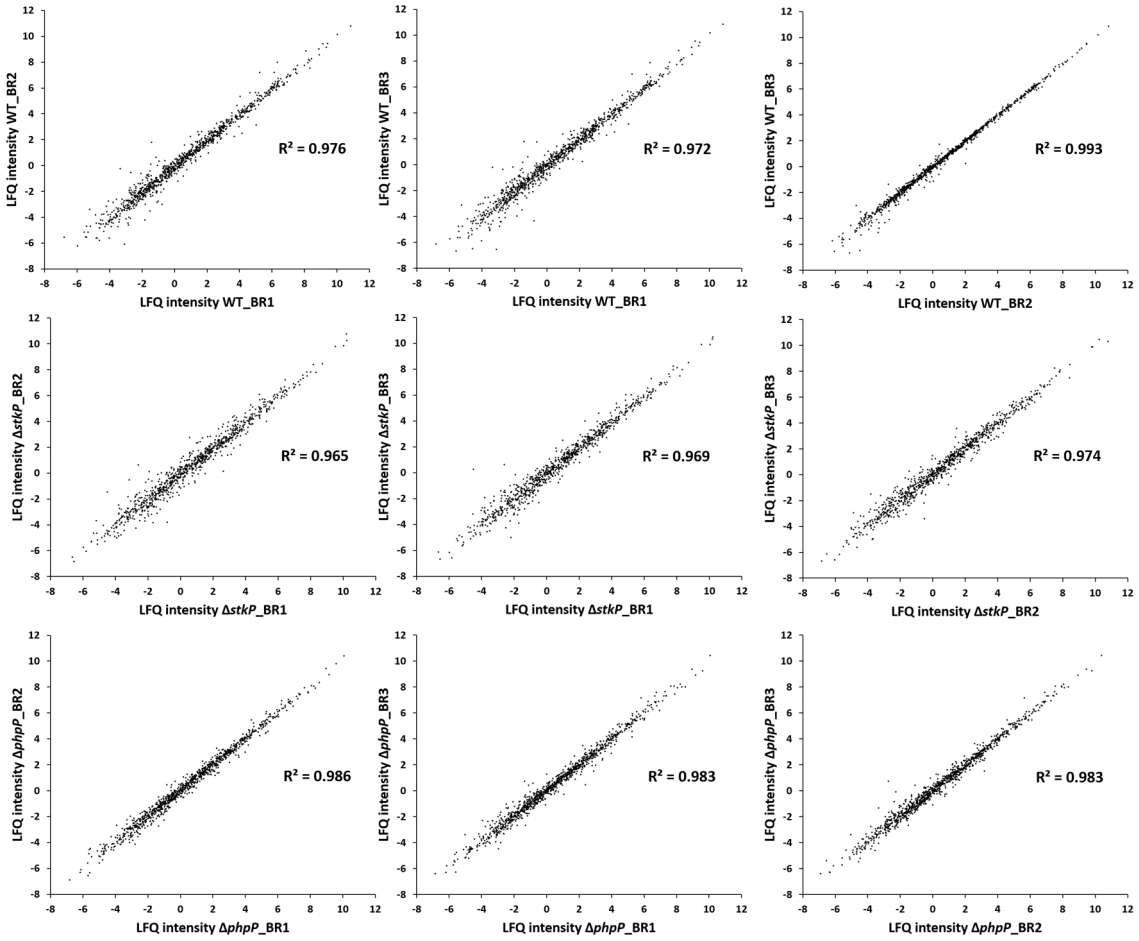

Figure 10-4: Scatter plots of biological replicates of pneumococci grown in THY medium, harvested in the stationary growth phase. The scatter plots were created from the quantitative data, i.e. the $\log_2$ transformed LFQ intensities of each biological replicate of the WT stain, the kinase mutant strain Δ*stkP* and the phosphatase mutant strain Δ*phpP.* The square of the correlation coefficient, R^2, is displayed within each plot.

10.1. SUPPLEMENTARY MATERIAL – ELECTRONIC APPENDIX

This section contains a list of the supplementary materials included on the attached CD-ROM.

FOLDERS

Database All samples were searched against the *S. pneumoniae* D39 database from UniProt (1,918 proteins, 2017) included in this folder. For TPP based spectral library construction the FASTA-header were shortened and replaced by the corresponding NCBI identifier.

MaxQuant For classical database search, spectra were searched separately for each strain with MaxQuant (1.6.1.0, Max Planck Institute of Biochemistry, (Cox and Mann, 2008)) and its implemented search engine Andromeda (Cox et al., 2011) against the *S. pneumoniae* D39 database from UniProt (2017).
The specific search parameters can be found in the mqpar files. The search output including the proteinGroups.txt file is attached as well.

- MaxQuant_search parameters
- MaxQuant_output

Perseus For shot gun proteomic data analyses the software Perseus 1.6.1.1 (Tyanova et al., 2016) was used.
The corresponding .sps files including the unique peptide identifications and the MaxQuant LFQ intensities are presented in this folder. Data were normalized over the median in Microsoft Excel and re-imported in Perseus.

- D39_RPMI_Unique peptides_and_LFQ
- D39_THY_Unique peptides_and_LFQ

SAM Statistical evaluation of quantified proteins was performed using RStudio (version 3.5.0) and the SAM (Significance analysis of microarrays (Tusher et al., 2001)) script by Michael Seo (https://github.com/MikeJSeo/SAM) with the implemented two-class unpaired test, which is analogous to a t-test between subjects. The input data tables and the original output tables (.xlsx files) can be found in the sub folders. Differentially expressed proteins with a minimum fold change of two and a q-value ≤ 0.01 were considered as significantly regulated.

- Input
- Original_output

Spectral library *S. pneumoniae* D39

The validated spectral library *S. pneumoniae* D39 was constructed using the Trans Proteomic Pipeline (TPP, 5.1.0-rc1 Sysygy, 2017) and can be applied for phosphorylation-centered searches.

- Final_Sp_D39_combined_splib_SILAC_fwd_decoy_CHi

DATA SHEETS

Annotation table - *Streptococcus pneumoniae* D39

Data Sheet 1 - Overview of data sets and raw files

Data Sheet 2 - LFQ results

Data Sheet 3 - ON_OFF_protein_identifications

Data Sheet 4 - STY phospho identifications_RPMI_exp

Data Sheet 5 - Summary LFQ and phosphoproteome results_RPMI_exp

Voronoi treemap collection

EIGENSTÄNDIGKEITSERKLÄRUNG

Hiermit erkläre ich, dass diese Arbeit bisher von mir weder an der Mathematisch-Naturwissenschaftlichen Fakultät der Universität Greifswald noch einer anderen wissenschaftlichen Einrichtung zum Zwecke der Promotion eingereicht wurde.
Ferner erkläre ich, dass ich diese Arbeit selbstständig verfasst und keine anderen als die darin angegebenen Hilfsmittel und Hilfen benutzt und keine Textabschnitte eines Dritten ohne Kennzeichnung übernommen habe.

Unterschrift des Promovenden